Comparison of the energy breakage efficiency of high compressive breakage with drop weight impact breakage

Research Report

Kelebone Sehlabaka

0705267R

Supervisor: Professor Henry Simonsen

February 2021

A research report submitted to the Faculty of Engineering and Built Environment, University of the Witwatersrand, Johannesburg, in partial fulfilment of the requirements for the Degree of Master of Science in Materials and Metallurgical Engineering.

Declaration

I declare that this thesis is my own, unaided work. It is being submitted for the Degree of Master of Science in Materials and Metallurgical Engineering. It has not been submitted before for any degree or examination in any other University.

Signed:

8 day of February 2021

Abstract

Ore particle size reduction is a process that has to be undertaken for valuable mineral liberation from host rock. In these comminution processes, appreciation of energy employment is required. Particle breakage is a function of the loading conditions as well as the particle properties. The loading conditions refer to the magnitude of the forces, loading velocity, temperature and the comminution tool properties while the particle properties refer to the particle shape, mechanical properties, size and internal structure

Mechanical processes, causing particle breakage, can be distinguished on the basis of the rate and direction in which the load is applied as well as the type of contact established. This is because of the stresses introduced, which may be localized, or distributed. The material hardness refers to the material's ability to withstand deformation while toughness is the material's ability to withstand stress without fracture and this is of great interest in comminution. Generally, brittle materials do not exhibit plastic deformation and rather exhibit a linear stress-strain relationship.

Particle breakage can occur in different ways as a function of the breakage mechanism and material properties. Material breakage behavior is important in the selection of size reduction equipment and is generally defined by breakage distribution functions. Single particle breakage is commonly used to determine particle breakage behavior for materials. As new surface is formed, the material behavior is observed to change since the change in size changes the particle behavior in terms of apertures it can accommodate, the downstream treatments it can be subjected to and such separation techniques as flotation and methods of particle handling.

When a particle is impacted, in the case of drop weight tests, it can never be pre-determined, with any certainty that it will actually break. However, what is known is that the probability of fracture is related to the amount of energy absorbed by the particle during impact. High pressure breakage also demonstrates similar behaviors, whereby a particle will experience fracture when subjected to increasing pressure. The main difference will, however, be in the conditions of the particle breakage since the impact breakage is an instantaneous process while the high pressure breakage is conducted at a slower rate and the particles receiving the pressure are retained in an enclosure.

Mechanisms of particle breakage investigated included the drop weight impact and high pressure compression tests. The impact drop weight test was conducted from two drop heights on individual and collections of particles while the high pressure compression was conducted at two compression forces on particles of a single layer and those in a multiple layer setting. Particle breakage from the tests was found to be influenced by several factors, namely the particle size, the input energy, stress distributions and the number of particles subjected to the breakage.

The impact tests indicate that less unit breakage energy is required for the single particle as compared to that required for a bed of particles of a similar size. Particle shape and size can affect breakage due to their influence on the resultant fragments obtained from the breakage, which has been indicated by the variation in the fragments obtained from breakage of particles of different sizes. The drop weight tests indicated that reducing the drop height resulted in a difference in the breakage energy used and single particles depicted higher breakage efficiency at both energy inputs analyzed in the test work, when compared to the single layer drop weight test.

The high pressure test indicated that the change in the energy input does have an effect on the degree of breakage obtained and the number of particles subject to the breakage also affects the degree of particle breakage. The increase in the input force resulted in a higher breakage of the smaller sized particles at the single layer set-up when compared to the multiple layers setting. As the particle layers increased, the resultant particle breakage is reduced due to the drop in the direct particle contact to the applied pressure as a result of the number of particles present in the system. The initial particle breakage also causes an effect on the particle breakage efficiency in a multiple particle layer set-up because of the particle re-arrangement which occurs between the adjacent particles as well as between the particle layers. An increase in the input energy resulted in a finer product particle size distribution when compared to that obtained from a lower input energy breakage. The effect could be noted on different size classes, where the d_{80} obtained from the breakage was finer when an increased energy was input into the system.

Looking at both the drop weight test and the high pressure test the highest particle breakage efficiency was obtained with the high pressure single layer test at 80kN. In this setting, more particle breakage was obtained. Random particle breakage can be summarized as "the independence of breakage from ore properties and mechanical properties during comminution." Evans C.L, *et al* [16]. This was seen in the energy utilization obtained from both the high pressure compression and drop weight impact tests. The energy utilization varied for the impact test to that of the high pressure compression test. Looking at the energy used per mass of particles subject to breakage it indicated for both tests that more energy is used for the small particle size breakage. This was seen in the energy utilization obtained from both the high pressure compression and drop weight impact test.

The high pressure compression test results in greater effectiveness in achieving particle breakage as could be seen from the daughter fragments produced. The specific energy employed for the high pressure test was the highest for the smaller particle sizes and decreased with increasing particle size. This value was higher for each particle size when 80kN of force was applied compared to the 50kN-applied force. The energy unitization and distribution is better controlled between the particles in the high pressure test due to the confined set-up. In the drop weight test, particles are less confined and this results in the more 'erratic' particle behavior as soon as it has been impacted. However, the specific energy use displayed a similar trend as that obtained in the high pressure test with the smallest particle size using the highest amount of energy

Acknowledgements

I would like to acknowledge the following for their contribution to this effort:

Professor Simonsen, I am not only grateful for his patient and wise mentorship to guide me on the road to become a quality researcher, but also the life-lessons he imparted.

Dr. Bwalya, who always willingly shared his expertise to help broaden my understanding of the subject matter. My knowledge of comminution modelling can be contributed to the generous knowledge and insights he shared.

I would like to thank my parents for their constant guidance, I am forever grateful for you. My husband, Sebanti Mofokeng, for his patience and unmeasurable support. Through his unrelenting humor, he has contributed greatly to my sanity during the completion of this dissertation.

Family members for the unfailing love, support and understanding though out the process of finalizing this work.

Lastly, I am eternally grateful for the grace offered to me by my Lord and savior to complete this work.

Table of Contents

List of tables

List of figures

Notation

Units:

kN	- kilo Newton
mm	- millimeters
g/cm^3	- grams per cubic centimeter
MPa	- mega Pascal
^oC	- Degree Celsius
GPa	- giga Pascal
J	- Joule
Kg	- kilogram
m/s	- meters per second
m/s^2	- meters per second squared
kWh/t	- kilowatt-hour per ton
µm	- micro meters

Abbreviations:

JKMRC	- The Julius Kruttschnitt Mineral Research Centre
DEM	- Discrete Element Methods
DWT	- Drop Weight Tester
UFLC	- Ultra-fast load cell device
SILC	- Short Impact Load Cell
HPGR	- High Pressure Grinding Rolls
SAG	- Semi Autogenous Grinding
AG	- Autogenous Grinding

Equation Symbols:

E (J)	= potential energy
m_{dw}	= mass of the drop weight (kg)
g	= gravitational acceleration (9.81 m/s^2)
h	= distance (meters) between the drop weight and the top of the specimen.
E (J/kg)	= the energy required per mass of feed
k_R	= Rittinger's constant
d_1 (m)	= the average initial size of the feed particles in Rittinger's Law
d_2 (m)	= the average size of the comminuted particles in Rittinger's Law
s_n (m^2)	= surface area of the comminuted particles
s_i (m^2)	= surface area of the feed particles
E (kWh/t)	= the energy required per mass of feed
W (kWh/t)	= the Bond Work Index work required to reduce a unit mass.
d_1 (µm)	= sieve aperture or mesh size that allows 80% of the mass of the feed to pass in Bond's Law
d_2 (µm)	= sieve aperture or mesh size that allows 80% of the mass of the feed to be retained in Bond's Law
Wi (kWh/t)	= work input
t_n	= the breakage index 'a' and 'b' = the ore impact breakage parameters.
E_{cs}	= the specific comminution energy (kWh/t)
v	= impact velocity (m/s)

Breakage and sizing parameters:

d_{80}	= 80% particle passing size
d_m	= modular particle size (mm)
lambda (λ)	= breakage constant "lambda"

1. Introduction

Comminution is a function of both equipment and material property. The breakage response of the material depends on the force loading that is applied under normal condition; an elastic body will extend in proportion to the magnitude of the applied force. However, if this force exceeds the elastic limit of the material, it is permanently deformed, or usually fractured. Most ores encountered in mineral processing are brittle material that exhibit little elasticity before fracturing, at least in the coarser size ranges, and this is advantageous to comminution.

Despite the advantage of brittle material fracturing more easily, it is well known that a lot of energy invested in comminution ends up being wasted and thus there is a need to improve the efficiency of loading the particles. In this research, we study two force-loading techniques on quartz; drop weight impact and slow compression and compare their efficiencies. While there are many ways of loading, we limit ourselves to these two types of force loading; impact by drop weight and compression loading.

The main objective of this research will thus be a comparison of efficiencies of the two force loading techniques on quartz. To tackle this, the dissertation is divided in five chapters, which are briefly summarized below:

Chapter 1 gives the introduction and gives an overview of each chapter.

Chapter 2: Reviews the relevant literature that discusses comminution mechanisms as it is applied to material of different properties. The different test methods for evaluating breakage properties of material are reviewed. The material properties of quartz are also reviewed to help explain the expected response to the two loading techniques being applied.

Chapter 3: Addresses the sample preparation techniques and the experimental procedures are discussed. The drop weight test equipment is described as well as the equipment used in pressure loading compression tests.

Chapter 4: The methodologies for computing energy that a particle is subjected to in a drop weight test is described and tables of results of product size distributions are presented. A similar procedure is applied to the compression test results. Same trend worth mentioning are highlighted.

Chapter 5: The results presented in chapter 4 are discussed in more detail. The two force loading techniques are compared more closely.

Chapter 6: In this chapter, the conclusions are drawn and recommendations for further work are made.

For particles to break, a sufficient force that exceeds the fracture limits must be applied.

How different material responds differently to applied forces:

Particle deformation, resulting from applied forces, produces a 3-dimensional compression-, tensile- and shear-stress field. This occurs by: [34]

- Elastic energy that is stored in the stress field for elastic material
- For sufficiently high stresses, fracture is initiated by tensile stresses in brittle material.
- The first total fracture determines the breakage.
- In situations whereby the elastically stored energy is higher than the energy required for breakage, some of it will be transferred to kinetic energy for the breakage fragments generated. This 'excess' energy will serve to facilitate breakage of the produced fragments of particles from the initial particle breakage, thus carrying on the breakage from the parent particle to the breakage of the daughter particles.

1.1. Crushing

Crushing refers to the first stage an ore is exposed to in processing. It is at this point that the initial material size reduction takes place. Minerals have the tendency, in comminution, to follow their natural crystal behavior but this can be detrimental as it can lead to over-representation of fines of the required minerals. As a result, it is essential that the crushing equipment is well suited to the ore to be treated.

Due to varying material properties, during crushing, the objective needs to be well established. The crushing stages, required for a particular ore, will not be those universally applicable for all ore bodies due to their distinct properties. This is the reason why the comminution stages employed in plants vary; each is designed for its particular material to be treated in the subsequent processes.

Size reduction, by crushing, has a size limitation for the final product size obtained due to the particle feed size it can treat and the reduction ratios that crushing equipment can offer. If further reduction is required, grinding stages should be added. Grinding is a comminution process that uses the mechanical forces of impaction, compression, shearing and attrition. The two main purposes for a grinding process are:

- To liberate individual minerals trapped in the rock for subsequent enrichment in the form of separation.
- To produce "fines" as a means of adequately liberating the economic mineral by increasing the specific surface.

1.2. Grinding

In comminution processes, grinding is the last stage. During grinding, particle sizes are reduced by both impact and abrasion. One process, where grinding takes place, is in a grinding mill. Ores have a particular particle size distribution, which is influenced, by several factors such as the extent to which the gangue is distributed and the mineral recovery processes to be used post grinding. It is for this reason that the particle size produced from grinding processes is closely regulated. Grinding is, for this reason, an essential part in the mineral recovery process because deficient grinding will result in material which is too coarse, thus leading to a low degree of mineral recovery while over grinding will lead to high energy utilization and size reduction of the favorable mineral to a size below that required for efficient separation.

Grinding is an energy intensive process because in units such as mills, the ore is broken down because of repeated, cataracting impacts, which affect the liberated, and the unliberated particles during the tumbling process [57]. The energy drawn by the grinding process gets dissipated as heat, noise and other losses during the grinding process. The main purpose of grinding is to achieve the correct degree of particle size reduction of the ore.

Grinding in mills is influenced by particle size, quantity, motion of the mill and spaces present between the grinding media and the ore particles. In this process, the degree of grinding is dependent on the probability of the ore particle entering a zone where it is in contact with the grinding media or the other particles, making grinding a more random process as compared to crushing. Mills have as a result mostly been installed with a classifier in order to produce a more consistent product size distribution.

Grinding processes occur by impact (compression), abrasion, or chipping. Impact breakage is experienced because of forces applied normally to the particle surface, while abrasion occurs due to forces acting parallel to the surface and chipping occurs when oblique forces act on a particle.

1.2.1. Issues related to crushing and grinding

Crushing

Crushing is the initial controlled size reduction process that reduces particle size and increases the specific surface area of the ore treated. As the primary stage in mineral recovery, crushing is quite energy intensive. It is imperative in comminution circuits that the crushing stage operates optimally so that the correct sized material is fed to the grinding stage.

Grinding

Dry / Wet grinding

The feed material to grinding circuits may be wet or dry. Dry grinding is required when there is a probability of physical or chemical changes to the mineral that may occur when wet grinding is applied. It, however, causes a higher proportion of fines, but results in less liner wear. Wet grinding on the other hand is usually applied because of the total operation cost of reduction simply because: [57]

- It results in lower power consumption
- Eliminates dust generation
- Allows various material handling modes, i.e.: pumping
- Allows close product control through wet screening, classification and cycloning.

High energy consumption

The grinding costs are mainly composed of the energy, liners and grinding media. These, however, differ for different mill types. These high costs are to some extent a product of high power inputs required by the milling processes.

Uncontrolled particle production

Overgrinding is also a very common challenge associated with comminution circuits. This result in energy utilized unnecessarily in the process and can cause inefficiencies in mineral recovery downstream. To solve the problem, classifiers are incorporated in the grinding circuit, whereby particles of the required particle size are removed and the oversize is returned into the grinding unit.

1.2.2. Mechanism of particle breakage

The mechanical processes causing particle breakage can be distinguished based on rate and the direction in which the load is applied as well as the type of contact established. This is because of the type of stresses introduced, which may be localized, or distributed. The stresses in contact with the loading may be applied to individual particles or transmitted through a bed of particles.

Rumpf *et al*., (1973) [48] established that the mode in which load is applied and the type of contact established result in four particle breakage mechanical processes, which are; impact, compression, shear and abrasion. However, it has been noted that combinations of these can be found in practice, such as impact compression of ceramic materials (Arbiter *et al.*, 1969) [2] or impact cutting of soft polymers (Okuda and Choi, 1981) [38].

Surface wear occurs when very small loads are applied to particles with a rough surface which are subjected to sliding or rolling. It is a form of material removal, which does not cause the material significant changes to its shape and size. (Ghadiri *et al*., 1995*)* [21].

Impact breakage refers to particle breakage experienced when a particle breaks because of high impact forces/energy. This breakage phenomenon is experienced by particles undergoing comminution. It is a sharp, instantaneous, collision. The Impact test employs a device used to measure how much energy is absorbed as material fractures, or breaks, under collision. This indicates the total amount of energy employed in the breakage. The impact testing is about measuring the material's resistance to impact and this is known as the material toughness. It is the amount of energy material can absorb before fracturing or breaking.

Abrasion refers to when surface material is directly removed from the particle because of sliding on a surface. It is the tearing-off of the particles from the body of material because of low energy forces [15].

Shear failure is sometimes referred to as attrition. This mode of particle breakage produces a significantly finer product thus making it unfavorable in some industry sectors. Shear occurs because of inter-particle interaction and may occur if a crusher is fed too fast, with particles contacting and increasing the degree of compressive stress and shear failure [16].

Compression occurs when work is being done on the material between two surfaces. Here material is subject to a compression force between two plates, which will initiate cracking, and particle breakage. Compression is used in High Pressure Grinding Rolls (HPGR), where the material size reduction occurs because of the force applied to it.

Ore size reduction is thus an essential process in industry as it allows for the increase in the particle surface area because, in some particle processing solid particle reactions, the reaction rate is proportional to the area of contact. It also allows one to achieve intimate or more homogenous mixing, easier disposal of solid waste and generally allows for better material handle-ability. Ore size reduction processes are found in various industries such as in cement, agricultural products, pulp and paper, pharmaceuticals and mining to name a few.

In 2012, Ballantyne *et al*. [V] indicated that the proportion of energy consumed through comminution in gold and copper producing mines is between 26-46% of the total energy use in the process. In resource intensive countries such as Australia, gold and copper processing amounts to 1.3% of the national electrical power consumption. The Department of Energy in the USA research revealed that comminution represents 2% of the world electrical power consumption (Ballantyne *et al*, 2012) [V].

Comminution technology employed in industry is generally energy intensive and inefficient. Size-reduction devices have been noted to be very costly to operate, equating to 25% or more of the total raw materials processing costs and are particularly inefficient with less than 1% of the input energy resulting in the generation of the new surface area produced. [14]

1.2.3. Objectives and structure of the thesis

This dissertation is aimed at evaluating the relative energy directed to comminution resulting from impact and high pressure compressive breakage. It will trace the energy utilized in particle breakage from a single particle, single particle layer and multiple particle layers using a drop weight impact system and a high pressure compression unit.

2. Overview of Particle Breakage

2.1. Introduction to material properties and how they respond to loading forces

Particles experience fracture because of applied stresses by pressure and/or impact, which is referred to as cleavage and shattering. While at high shearing stresses, subsidiary fracture occurs on the particle surface, which leads to attrition and wear. In their natural form, materials can resist fracture to a particular extent, which is why materials exhibit different fracture thresholds when subject to stress.

The material hardness refers to the material's ability to withstand deformation while toughness is the material's ability to withstand stress without fracture, or failure, and this is of great interest in comminution. Brittle materials have a high resistance to plastic deformation and exhibit a linear stress-strain relationship; nevertheless, these are mostly not tough and can thus be easily fractured. [57, p109]

Low material toughness can be attributed to the presence of micro and macro flaws in the material. When subjected to stress, the stress intensity of the flaw is expected to increase at the flaw tip or edge. In this manner, the material is stressed beyond its strength at the flaw tip. In the 1920s, Griffith [24] developed the theory of brittle fracture which stated that "Fracture occurs when the tensile stresses at some crack tip exceeds theoretical cohesive strength of the material." This theory was able to explain why the strength of brittle materials is less than that expected from theoretical calculations. The low strengths were thus suggested to be because of the small cracks or flaws in the material. Thus, when a material with flaws is stressed, the flaws act as stress raisers or concentration points.

Several factors contribute to the fracture of particulate matter, but the result is unpredictable, thus making the process random. The certainty of a particulate particle breaking on impact is very narrow; all that is known is that the fracture probability is related to the amount of energy absorbed by the particle during impact. R Mariano, et al.[16], describes in particle breakage literature that random and non-random breakage can be categorized into 5 groups which are: (1) the explicit definition of random breakage, (2) definition of random breakage through its contrary, whereby non-random breakage is explicitly defined, (3) random breakage defined using examples and methods, (4) context clue definition without directly mentioning random breakage and (5) definitions of random and non-random breakage which do not fall under the four above-mentioned categories (impact, abrasion, shear and compression). From this paper, it was established that random particle breakage could be summarized as "the independence of breakage from both ore properties and mechanical properties during comminution."

2.1.1. Properties of test material

The test material used in this research is silica, also referred to as quartz. Silica is found mostly in its crystalline state, but it also occurs in an amorphous form, which is a result of weathering.

Silicon dioxide has a giant covalent atomic structure. The covalent bonds allow each silicon atom to bond to four oxygen atoms. Silicon dioxide is insoluble in water and does not conduct electricity, which is one of the features derived from the strong covalent bonds it has. [IV]

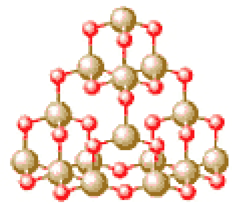

Figure 2-1: Silicon Dioxide atomic structure

[http://www.bbc.co.uk/schools/gcsebitesize/science/add_ocr_pre_2011/chemicals/rocksmineralsrev3.shtml]

Silicon dioxide is also found as quartz in granite and it is the main compound in sandstone. Beach sand is mainly made up of silicon dioxide. [IV]

2.1.1.1. Mechanical properties of test material [VII]

The density of silica is 2.20 g/cm^3 while the thermal conductivity is 1.4 Wm^{-1}K^{-1}. The tensile strength of silica is 110 MPa. The melting point of silica is 1830 ^{o}C with excellent thermal shock resistance.

2.1.1.2. Young's Modulus

The Young's modulus is a property used for quantifying a material's stiffness. The Young's modulus for silicon is higher than that of materials such as aluminum, copper and titanium metal at 66.3 GPa.

2.1.1.3. Hardness

Silica is a solid, crystallized material under ambient temperature and pressure. It is relatively hard, recording seven on the Mohs scale.

2.1.1.4. Fracture Toughness

Fracture toughness refers to the material's ability to resist fracture. The fracture toughness varies with material thickness and it is an indication of the amount of stress, which is required to propagate an existing flaw. The fracture toughness for silica is 0.79 MPa.

2.2. Comminution Laws that elucidate the process of size reduction

In 1867, Rittinger [26] proposed a law, which states, “The energy required in crushing is proportional to the new surface created as a result of particle fragmentation.” This law has been noted to give better results with fine grinding because of the larger increase in surface area. Rittinger’s Law has no incompatibility to the laws of elastic bodies. This is such because, up until the elastic limit, deformation is directly proportional to the stress and the energy absorbed. It is proportional to the volume of the stressed particle as stated by Rittinger’s Law [26]. This may be expressed as:

$$E = k_R\left(\frac{1}{d_2} - \frac{1}{d_1}\right) \quad \textit{Equation 1}$$

Where E (J/kg) = the energy required per mass of feed

k_R = Rittinger’s constant

d1 (m) = the average initial size of the feed particles

d2 (m) = the average size of the comminuted particles

From this equation, the 1/d ratio equates to the surface area(s). As a result, the equation can be represented as follows:

$$E = k_R(s_n - s_i) \quad \textit{Equation 2}$$

Where E (J/kg) = the energy required per mass of feed

k_R = Rittinger’s constant

s_n (m^2) = surface area of the comminuted particles

s_i (m^2) = surface area of the feed particles

A few years later in 1885, Kick [19] proposed, “The energy required for particle size reduction is proportional to the size reduction ratio, or the volume reduction.” This may be expressed as follows:

$$E = k_K ln\frac{d_1}{d_2} \quad \textit{Equation 3}$$

Where	E (J/kg)	= the energy required per mass of feed
	k_K	= Kick's constant
	d_1 (m)	= the average initial size of the feed particles
	d_2 (m)	= the average size of the ground particles

The d_1/d_2 ratio is known as the size reduction ratio, which is used to evaluate relative performance of different types of equipment. The reduction ratio in coarse grinding is 8:1 while in fine grinding it exceeds 100:1. [VI]

Both laws give widely different results even though they do have a relationship. As it was stated by Rittinger, the energy required is proportional to the surface area created. The abovementioned laws indicate that the stresses in the compression machine are bigger along certain planes of fracture for the particle, which is where relative movement will be the greatest as well as the amount of energy expended.

In 1961, Bond [19] published a law, which stated, "The total work input represented by a given weight of crushed product is inversely proportional to the square root of the diameter of the product particles." Also known as "the energy used for the size reduction being proportional to the new crack length formed". This law is represented by the following equation:

$$\frac{E}{W} = \sqrt{\frac{100}{d_2}} - \sqrt{\frac{100}{d_1}}$$ *Equation 4*

Where	E (kWh/t)	= the energy required per mass of feed
	W (kWh/t)	= the Bond Work Index work required to reduce a unit mass.
	d_1 (µm)	= sieve aperture or mesh size that allows 80% of the mass of the feed to pass
	d_2 (µm)	= sieve aperture or mesh size that allows 80% of the mass of the feed to be retained

2.2.1. Evaluation of ore test methods used for mill design

2.2.1.1. The Bond Test

This test is used to determine the materials grindability. The apparatus used is a ball mill of a 305mm diameter and length. The test is conducted as a dry, locked-cycle, test with screening of the mill product after each stage. The same amount of material is maintained in the mill by adding the same amount of ore as that of the fines removed. The grinding time is maintained in order to allow for a 250% circulating load. The test requires a sample with a mass of 10kg and a minus 3.35mm size distribution.

The Bond ball mill work index (Wi) can be determined as follows: [36]

$$Wi\ (kWh/t) = (1.1x44.5) / [x_s^{0.23} \times G^{0.82} \{10/\sqrt{x_{80,P}} - 10/\sqrt{x_{80,F}}\}]$$

Equation 5

Where x_S = screen aperture in microns

G = grindability (in grams of product per mill revolution),

$x_{80,F}$ *and* $x_{80,P}$ = 80% passing particle sizes in µm for the mill feed and product, respectively.

The results obtained are used to calculate the change in particle size during grinding based on the grinding work input Wi (kWh/t), as well as to size mills in order to yield a desired particle size reduction based on the Bond law.

Originally, the Bond test was developed for determining the grindability in ball mills; however, it has been adapted for other types of mills. For the rod mill, a 305mm x 610mm sized mill requiring a 20kg sample is used, while the circulating load is maintained at 100%. In the autogenous and semi-autogenous mills and in high pressure grinding rolls the use of the Bond test method would require extensions by empirical relations.

In grindability tests, a combination of attrition and impact forces is involved. The test can be quite complex simply because one requires several grinding cycles in order to attain steady state of the closed circuit. In addition, a large amount of sample is required for the test.

On the positive side, the test is quite reliable and does have good repeatability in cases where the procedure complies with the standard.

In order to determine the grindability of an ore, the bond work index is used. It represents the kilowatt-hours per ton required to reduce the material from theoretically infinite feed size to 80 percent passing 100μm. This bond index is useful in designing the grinding circuit and it is used in determining the size of the mill to be incorporated in the circuit as well as the grinding power required for the desired ore throughput.

This work index varies vastly with material hardness as follows:

Table 2-1: Bond Work Index Properties [VIII]

Property	Soft Ore	Medium Ore	Hard Ore	Very Hard Ore
Bond Work Index (kWh/t)	7 - 9	9 - 14	14– 20	>20
Bond Work Index (J/g)	25.2 – 32.4	32.4 – 50.4	50.4 – 72.0	> 72.0

The test is conducted in a closed circuit grinding test performed in a mill. This test is applied at sizes ranging from 600-44 microns.

2.2.1.2. Population balance modelling

However, the Bond test, though widely used, has limited accuracy and other methods have been proposed to improve precision such as Population Balance Modelling, which involves use of the selection and breakage function parameters to predict the rate of grinding. These test are however dependent on comminution equipment being used. For this reason JKMRC proposed a test that would purely focus on the material's resistance to breakage as discussed in the next section.

Population balance is a balance of particles of a particular state and the equations thereof are used to describe the evolution of a population of particles. In their paper, Broadbent and Callcott (1956) [10] indicated that comminution consists of two processes, namely the selection and breakage of particles and the modelling of comminution will thus be dependent on the description of both functions. The selection function expresses the breakage probability encountered in the size reduction equipment failure zone while the breakage function refers to the size distribution obtained from the particle breakage process. Both these functions are incorporated in the population balance model such that the mass balance of each size class maintains its stability.

The population balance model is based on first order kinetics and is a discrete-size and continuous time model. In this model, the breakage rate is at its maximum, but above this breakage rate, the optimum size decreases drastically for an optimum size. This model takes into consideration the abnormality of large particle breakage.

2.3. A survey of breakage mechanisms that are involved in size reduction of the particles

2.3.1. Modes of particle breakage

Particle breakage can occur in different ways as a function of the breakage mechanism and the material properties. Material breakage behavior is important for size reduction equipment and is generally defined by breakage distribution functions. Single particle breakage is commonly used to determine particle breakage behavior for materials, which assume that breakage is not size dependent. As new surface is formed, the material behavior is observed to change.

When particle breakage occurs, the fracture is prompted by the different stresses the particle is subjected to. When a particle shatters, a wide spectrum of product sizes is produced thus making it evident that the process occurs in a series of steps in which the sequential shattering occurs at a rapid rate. The size distribution of such product population forms the basis for breakage function models. When dealing with particles that have a preferred fracture surface, cleavage occurs. The size distribution from cleavage breakage is narrow and bimodal. With attrition and chipping, the applied stresses are not high enough to cause fracture with the resultant creation of smaller product particles. This is the reason why in this process, the parent particle is modified but not depleted. [30, p129-132]

When a particle is impacted, it can never be pre-determined if it will actually break. However, what is known is that the probability of fracture is related to the amount of energy absorbed by the particle during impact. This energy absorbed before fracture is the particle's fracture energy, which is an intrinsic particle property. The fracture energy requirement is modified by the presence of flaws in the material. [30]

2.3.1.1. Ductile breakage

Ductile material fracture refers to the breakage material experiences post extensive plastic deformation. This is encountered by materials, which have a particularly high ductility and fracture toughness. In this phenomenon, rather than cracking, the material pulls apart when under tension and leaves a rough surface. In this case, there is a moderate propagation and absorption of energy before fracture occurs.

2.3.1.2. Brittle breakage

Materials which do not fail in a ductile manner, will do so in a brittle manner. Brittle fracture is characterized by little to no plastic deformation resulting in a distinct and reasonably smooth fracture surface. Materials that characteristically fracture in this manner include glass, ceramics and some polymers. [30]

2.3.1.3. Particle size effects on breakage

Particle breakage is used extensively in various industries and the shape and size of the particles is very important in, inter alia, mineral processing plants. This is because of its effects on the downstream unit processes and because the particle shape and size determine a range of physical and chemical properties, which can affect product quality. [44]

It has been noted that the particle strength decreases with increasing particle size and this can be attributed to more impurities and micro-cracks found in larger particles. However, the number and length of these micro cracks can vary. Particle shape also plays a role in particle breakage especially when the particle has sharp edges, which could allow large local stresses to be created.

2.3.2. Mechanisms of particle breakage investigated

2.3.2.1. Impact breakage

When objects collide, breakage is, in most instances, imparted on either one of them, or on both. The degree to which a particle can resist damage is the particle's impact resistance. The impact test is used to estimate the amount of energy absorbed when particles fracture, or break, under the impact.

Impact testing is a means of assessing a particle's resistance to impact loading and is often referred to as material toughness. It is the amount of energy particles can absorb before breaking. In impact breakage testing, the impact energy is the kinetic energy of the mass upon impact. The energy input can be varied.

Fang *et al*, 2018 [17] identified that, with a decrease in the initial particle size or the impact velocity, the fragments particle size distribution becomes more distinct. The optimal impact velocity is achieved at minimum energy consumption per unit of product and that, for the smaller initial particle size, the lower the energy consumption per unit produced. [17]

2.3.2.2. High Pressure Compression

During high pressure compression, particles comminute in response to the pressure applied. The breakage energy required is a function of the particle strength. The mechanism of particle breakage differs for fine and coarse material, whereby the coarser material undergoes breakage in high pressure compression as a result of brittle behavior while the finer particles undergo a degree of plastic deformation which is the reason why increased or multiple stressing will be required.

In the paper 'Particle Breakage and Attrition', H.Kalman [29] identified that, in single particle compression breakage, the fracture behavior is dependent on the size and shape of the primary particle as well as on the loading conditions. The relation between the particle size and strength of the fine particles was also found to be similar to that of coarser particles. For particle beds, the percentage of broken particles is dependent on the compression load.

2.3.3. Factors affecting particle breakage

The mode of particle breakage is related to the type of fracture, which can be trans-granular or intergranular. Intergranular particle breakage does result in higher particle breakage when compared to trans-granular breakage.

For impact fracture, it has been observed that the pattern of particle impact breakage, in two-dimensional systems, is a result of two mechanisms, namely mechanism I and II. When a particle experiences impact, tensile stresses are generated along the radially outward projecting lines from the point of contact. Cracks will thus generate along these lines which are referred to as mechanism I breakage. This will be the dominant mode of breakage at the initial impact stage. Mechanism I thus accounts for the breakage, which is induced by the stresses, which appear in unbroken particles while mechanism II occurs as a result of mechanism I undergoing buckling [46] . This is depicted below:

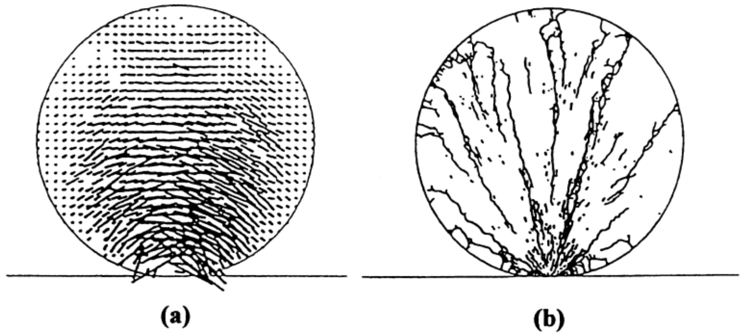

Figure 2-2: Figure (a) refers to mechanism I, figure (b) refers to mechanism II [46]

Before breakage is complete, cracks will form perpendicularly to the mechanism I cracks. The breakage, which occurs because of the buckling of mechanism I fragments is mechanism II breakage. No tensile stresses will appear in an unbroken particle in directions perpendicular to mechanism I cracks, the stresses that lead to mechanism II breakage probably only appear because of mechanism I breakage. The simulations show that the mechanism II breakage appears because of the buckling of the fragments remaining after the mechanism I breakage.

In high velocity impact, mechanism I stresses are higher and this makes mechanism I breakage more dominant, while at lower impact velocities mechanism II plays the dominant role in the particle breakage.

The characteristics of particle breakage depend on the physical properties of the material such as its shape and size. The breakage will thus be characterized by the fractional rate of particle breakage for each distinct size class and the average size distribution of the generated fragments from the breakage.

2.3.4. How material responds to breakage

Particle breakage is dependent on the particle's physical properties, such as the shape and size. The breakage process is characterized with the aid of two functions, namely the selection function and breakage function. The selection function represents the breakage rate of the particles while the breakage function gives the average size distribution of the fragments produced during primary breakage repetition [7]. The amount of breakage encountered is represented by the breakage index (t_{10}). This refers to the particles, in percent terms, passing a tenth of the original mean particle size. This function can be represented using the following equation [44]:

$$t_n = a \times \left[1 - e^{(-E_{cs} \times b)}\right] \quad \textit{Equation 6}$$

Where t_n = the breakage index (the progeny percent passing one 'n'th of the initial mean particle size)

'a' and 'b' = the ore impact breakage parameters.

E_{cs} = the specific comminution energy (kWh/t)

Where t_{10} is a breakage index defined as the progeny percent passing one tenth of the initial mean particle size.

The breakage function is a parameter, which is difficult to measure experimentally simply because it requires the fractured products to be observed after each impact during comminution. The breakage function also takes into account the effects of the particle size and shape.

In a particle breakage set-up, each fracture event, which takes place, contributes to subsequent breakage events. This is because the energy employed in the particle breakage causes primary fracture while the daughter fragments thus initiating their breakage behavior will absorb the residual energy available in the particle breakage event. This successive particle breakage occurs until all the energy in the drop weight has been dissipated. [30]

The successive particle breakage of the fragments means that the breakage function obtained from the test is a composite of several primary breakage functions. Thus, the primary breakage function is dependent on the initial particle size while subsequent breakage functions are a result of the primary breakage fragments. The breakage test "breakage function" is therefore a sum of the breakage functions generated during the breakage test. [30]

High pressure particle breakage affects the particle bonding behavior as pressure increases. At lower comminution pressure, a change in the particle morphology is experienced by the particles but this change to inter-particle attrition as the pressures increase, which is characteristic of the inter-particle bonding process. Excessively high pressure results in electrons obeying the uniform electron gas theorem. With electrons, their kinetic energy increases with a change in the density. This is what is experienced at high pressure, whereby the kinetic energy dominates. [52]

In comminution however, crack propagation facilitates the particle breakage thus leading to particle liberation. The behavior of silica in this test work will be of interest especially considering its brittle nature.

2.3.5. Other means to characterize the extent of particle breakage

The extent of particle breakage can be characterized in several ways. The ore subjected to breakage is composed of mineral grains, which exhibit a range of properties such as grain shape, Young's modulus and grain size. These properties, as well as the intergranular bond strength, can affect the way in which the ore breaks.

The mode of particle breakage contributes to the extent of particle breakage experienced. One of the internationally renowned mineral research centers is The Julius Kruttschnitt Mineral Research Centre (JKMRC) of the University of Queensland. Several breakage test devices for comminution research and commercial use have been developed at this center. Amongst these developments there is the twin pendulum by Narayanan in 1985 [43], the Drop Weight Tester (DWT) by Napier-Munn et al., 1996[42] and the two types of drop-weight testers, the larger drop weight for the breakage of basalt particles ranging in size 45mm and 8 mm and a smaller one for the breakage of particles ranging between 8mm and 2.8mm by Man, 2000[35]. These devices have been extensively used in particle breakage experiments and the quantification thereof.

Literature includes many referrals to breakage indices in describing particle breakage as an alternative to particle size distributions. The degree of fragmentation obtained during impact can be quantified by the mass ratio of the final particle size to the initial particle size [27]. This can also be referred to as the size reduction ratio of the particles. The use of criteria based on measurements of the specific surface area of the breakage product was done by Rizk et al., 1994 [47]. In this method the specific surface area is measured, or calculated, from the product material particle size distributions. In this instance the grindability index, is thus defined as the amount of surface area produced during the grinding process on a closely sized sample material [6]. This can also be analyzed in terms of the specific area generated in terms of the energy input in initiating the particle breakage.

Energy criteria have also been used as a means of characterizing particle breakage in energy-controlled conditions. The input energy in such applications is the particle's kinetic energy. In 1973, Rumpf et al., [48] proposed the use of the amount of energy, which is required to fragment 50% of the particles down to the required particle size. The amount of energy exerted on particles to induce breakage will determine the extent to which the breakage occurs. Depending on the degree of breakage required, the energy input into comminution equipment is controlled. Too little energy input can also result in no, or insufficient particle breakage, which is also undesirable.

2.4. Mineral testing methods

2.4.1. Drop weight test

The drop weight tester was developed to quantify the fracture response of an ore to the energy spectra. Initially the aim of these tests was to establish a relationship between the probability of a fracture occurring and the related energy input. However, in recent years, drop weight tests have been useful in addressing the progeny distribution from a fracture event.

The JKMRC drop weight test was developed to determine the input energy for particle breakage when a steel disk of known mass is dropped from a known height.

The drop weight test is used in applications for autogenous mill sizing when designing a grinding circuit or in order to perform sensitivity analyses on the operating parameters of a grinding circuit.

This test serves as a simplest way in which the behavior of the material's breakage characteristics can be investigated. Through experiments, larger particles have been found to be weaker per unit mass when compared to smaller particles. Based on the particle size, different particle strengths are present such that, as the striker impacts the particle, it can break some of the particles while some are left unbroken. The relative strength required to break smaller particles is normally higher than that required for the larger particles.

In impact induced breakage, the mass of the particles impacted, as well as the pressure applied, is not known because it is not evenly spread. In this case, only the energy of the impact is known. As a result, the particle breakage is to be correlated to the input energy and not the grinding pressure.

Literature has suggested and experimental work has demonstrated that, based on the same input energy, particle strength is related to their size, where larger particles are generally weaker than the smaller particles. This is what sparked the interest in the JKMRC drop weight test. The test involved fixing the drop weight energy input and breaking the particles of a specific group (based on size) one at a time. The larger sized particle group was broken until a size group was introduced whereby some of the particles could not be broken. (i.e. the same weight of material was involved but the diminishing particle sizes reduced the contributory effects of cracks and other comminution facilitators).What this indicated was that the size group was too strong for the set energy levels, thus a higher energy level was needed. In so doing, the minimum energy required to break the particles of a particular size when the number of impact attempts is thirty was established.

In this test, a weight is lifted to a particular height and released to fall onto an ore particle situated on an anvil underneath. The breakage product from this test is collected and analyzed to determine the product size distribution. Several drop weight breakage tests have been conceived with the Julius Kruttschnitt Mineral Research Centre (JKMRC) drop weight test being the most well known. This drop weight test was developed at the JKMRC in order to measure the breakage parameters of a test sample.

In drop weight tests, the impact level and the amount of comminution energy can be obtained through varying the drop weight, the falling height, or the ore fragment mass. The energy provided can thus be described by the potential energy (in J/kg) of the drop weight at the initial height:

$$E = m_{dw} \cdot g \cdot h$$

Equation 7

Where E = potential energy (J/kg)

m_{dw} = mass of the drop weight (kg)

g = gravitational acceleration (9.81 m/s^2)

h = distance (meters) between the drop weight and the top of the specimen.

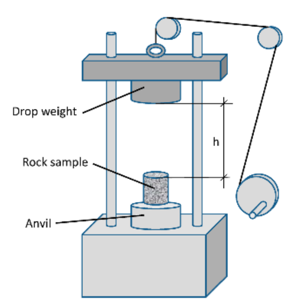

Figure 2-3: Drop weight test

2.4.2. Instrumented Drop Weight Test

This is an extension of the drop weight test by adding instrumentation for measurements during the test. An example of this instrumented drop weight test is the Ultra-fast load cell device (UFLC) developed at the University of Utah [54] as depicted below:

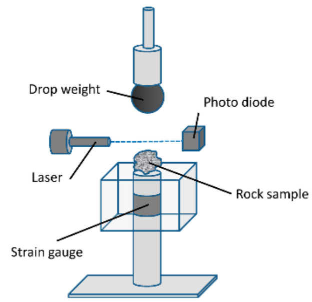

Figure 2-4: Instrumented drop weight test

In this test, a particle or bed of particles is placed on a vertical steel bar where it is impacted by the falling mass. The steel bar has a pair of strain gauges, which detect impact waves which allow the determination of the actual load applied to the sample. Unlike in the conventional drop weight test, here the actual energy transferred is determined by using the load-time profiles and the calculated test sample deformation/breakage.

A portable impact load cell, using the same principles as in the Ultra-fast load cell, has been developed by Bourgeois et al. [9] for in situ quantification of ore breakage properties. The so-called SILC—Short Impact Load Cell—is reduced in height and weighs only 30 kg.

2.4.3. Pendulum

A pendulum was initially proposed for the test work, but is considered to have a number of disadvantages. As a result, a more flexible and easier to use type of equipment was developed which was known as the “drop weight test”. The JK Drop Weight Test was developed by Julius Kruttschnitt Mineral Research Centre (JKMRC) lab in 1992 in order to determine the breakage characteristics behaviour of an ore in a SAG (Semi Autogenous Grinding) and AG (Autogenous Grinding) mill. The drop weight test measures the impact resistance of a sample. Dr Bwalya at the University of the Witwatersrand [13] developed a simplified drop weight machine. This equipment was designed and developed in order to quantify material fracture responses taking energy input into account.

During the 1980s – 1990, a lot of research went into development of various types of impact tests worldwide. Attempts were mainly to develop different size and shapes of specimen as well as the testers. The specimen was then subject to impact loading in the form of tensile, compression, torsion and impact loading.

The pendulum impact test is used to measure the susceptibility of a specimen to a pendulum-type impact load. In this test, the energy required for specimen breakage is the sum of energy needed to deform it, to initiate fracture, to propagate the fracture and the energy expended in "tossing" the broken particles [22].

The pendulum test is an alternative to the drop weight test with different types of pendulum tests being used for single particle testing. The most popular configuration is one standardized by Fred Bond, which was used to determine the resistance of rock to crushing. In this set-up, two pendulum hammers are dropped from 10 degrees on each side of the particle, which is mounted on a pedestal. The procedure is repeated until the particle breaks. When lifting only one pendulum and mounting the particle on the other one, you allow for determining the energy transferred to the sample by evaluating the rebound movements of the two pendulums after collision. The advantage of the pendulum testing over the drop weight is the potential to measure that fraction of the energy that is absorbed by the particle through measuring the residual energy of the strikers. [53]

2.4.4. Bond Twin Pendulum Tests

In this test, a single particle is fractured between two pendulums, which are released from a predetermined height as per the figure below:

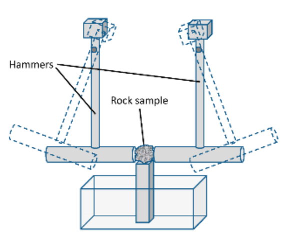

Figure 2-5: Bond twin pendulum test

The hammers hit the particle simultaneously and this process is repeated until the particle breaks. This test has been extended by Narayanan [43] [55] through the addition of instrumentation to allow for recording of the pendulum motion. The energy transferred to the sample can be done by mounting the particle onto one pendulum and evaluating the post collision rebound movements of the pendulums

2.4.5. Split Hopkinson Pressure bar test

This test was initially used when testing the material stress propagation from explosives. This test has subsequently also been used for fracturing a particle between two horizontal steel bars, the incident bar and the transmitted bar as depicted below;

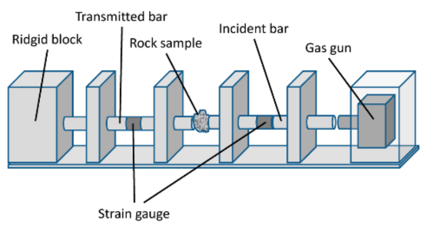

Figure 2-6: Split Hopkinson pressure bar test

2.4.6. Rotary single impact tester

During single impact tests, stress applied to the particle results from collision with a single impact surface, which can be achieved by accelerating the particle towards the plate (usually facilitated by gravitational forces). The rotary impact tester can be seen below:

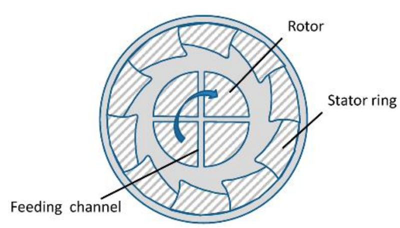

Figure 2-7: Rotary single impact test

Particles are fed into the impact chamber by the centrifugal action of the revolving rotor. The stator has a saw-tooth profile, which allows for perpendicular particle impact, enabling more particles to be tested within a given time.

From the tests mentioned above it can be noted that particle breakage tests rely a lot on the impact stresses for breakage and the repeatability is often affected by the sample characteristics and not the test method itself.

2.4.7. High Pressure Compression

During comminution processes, particle breakage is obtained because of particle-particle and particle-equipment interactions. This process is related to the particle properties as well as the loading applied to it. In the event where compression is taking place and in the event whereby the stored strain energy in the particle is not enough to generate the development of a new surface, a degree of crack growth could then emerge.

Looking at the work done by L.Wang, et al [54], it could be noted that, during high pressure compression loading, using X-ray computed tomography and digital image correlation, it was identified that crack development takes place until the high pressure loading is applied to 76% of the particle. Until then the crushing force is inadequate because of the absence of enough strain energy to generate a new surface. Thus having enough strain energy allows the conversion of crack propagation into new surface once the crack has developed. This mechanism could be expected in the drop weight impact test. However, in the drop weight impact test, the particles are not dimensionally constrained and energy leakage into the environment potentially exists.

The late Professor Schönert first developed high Pressure Grinding technology in 1985. Schönert undertook extensive research in single particle breakage under compressive and impact loading. In 1988, he concluded that the highest particle breakage efficiency is obtained through slow compression of single particles. This was because when, looking at the breakage of particle beds, using a piston die press, he noted that confined particle bed breakage was less energy efficient in comparison to the single particle breakage, but was much more efficient than the tumbling mill grinding particle breakage [51]. This could be attributed to the energy distribution to the particles and the particle-particle interaction taking place, which is not the case for single particle breakage [1]. Particles stressing, under uniaxial loading conditions, will result in fragmentation thereof. This is a result of the tensile stresses, which form in all the directions normal to the uniaxial loading. Therefore, the uniaxial load provides the compressive stress, which, in turn, results in the emerging tensile stresses.

In this dissertation, we will look at drop weight impact test and high pressure compression.

2.5. Summary

Understanding the fracture of a single particle is a fundamental concept in size reduction because it provides a means to distinguish a material's fracture behavior based on the comminution equipment employed. Particle fracture occurs as a result of the applied force.

Minerals' ability to withstand deformation talks to the material's toughness. Low material toughness can be attributed to the presence of micro and macro flaws in the material. When subjected to stress, the stress intensity of the flaw is expected to increase at the flaw tip or edge.

The random nature of particle fracture is unpredictable due to the different stresses the particle is subjected to during breakage. The particle strength is closely dependent on the particle size. This is because of the greater presence of impurities and micro-cracks, present in larger particles, as compared to smaller particles, and the size and amount thereof, which can vary.

The particle breakage mechanisms differ and will facilitate the breakage phenomenon differently. This is why particle breakage, in impact, differs from that in high pressure compression. In both of these breakage mechanisms, the energy absorbed, crack propagation and stresses induced upon the particles, vary. In the compression, derived energy input into the system for particle breakage will get used for the different aspects of the breakage process. Some of the energy will be utilized to initiate crack propagation, some to facilitate breakage of the daughter particles and some will be lost to the system. The particle breakage obtained from an impact or compression test is a result of the energy input enabling the particle breakage to take place to a particular extent.

An important experiment consideration is that some of the energy employed in unrestricted drop weight tests can be lost to the environment whereas compression tests take place in a constrained environment suggesting that more of the otherwise "leaked" energy can be employed in further particle comminution.

3. Experimental set-up and procedure

3.1. Drop Weight Impact Test

In a drop weight impact test, the impact energy imparted on the particle is kinetic energy. The energy which the particle absorbs is the impact energy. In this research, the drop weight impact was imparted on single particles of different size as well as on single particle layers of different sizes and the product distributions were obtained.

3.1.1. Material Preparation

Test sample of quartz obtained from the School of Chemical and Metallurgical Engineering comminution lab was used for the tests. The first step taken was to screen the quartz sample in the size ranges outlined below:

Table 3-1: Size ranges investigated

Class Number	Top size	Bottom size
1	31.50	26.50
2	26.50	19.00
3	19.00	16.00
4	16.00	13.20
5	13.20	9.50
6	9.50	6.70

The screened samples were to be subject to impact drop weight test for single particles as well as for single particle layer test.

3.1.2. Drop Weight Impact Test Experimental Conditions

3.1.2.1. Drop Weight test-work 1 – Particle Layer Drop Test

For this test, the particles were placed in a single layer on a 120mm diameter anvil to cover the surface area. The particle layer was weighed for each size class and arranged to cover the anvil for each particle size. The particles were subjected to a single impact from a fixed drop weight of 2.64kg from an initial drop height of 0.94 meters.

The particle layer masses subject to the impact were as follows:

Table 3-2: Particle layer impact test

Class Number	Top size	Bottom size	Particle Layer Mass (g)
1	31.50	26.50	96.38
2	26.50	19.00	99.88
3	19.00	16.00	103.35
4	16.00	13.20	102.70
5	13.20	9.50	99.94
6	9.50	6.70	60.95

This process was carried out separately for all the size classes and the fragments from each of the impact tests were collected for screening.

3.1.2.2. Drop Weight test-work 2 – Single Particle Drop Test

For this test, 10 particles from each size class were placed on the anvil, one at a time, and subjected to the drop weight impact. Each particle was impacted once then the fragments from each impact were collected. The fragments obtained from the 10 particles from each size class were then collected and combined for screening. This test was conducted from a fixed drop weight energy input of 2.64kg from an initial drop height of 0.94 meters.

3.1.2.3. Drop Weight test-work 3 – Particle Layer and Single Particle Drop Test at drop height 2

Drop Weight Test 1 and 2 were in this instance conducted for two size classes from a fixed initial drop height of 0.62 meters. The size classes subject to this impact breakage were the -19+16mm and the -13.2+9.50mm.

Table 3-3: Summary of the drop weight tests to be conducted

Particle size (mm)	1 Particle at 0.94m	1 Particle layer at 0.94m	1 Particle at 0.62m	1 Particle layer at 0.62m
-31.50+26.50	X	X		
-26.60+19.00	X	X		
-19.00+16.00	X	X	X	X
-16.00+13.20	X	X		
-13.20+9.50	X	X	X	X
-9.50+6.70	X	X		

3.1.3. Drop Weight Testing

There are several methods of estimating the energy required for crushing ores. An apparatus was developed by Brown et al [11] which allows for the energy required during impact breakage to be determined. Here a rock is placed on a rigid base-plate and is then crushed by weights falling from pre-determined heights as illustrated below:

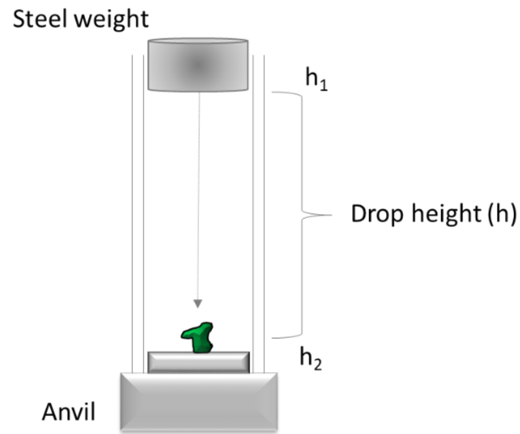

Figure 3-1: Drop weight test [13]

This is the drop weight test. The conditions set for this test include a weight mass while the drop height is also varied. The input energy mechanism for the drop test is illustrated in Figure 3-1: Drop weight test energy input, can be calculated by using the formula:

$$E = mg(h_1 - h_2) \qquad \textit{Equation 8}$$

Where: E = Input Energy (J)

m = mass of the steel weight (kg)

$h_1 - h_2$ = drop height (m)

g = gravitational acceleration (m/s^2)

The drop weight test serves as the simplest way in which the behavior of the material's breakage characteristics can be investigated. Through experiments, larger particles have been found to be weaker, per unit mass, when compared to smaller particles. Based on the particle size and orientation, different particle strengths are present such that, as the striker impacts the particle, it can break some of the particles while some are left unbroken.

The strength required to break smaller particles is normally higher than that required for the larger particles. Larger particles have more cracks and this is why they have lower strength as compared to smaller particles. In smaller particles, the diminishing presence of cracks and impurities has a smaller effect and thus do not play as large a role in weakening the particles.

In impact induced breakage, the mass of the particles impacted, as well as the individual pressure applied, is not known because it is not evenly spread. In this case only the energy of the impact is known. As a result, the particle breakage is to be correlated to the input energy and not the grinding pressure. Here particle breakage refers to the processes employed to reduce a particle size to a desired size suitable for subsequent processes or for mineral liberation purposes.

This experiment thus serves to indicate that a relationship exists between the energy input to yield fracture in 30 or less attempts, but it does not consider the effect of the number of impact attempts on the particle breakage.

The aim of this project is to evaluate the relative energy directed to comminution resulting from impact and high pressure compressive breakage. It is to investigate the conditions which affect this breakage and to determine the degree of the breakage.

3.1.4. Drop Weight Test Energy

For the drop weight test, a weight of 2.64kg was dropped for the tests at drop height 1 of 0.94m and at drop height 2 of 0.62m. From the drop weight test, the energy input can be calculated from each of the drop heights using the equation 7.

Therefore the energy at drop height 1 is 24.34 Joules while at drop height 2 it is 16.06 Joules. The impact velocity could also thus be calculated using the equation:

$$v = \sqrt{2gh} \qquad \textit{Equation 9}$$

Where v = impact velocity (m/s)

g = gravitational acceleration (m/s^2)

h = drop height (m)

Using equation 9, the impact velocity at drop height 1 and drop height 2 was calculated as 4.30m/s and 3.49m/s respectively.

3.2. High Pressure Compression Test

In the high pressure compression test, the particles are placed on the base of the test cylinder and these are then subjected to compressive forces from the plunger. In this test the particle is subject to compressive forces from the plunger and if there are multiple particles present in the test, these will be subject to interparticle compression.

3.2.1. Material Preparation

Test sample of quartz obtained from the School of Chemical and Metallurgical Engineering comminution lab was to be used for the tests. The sample was screened at the following screen sizes:

Table 3-4: High pressure test size classes

Class Number	Top size	Bottom size
1	31.50	26.50
2	26.50	19.00
3	19.00	16.00
4	16.00	13.20
5	13.20	9.50
6	9.50	6.70

The screened samples were to be used for the single layer and the three layer high pressure compression test.

3.2.2. High Pressure Compression Test Experimental Conditions

The test apparatus used is a plunger which allows for a steady compression action onto the particles situated in the 60mm diameter cylinder which is 75mm high. The setup was as follows:

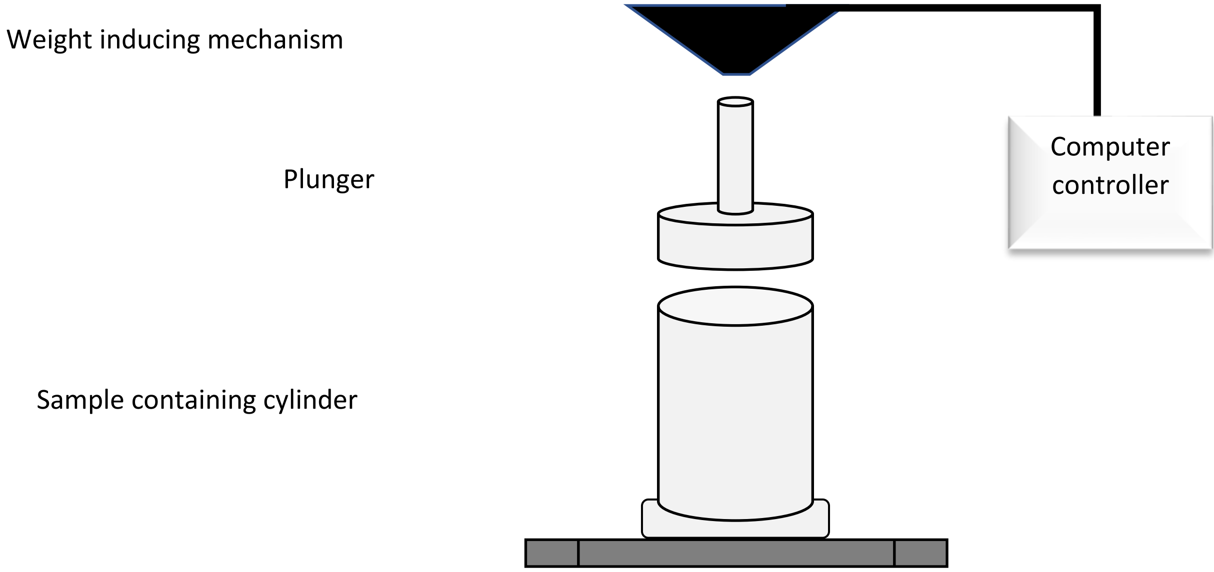

Figure 3-2: High Pressure compression test apparatus

The computer controller allows for the compression force and rate to be set. These include the pressure application speed and the maximum force to be applied. The computer controller will thus ensure that the load is applied so as to guarantee uniform stress application on the particles. The experimental conditions for the test were set such that the effect of force on the particle breakage can be noted and can be interpreted in terms of energy effects. The experiments were conducted at a maximum applied force of 50kN and 80kN. The force was applied at a plunger speed of 3mm/min at room temperature.

Table 3-5:50kN Compressive Force samples

Class Number	Top size	Bottom size	Single Layer Mass (g)	Three Layer Mass (g)
1	31.50	26.50	59.46	
2	26.50	19.00	60.87	
3	19.00	16.00	49.94	
4	16.00	13.20	45.42	89.64
5	13.20	9.50	37.61	70.73
6	9.50	6.70	25.71	55.70

Table 3-6:80kN Compressive Force samples

Class Number	Top size	Bottom size	Single Layer Mass (g)	Three Layer Mass (g)
4	16.00	13.20	38.71	121.77
5	13.20	9.50	39.69	60.40
6	9.50	6.70	20.64	48.03

At both the plunger force settings, the particles in a single layer and in a three layer configuration will be treated in size classes as follows:

Table 3-7: Summary of the High pressure compression tests to be conducted

Particle size (mm)	1 Layer at 50kN	3 Layer at 50kN	1 Layer at 80kN	3 Layer at 80kN
-31.50+26.50	X			
-26.60+19.00	X			
-19.00+16.00	X			
-16.00+13.20	X	X	X	X
-13.20+9.50	X	X	X	X
-9.50+6.70	X	X	X	X

Below kindly find a graph obtained from the high-pressure compression tests:

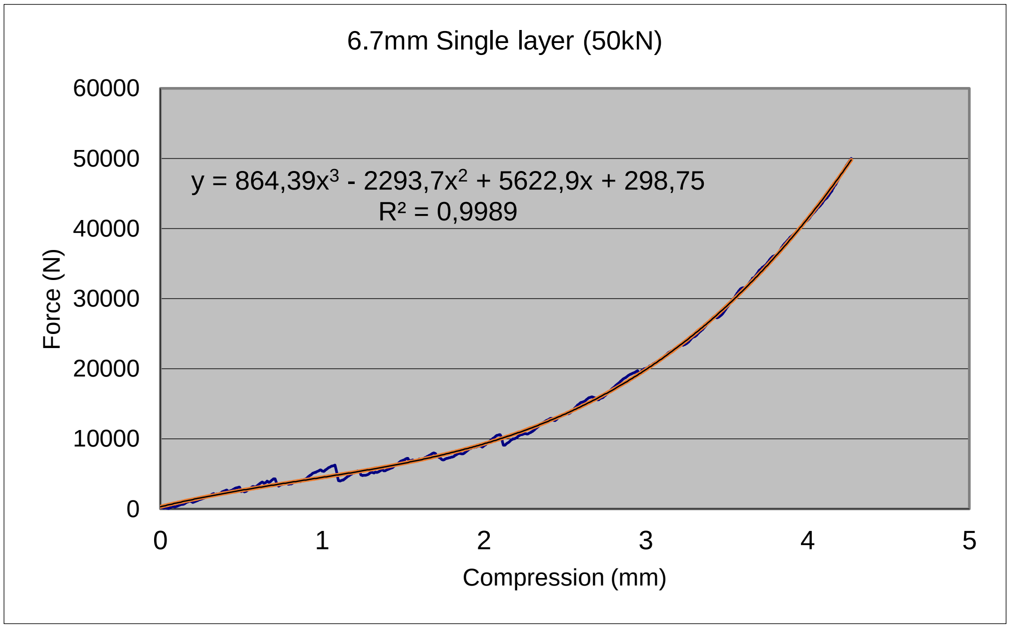

Figure 3-3: Compression test graphs used for energy calculation:

Using these graphs, the energy for each test was calculated by computation of the area under the curve.

3.2.3. High Pressure Compression Testing

The high pressure test is used to measure the effect of pressure on the particle size breakage. It is also used to serve as a comparison to the drop weight test. The high pressure test was used for single and multi-layered events in order to note the effect of the particle size and number of layers on the breakage phenomenon. The energy transmission was noted for both the single and multiple layer systems.

Compression tests are used to determine the behavior of material under compressive loading. Compressive high pressure tests are used in various industries to assess material strength, characterize materials' compressive properties as well as to assess product performance. Materials of different types behave differently to compressive forces, with some displaying a linear stress-strain relationship.

High pressure tests also serve as a means to also determine the behavior of ores to High Pressure Grinding Rolls (HPGR) in industry. HPGR have made an impact in the nonferrous minerals industry with the technology used as a primary milling alternative. This unit is most used for very hard and abrasive ores due to the magnitude of force it can impart on the particle to initiate breakage. HPGR gained great popularity based on the unit's ability to improve the overall comminution efficiency, the increased unit sizes and the reduction in the overall equipment maintenance due to the improved wear life

3.2.4. Particle bed configuration effect on particle breakage

Even as presented in a comminution unit, particles are arranged in a particular manner. In this respect it is essential that the effect of the particle loading on the crushing efficiency be noted in order to ensure that the unit's crushing ability is always optimized. Particle arrangements, as illustrated by K.Schönert, *et al* [18], can be classified as: single particle, one particle layer, closely or widely confined particle bed and an ideal particle bed. All of these confinements are very relevant to the particle crushing behavior in the HPGR because they all influence the stress distributions experienced. In this unit, the size reduction is demonstrated by the fraction of broken particles, the breakage function and the degree of particle surface increase. The energy transfer efficiency can, moreover, be determined by using the shape and packing density characteristics of the material.

High pressure tests are often referred to as compression tests. These are used to establish the response of a material to compressive force when it's subject to a force at a pre-set rate of application. In high pressure compression, the sample is usually compresses in the direction of the applied load and thus experiences expansion in the direction perpendicular to the force. In these tests, the response of material to compression, by measuring the strain, stress and deformation, can be determined. However, to some extent there will be the effect of constraint, by the particle holding vessel, which will retard the particle bed expansion.

The high compression test machines are configured to evaluate the ultimate compressive strength, yield strength, modulus and the deflection, which refers to the degree of deformation.

4. Overview of Results

The figure below gives an overview of all the experiments which have been conducted. The results are presented in the sections that follow:

Figure 4.1 provides an overview of the experiments conducted to evaluate the efficacy of impact and compression. The results obtained are presented in the sections that follow:

Figure 4-1: Sequence of Impact and Compression Tests Undertaken

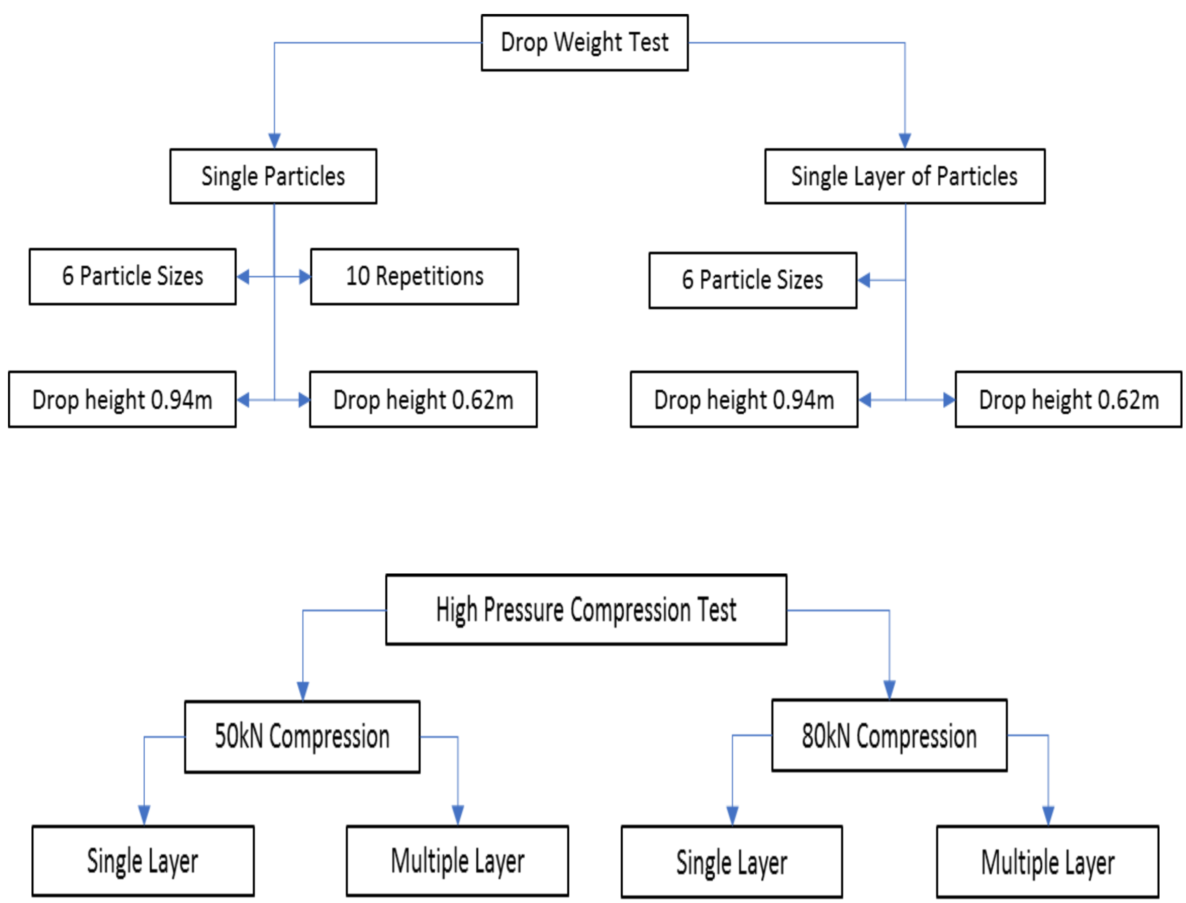

4.1. Drop weight Impact results

The mechanism employed in drop weight testing is described in section 3.1.3 and is illustrated in figure 3-1.

4.1.1. Single Particle at 24.34J of Applied Impact Energy

To each of the particles of different sizes, a fixed energy input of 24.34J was applied using one impact attempt per particle. The daughter particles, obtained from each attempt, were screened to determine particle size distribution.

The size distribution obtained for six initial particle sizes, broken individually, employing 24.34J of drop weight energy are shown in Figure 4-1 below:

Figure 4-2: Single particle impact test at 24.34J impact

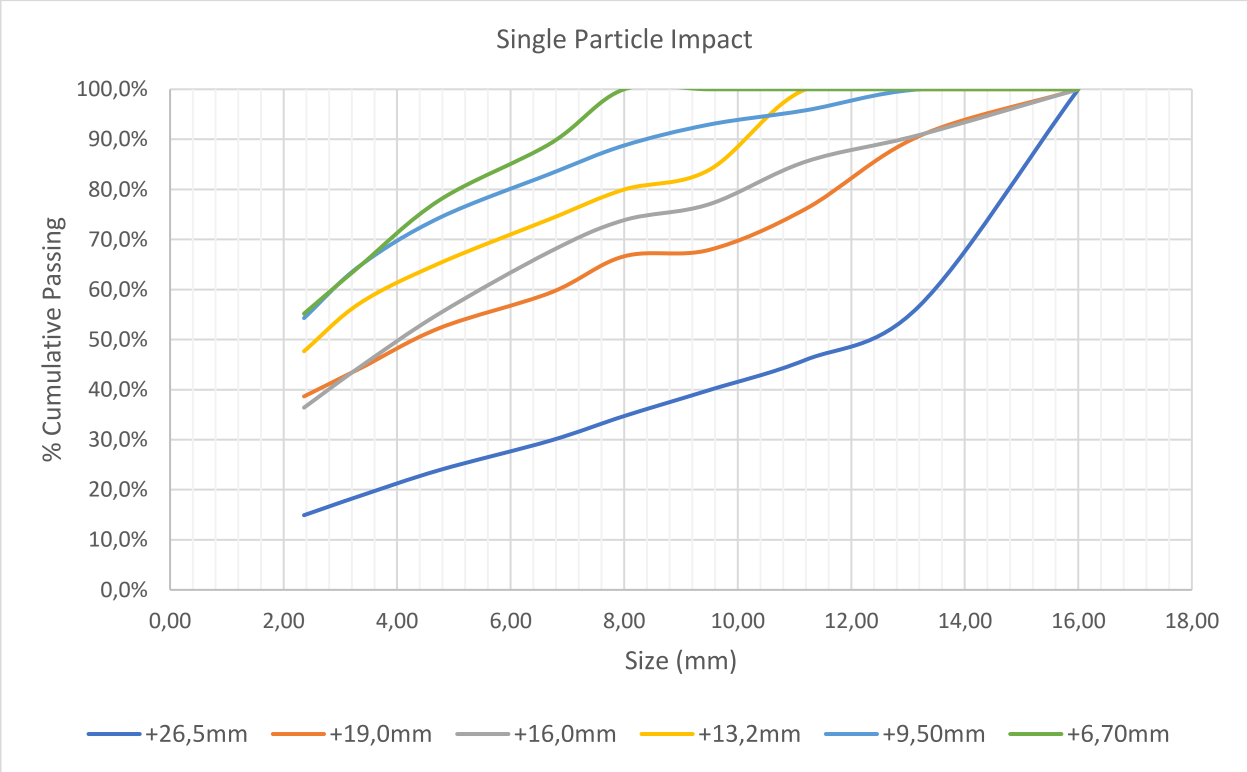

4.1.2. Single Particle at 16.06J of Applied Impact Energy

The same breakage test was conducted for single particles at 16.06J impact energy for the -19.0+16.0 mm and -13.2+9.50 mm size classes. These impact tests resulted in the product size distributions shown in Figure 4-2:

Figure 4-3: Single Particle Impact test result at 16.06J

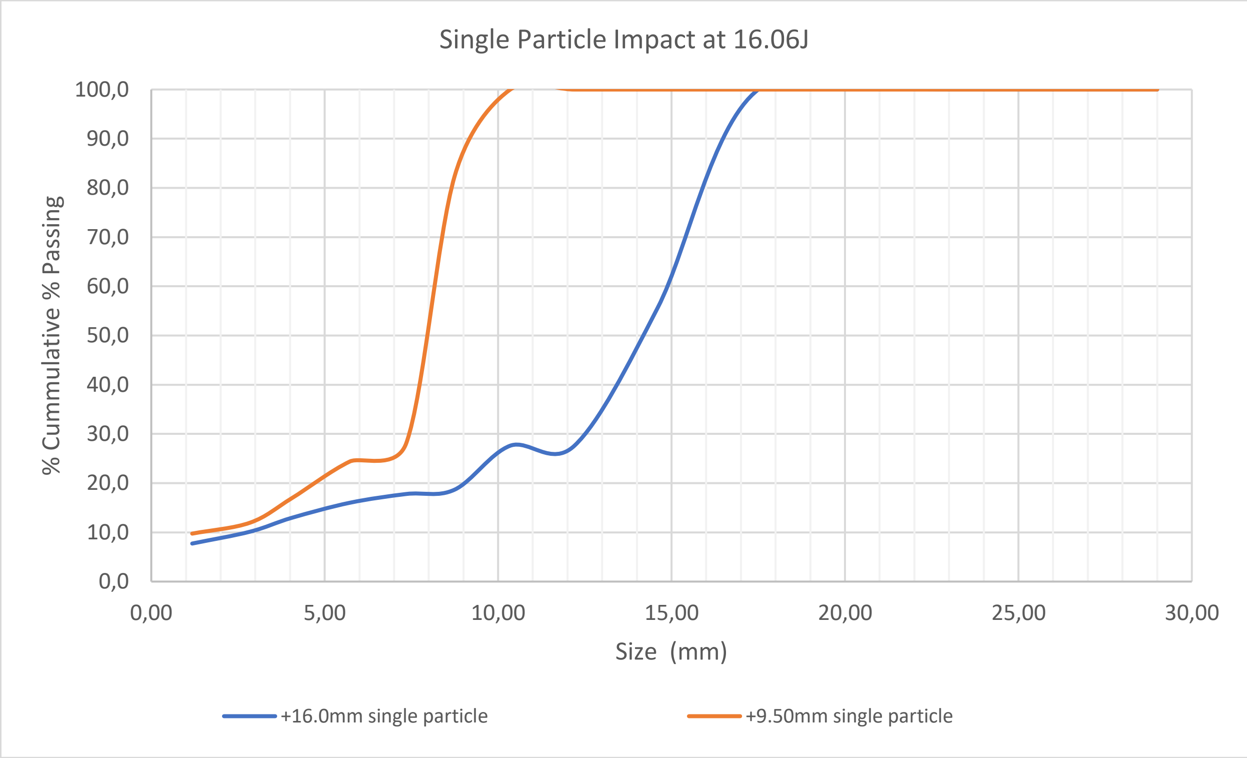

The normalized graphical representation is shown below:

Figure 4-4: Normalized Single Particle Impact test result at 16.06J

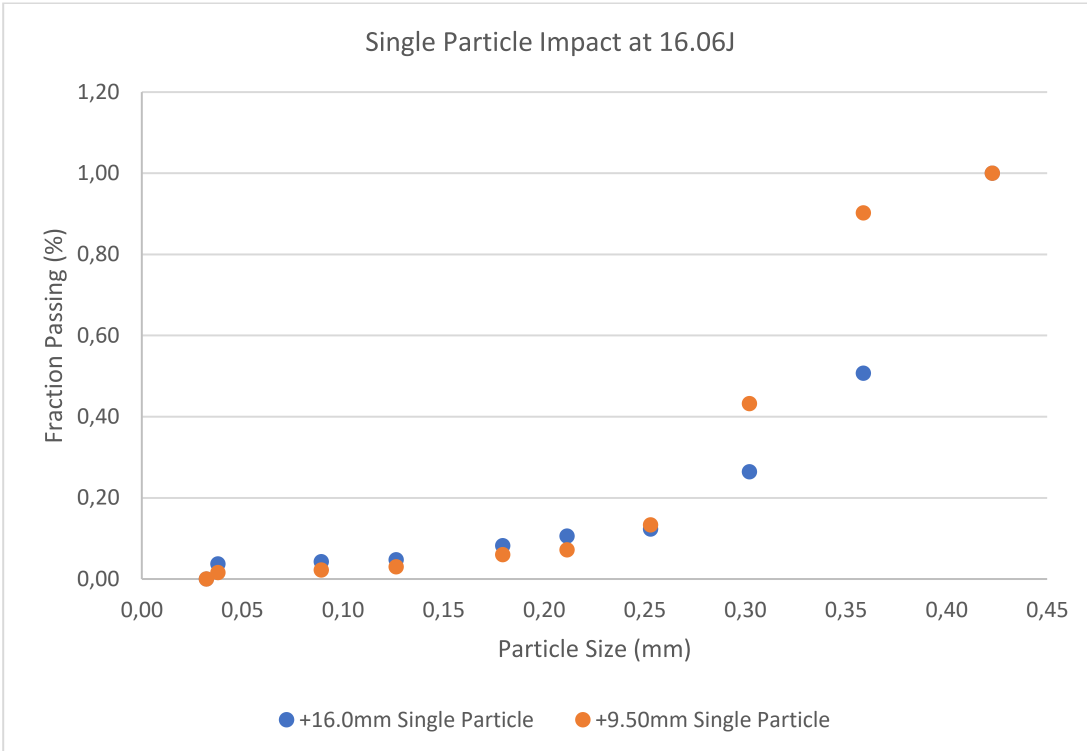

The above suggested that at 16.06J of impact, more particle breakage is obtained for the +9.50mm sized particle than for the +16.0mm size particle

4.1.3. Analysis of Single Particle at 24.34J of applied impact energy (Drop Weight)

The specific energy employed in each weight drop is a product of the input energy and the mass of the particle(s) employed:

Specific Energy Input (SI) = Input Energy (J) / Sample Mass (g)

The calculated specific energy employed for single particle impacted at 24.34J is detailed in Table 4-1 below.

Table 4-1 :Specific Energy Employed for Single Particles (24.34J)

Initial Particle Size (mm)	Input Energy (J)	Sample Mass (g)	Specific Input Energy (J/g)
+26.50	24.34	369.05	0.006596531
+19.00	24.34	151.04	0.016117913
+16.00	24.34	87.06	0.027962895
+13.20	24.34	44.27	0.054990956
+9.50	24.34	23.87	0.101987834
+6.70	24.34	8.68	0.280466544

The energy adsorbed by the particle is based on the size reduction achieved using the Bond formula that is formulated as follows:

Energy Adsorbed per gram (W) = (((10 x 14.05 (Wi)) *((1/square root Feed (Microns))-(1/square root Product (microns))) x 3.6

The W values obtained are recorded in Table 4.2:

Table 4-2: Energy Employed for the Comminution of Single Particles (24.34J)

Initial Particle Size (mm)	Feed (mm)	Feed (microns)	Product d80 (mm)	Product d80 (microns)	W (J/g)
+26.50	28.89	28892.04	14.80	14 800	1.181946
+19.00	22.44	22438.81	10.10	10 100	1.656303
+16.00	17.44	17435.60	6.00	6 000	2.699306
+13.20	14.53	14532.72	11.70	11 700	0.480414
+9.50	11.20	11198.21	8.00	8 000	0.875274
+6.70	7.98	7978.10	5.10	5 100	1.419843

The ratios of SI employed to computed W achieved are recorded in Table 4.3:

Ratio of Energy Applied to Energy employed (EP) = SI/W

The greater the EP value, the greater the energy required to effect comminution, as suggested in Table 4.3 the energy required to effect comminution increases with decreasing particle size.

Table 4-3: Ratio of Energy Applied (SI) to Energy Employed (W) in Comminution of Single Particles (24.34J)

Particle Size (mm)	**Ratio of Energy Employed to Energy Adsorbed**
+26.50	0,56
+19.00	0,97
+16.00	1,04
+13.20	11,45
+9.50	11,65
+6.70	19,75

The EP value trend, for single particles and 24.34J of energy input is shown graphically in Figure 4.5:

Figure 4-5:Relationship between energy applied and energy employed with 24.34J of impact on single particles

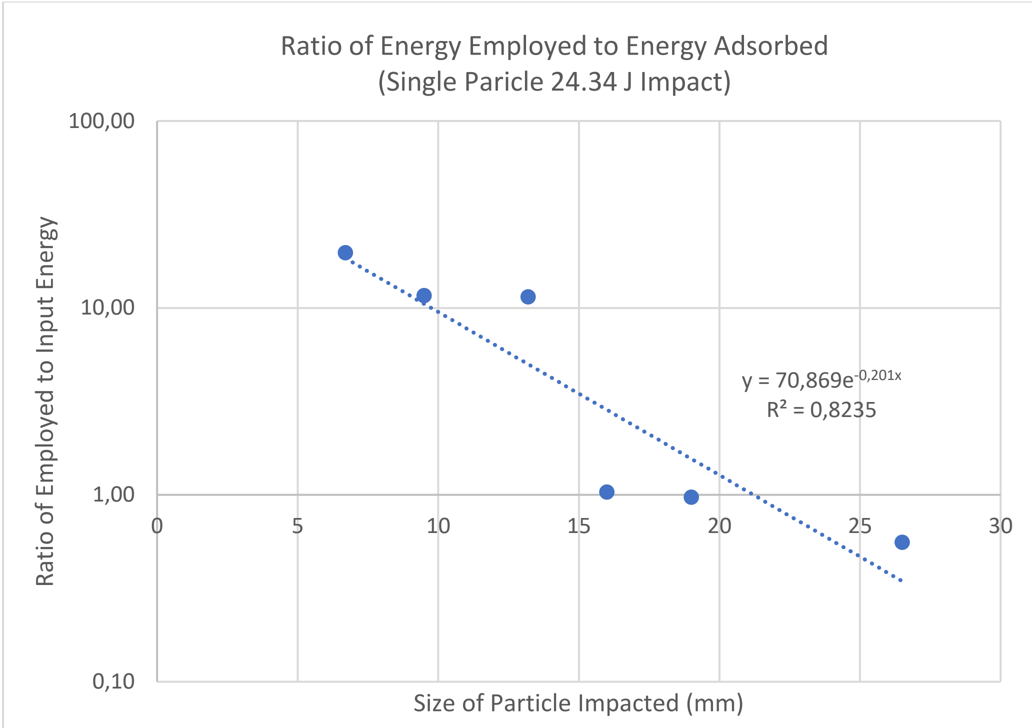

Ratio of Energy Employed to Energy Adsorbed
(Single Paricle 24.34 J Impact)
100,00
10,00
1,00
0,10
0
5
10
15
20
25
30
Ratio of Employed to Input Energy
Size of Particle Impacted (mm)
y = 70,869e-0,201x
R² = 0,8235

4.1.4. Analysis of Single Particle at 16.06J of applied impact energy (Drop Weight)

Reduction of the energy input, employing single particles, to 16.06 J produces SI values, for +16.00 and +9.50mm, as shown in table:

Table 4-4:Specific Energy Employed for Single Particles (16.06 J)

Initial Particle Size (mm)	Input Energy (J)	Sample Mass (g)	Specific Input Energy (J/g)
+16.0	16,06	83,90	0,191418355
+9,5	16,06	25,87	0,620796289

The energy employed in the comminution of single particles employing 16.06 J is detailed in table 4-5 below:

Table 4-5: Energy Employed for the Comminution of Single Particles (16.06 J):

Initial Particle Size (mm)	Feed (mm)	Feed (microns)	Product d80 (mm)	Product d80 (microns)	W (J/g)
+16.0	17,44	17435,60	15,90	15 900	0,180711
+9.50	11,20	11198,21	8,60	8 600	0,674440

The EP ratios for the 16.06J when applied to single particles are recorded in table 4-6:

Table 4-6: Ratio of Applied and Employed Energy in Comminution of Single Particle (16.06J)

Initial Particle Size (mm)	Ratio of Energy Employed to Energy Adsorbed
+16.0	0,94
+9,50	1,09

The EP results obtained for both the 24.34 and 16,06 J energy inputs suggest that there is a considerable increase in EP values when transiting from the lower to the higher energy inputs.

4.1.5. Single Particle Layer at 24.34J of Applied Impact Energy

A 24.34J impact energy input was applied to a particle layer of the same sized particles. The mass of the particle layers subject to the drop weight impact are recorded in Table 4-7:

Table 4-7:Details of impact energies on layers of segregated particle sizes

Class Number	Top size	Bottom size	Particle Layer Mass (g)
1	31.50	26.50	96.38
2	26.50	19.00	99.88
3	19.00	16.00	103.35
4	16.00	13.20	102.70
5	13.20	9.50	99.94
6	9.50	6.70	60.95

The particle size distribution results from the different test particle sizes are shown below for the single layer impact test:

Figure 4-6: Single Particle Layer Impact from 24.34J impact

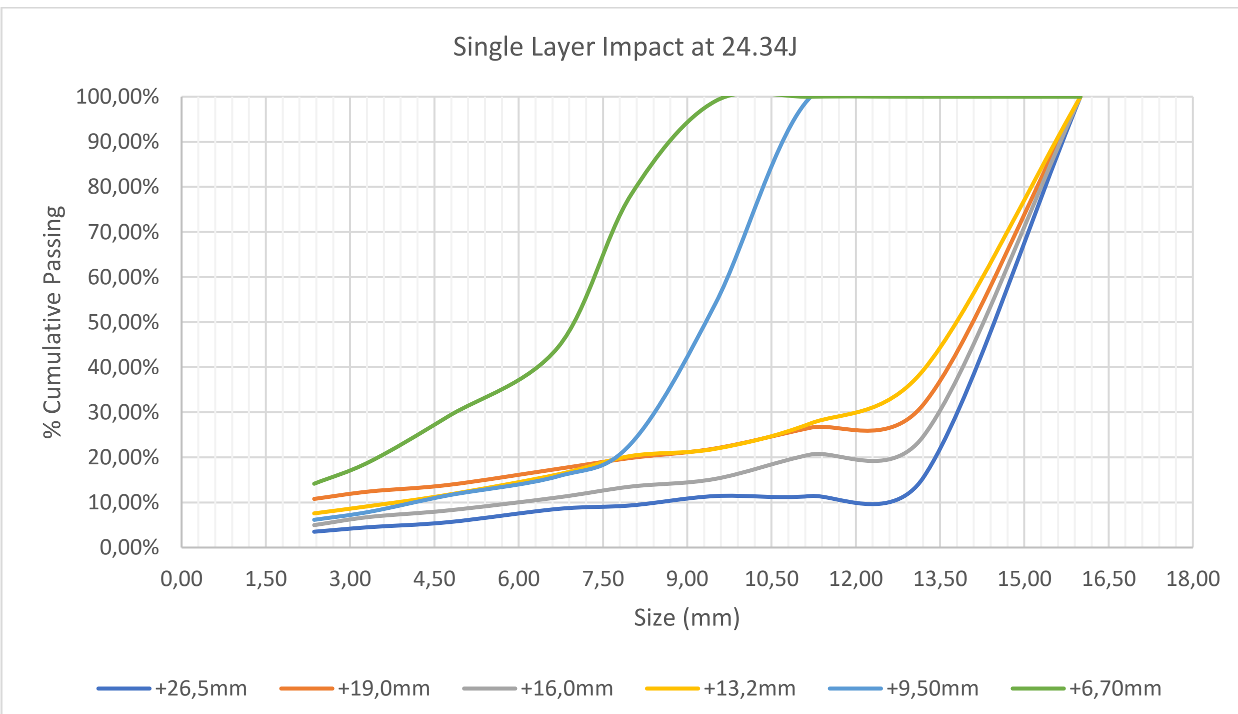

It can be noted from the above that the different particle size layers behave differently to the drop weight single particle impact test. These distributions differed even though the drop weight input energy was 24.34 J at an impact velocity of 4.30 m/s in each case.

4.1.6. Single Particle Layer at 16.06J of Applied Impact Energy

As the input energy height was decreased from 24.34J to 16.06J, the impact test was conducted on the -19.0+16.0 mm and -13.2+9.50 mm size classes. These impact tests resulted in the following:

Figure 4-7: Single layer impact at 16.06J

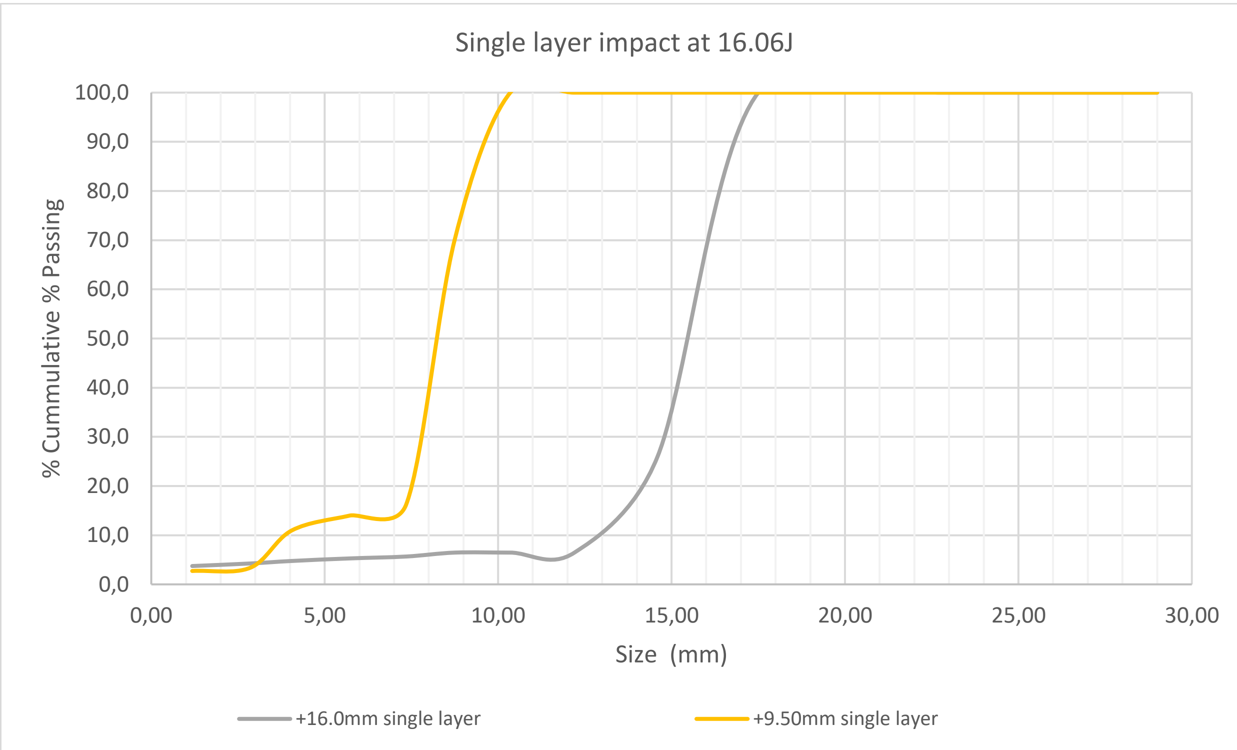

The graphical representation of the normalized data can be seen below:

Figure 4-8: Normalized Single layer impact at 16.06J

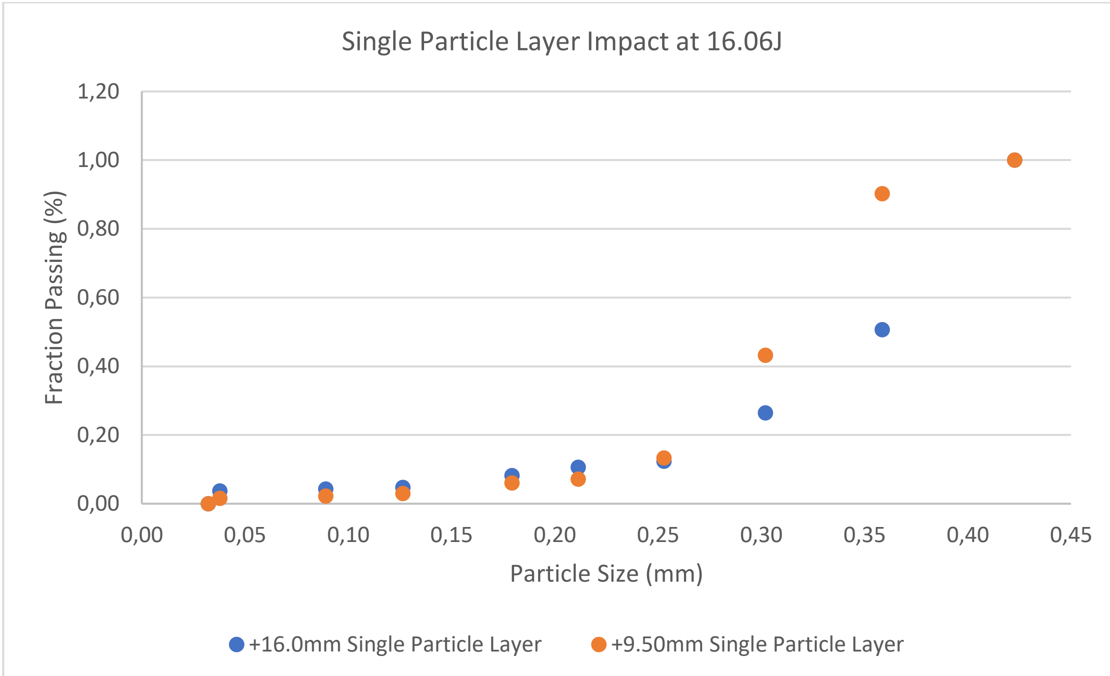

From the above it is indicated that at 16.06J impact energy, the particle breakage obtained is more extensive for the +9.50mm particle.

4.1.7. Analysis of Particle Layer at 24.34J of applied impact energy (Drop Weight)

The sequence of drop weight experiments was repeated, this time onto layers of a mono-sized particle, rather than particles broken individually.

The fixed energy input of 24.34J was applied to particle layers The values for energy absorbed are calculated using the same approach, the results are recorded in Table 4-8.

The resulting EP values are calculated for the data in Tables 4-8 and 4-9 and recorded in Table 4-10.

Again the trend in EP values confirms the increasing energy requirements with smaller particle sizes.

Table 4-8:Specific Energy Employed for Particle Layer (24.34J):

Initial Particle Size (mm)	Input Energy (J)	Sample Mass (g)	Specific Input Energy (J/g)
+26.5	24.34	95.5715	0.025472548
+19.0	24.34	99.035	0.024581709
+16.0	24.34	102.755	0.023691787
+13.2	24.34	100.865	0.024135722
+9.50	24.34	98.64	0.024680146
+6.70	24.34	59.06	0.041219939

The energy absorbed by each sized layer is computed as follows using the relationship determined for W above**.**

Table 4-9:Energy Employed for the Comminution of Particles Layer (24.34J)

Initial Particle Size (mm)	Feed (mm)	Feed (microns)	Product d80 (mm)	Product d80 (microns)	W (J/g)
+26.5	28.89	28892.04	13.90	13 900	1.314436
+19.0	22.44	22438.81	13.64	13 640	0.954240
+16.0	17.44	17435.60	13.80	13 800	0.475112
+13.2	14.53	14532.72	13.62	13 620	0.138305
+9.50	11.20	11198.21	11.03	11 030	0.036309
+6.70	7.98	7978.10	7.42	7 420	0.209102

Table 4-10:Ratio of Applied and Employed Energy in Comminution of Particle Layer (24.34J)

Particle Size (mm)	**Ratio of Energy Employed to Energy Adsorbed**
+26.5	0,19
+19.0	0,26
+16.0	0,50
+13.2	1,75
+9.50	6,80
+6.70	1,97

The relationship between EP and size employed in the particle layer is illustrated by Figure 4-9.

Figure 4-9:Relationship between Energy Applied and Energy Employed with 24.34J of Impact on Single Layer of Particles

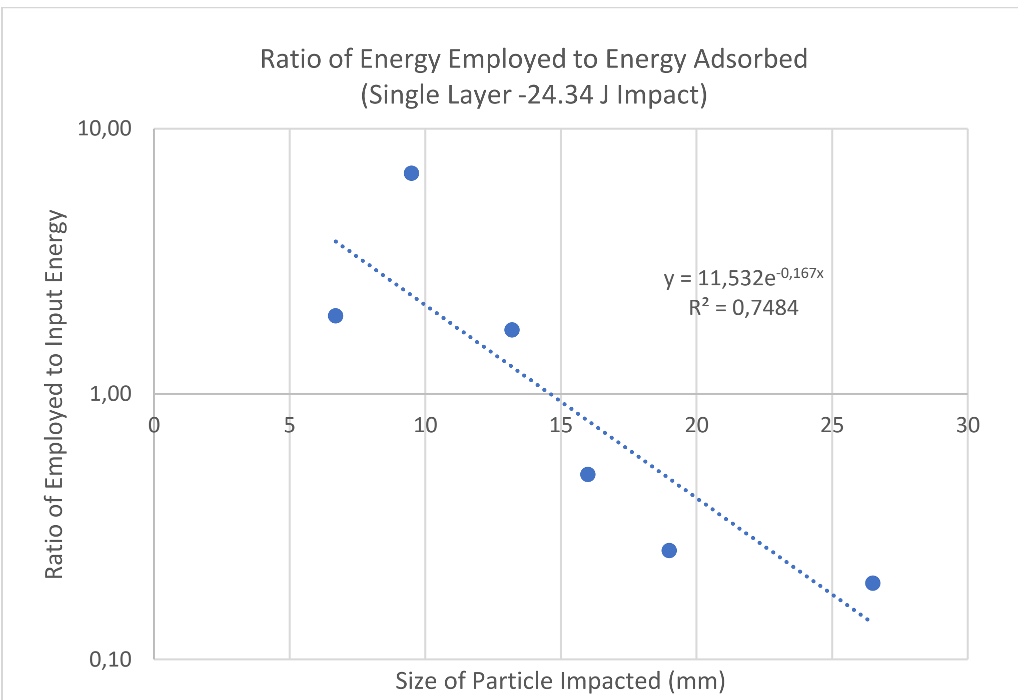

4.1.8. Analysis of Particle Layer at 16.06J of applied impact energy (Drop Weight)

The drop weight tests were repeated using layers of single size particles but, this time, employing only 16.06 J of drop weight energy.

The values obtained for SE, W and EP are recorded in Tables 4-11, 4-12 and 4-13.

Table 4-11:Specific Energy Employed for Particle Layer (16.06J)

Initial Particle Size (mm)	Input Energy (J)	Sample Mass (g)	Specific Input Energy (J/g)
+16.0	16,06	101,74	0,157853352
+9,5	16,06	92,46	0,173696734

Table 4-12:Energy Employed for the Comminution of Particles Layer (16.06J)

Initial Particle Size (mm)	Feed (mm)	Feed (microns)	Product d80 (mm)	Product d80 (microns)	W (J/g)
+16.0	17,44	17435,60	16,40	16 400,00	0,119091
+9.50	11,20	11198,21	9,20	9 200,00	0,493588

Table 4-13:Ratio of Applied and Employed Energy in Comminution of Particle Layer (16.06J)

Initial Particle Size (mm)	Ratio of Energy Employed to Energy Adsorbed
+16.0	0,75
+9,5	2,84

The EP values again support the additional energy required for finer particles.

The data obtained in the single and layer experiments employing 24.34J and 16.06J were employed in the derivation of algorithms. It is intended that the data provided by the algorithms removes some of the outliers (noise) resulting from experimental inaccuracies.

The results provided by the algorithms are recorded in Table 4-14 and are shown graphically in Figure 4-10.

Table 4-14: Comparison of EP Values for Single Particle and Particle Layer Responses to 24.3 J and 16.06 J Energy Inputs

Particle Size (mm)	**W/Input Energy Values (J/g)**			
	Single Particle Impact	**Single Particle Layer Impact**	**Single Particle Impact**	**Single Particle Layer Impact**
	24.34J	**24.34J**	**16.06J**	**16.06J**
5.00	25.94	5.00	1.19	9.04
10.00	9.50	2.17	1.07	3.53
15.00	3.48	0.94	0.96	1.38
20.00	1.27	0.41	0.86	0.54
25.00	0.47	0.18	0.77	0.21

Figure 4-10:Graphic Representation of Single and Layer Particles Impacted by 24.34 J and 16.06 J

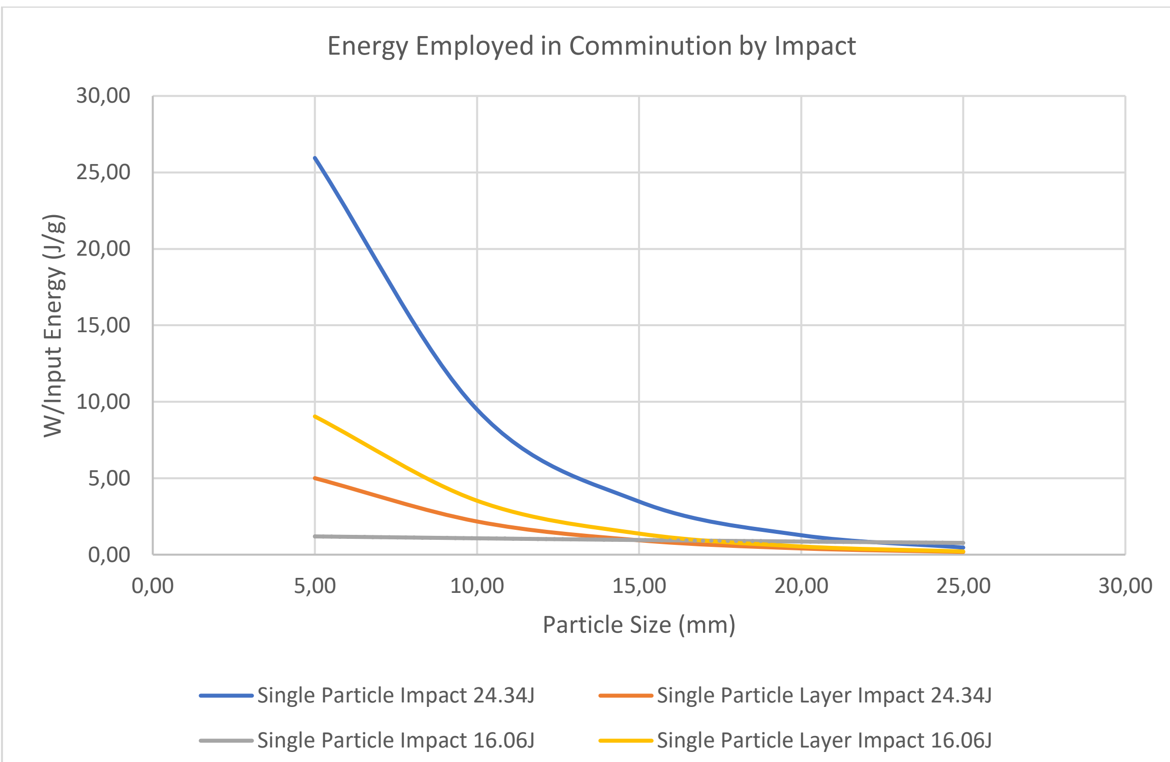

The results from the algorithms support the findings that the finer the particle, the more energy is required for comminution.

If the data obtained for impact on single particles at two energy levels is examined the relationships shown in Table 4-15 and Figure 4-11 can be established

Table 4-15:Size Reduction Accomplished on Single Particles using Two Level of Energy

Drop Weight - Single Particle at Two Energy Levels		
Particle Size (mm)	**D_{80} @ 24.34J (mm)**	**D_{80} @16.06J (mm)**
26,50	14,80	
19.00	10,10	
16.00	6,00	15,90
13,20	11,70	
9,50	8,00	8,60
6,70	5,10	

Figure 4-11:Graphic Representation of Size Reduction Accomplished on Single Particles using Two Levels of Energy

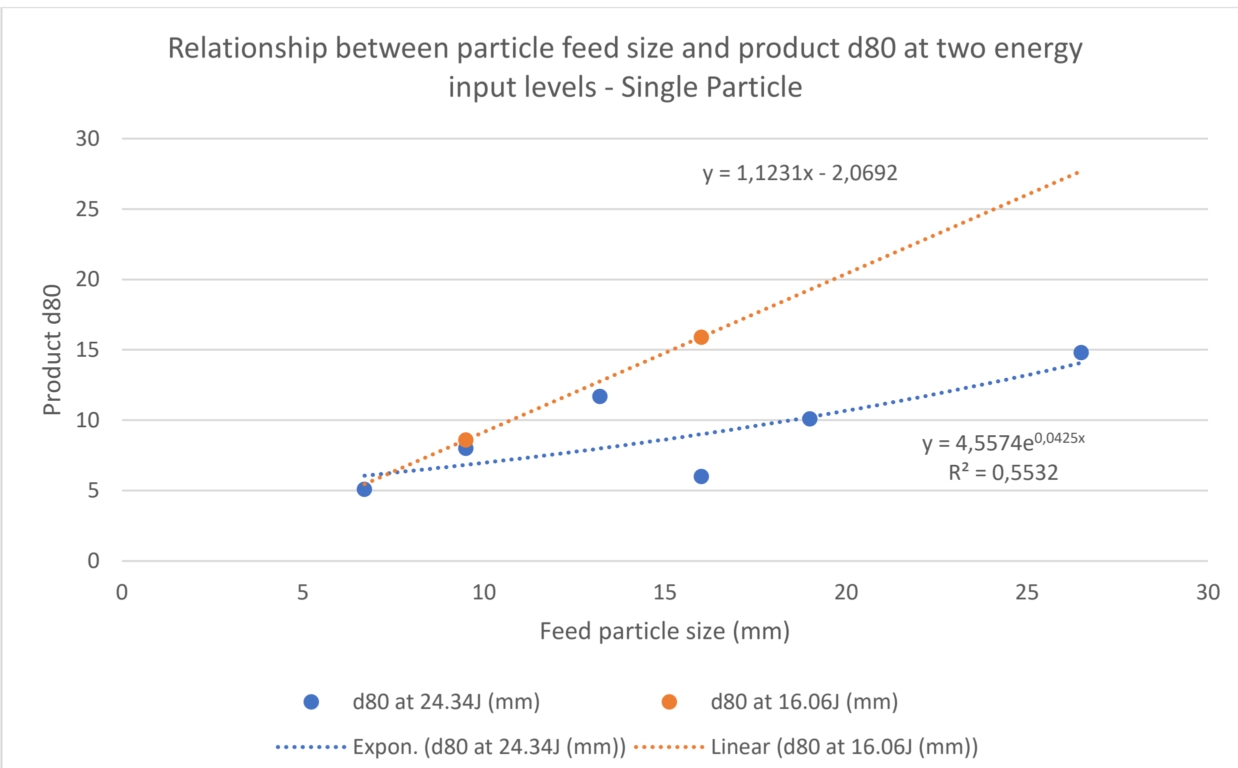

The situation can also be interpreted in terms of single particle and mono-size particle layers as shown in Figure 4-12.

Figure 4-12:Degree of Comminution of Single Particle Employing 24.34 J of Energy

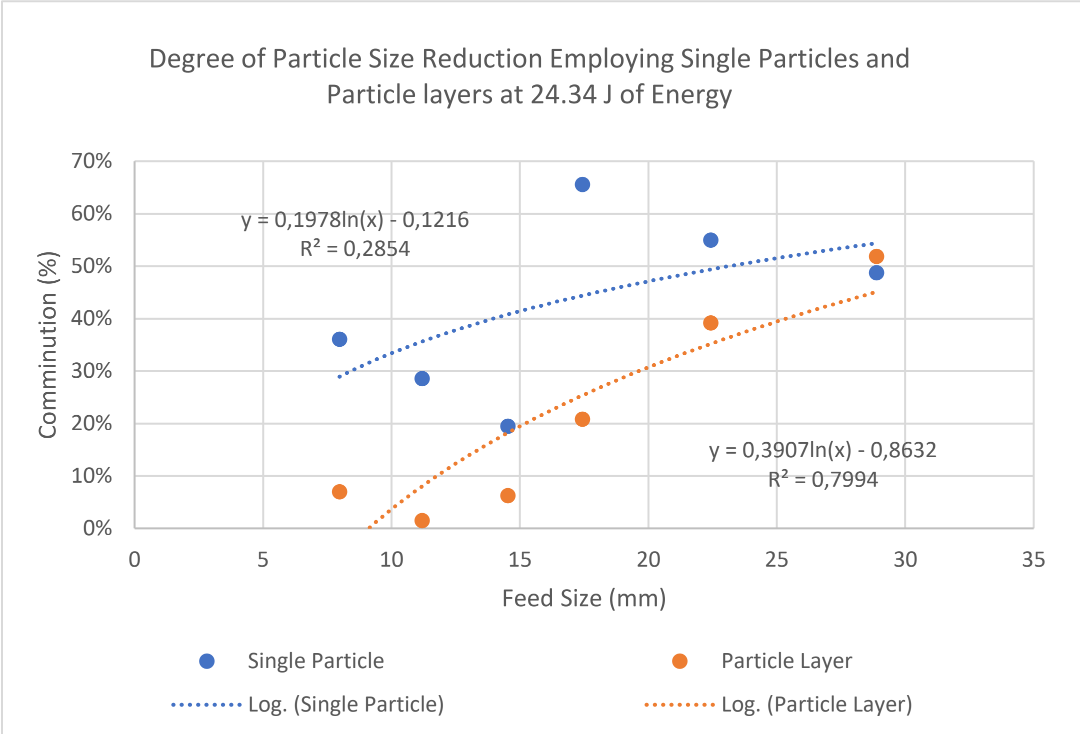

Comminution, which refers to the process of reducing material size to smaller particles or fragments can be seen in the figure above relative to the initial particle size. It can be seen that finer particle size or higher comminution is obtained for the single particle than for particle layer.

4.2. High Pressure Compression results

4.2.1. Single Particle Layer at 50kN of compressive force

During this test the single layer of each particle size of the masses shown below, were subject to a 50kN breakage force applied at a plunger speed of 3mm/min.

Table 4-16:Particle sizes and their masses employed in high pressure compression

Initial Particle Size (mm)	Sample Mass (g)
26.50	25,71
19.00	37,61
16.00	45,42
13.20	49,94
9.50	60,87
6.70	59,46

The fragments obtained from each test were screened for sizing. The following distribution was obtained:

Figure 4-13:Single layer 50kN applied force particle size distribution

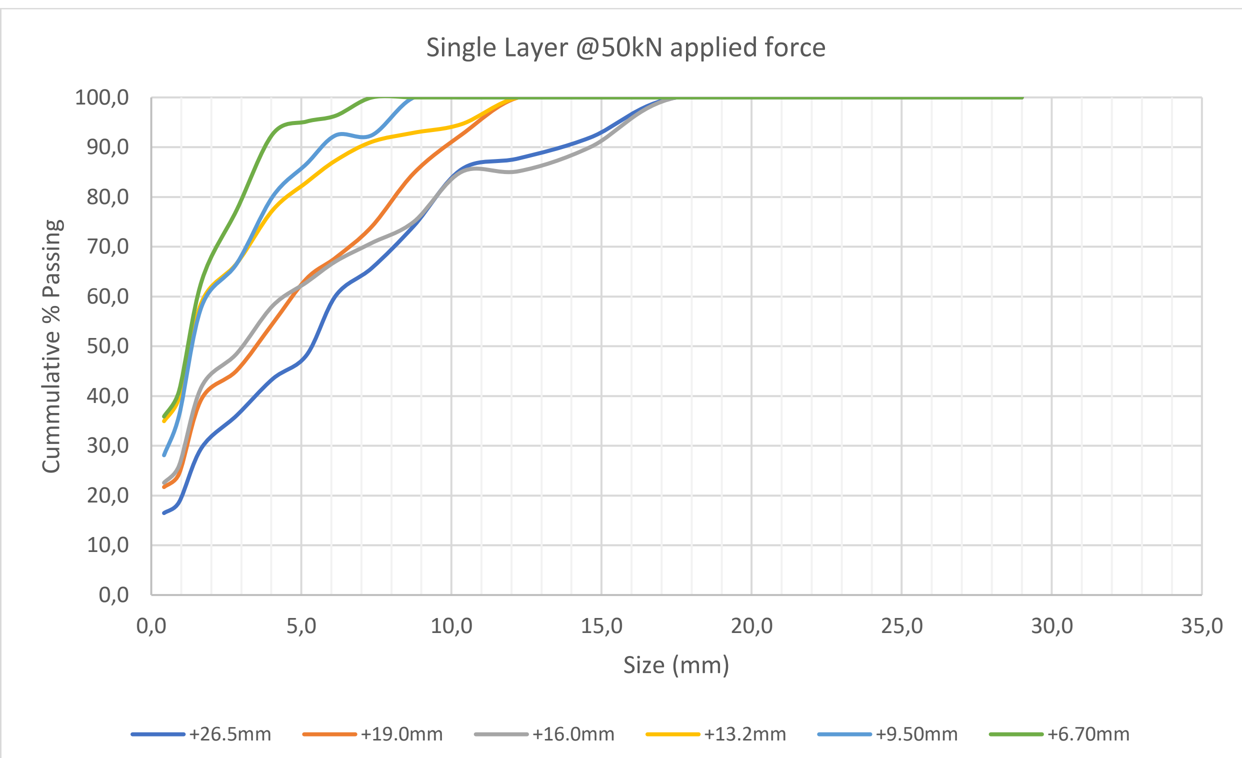

Below kindly see the single layer at 50kN compression normalized data:

Figure 4-14: Normalized data for 50kN single layer applied force

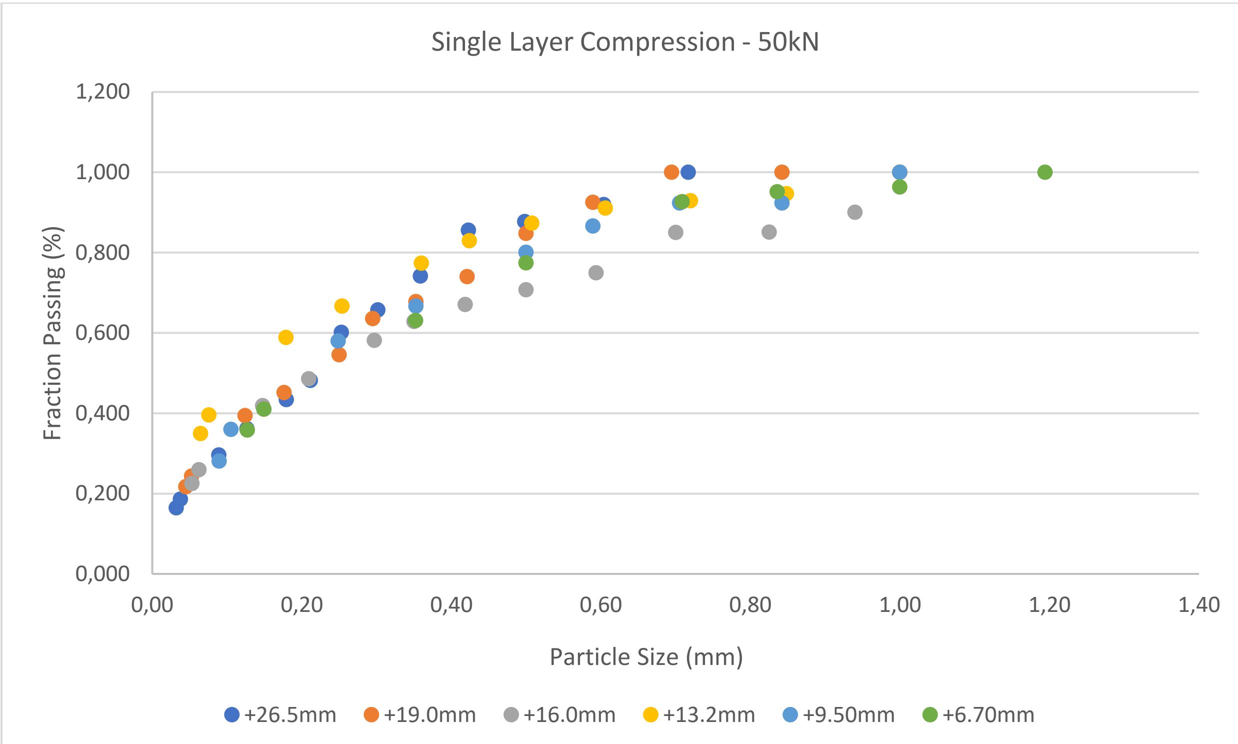

The single particle layer compression graph above indicates that the particle breakage the particles experience for a single particle layer at 50kN input force is similar for the different initial particle sizes.

4.2.2. Single Particle Layer at 80kN of compressive force

The applied force, or compression load, was then increased to 80kN at the application rate of 3mm/min. For the single layer test, the size classes considered were class 4 (-16.0 +13.20mm), 5 (-13.20 +9.50mm) and 6 (-9.50 +6.70mm). The sizing obtained from this test was as follows:

Figure 4-15:Single layer 80kN applied force particle size distribution

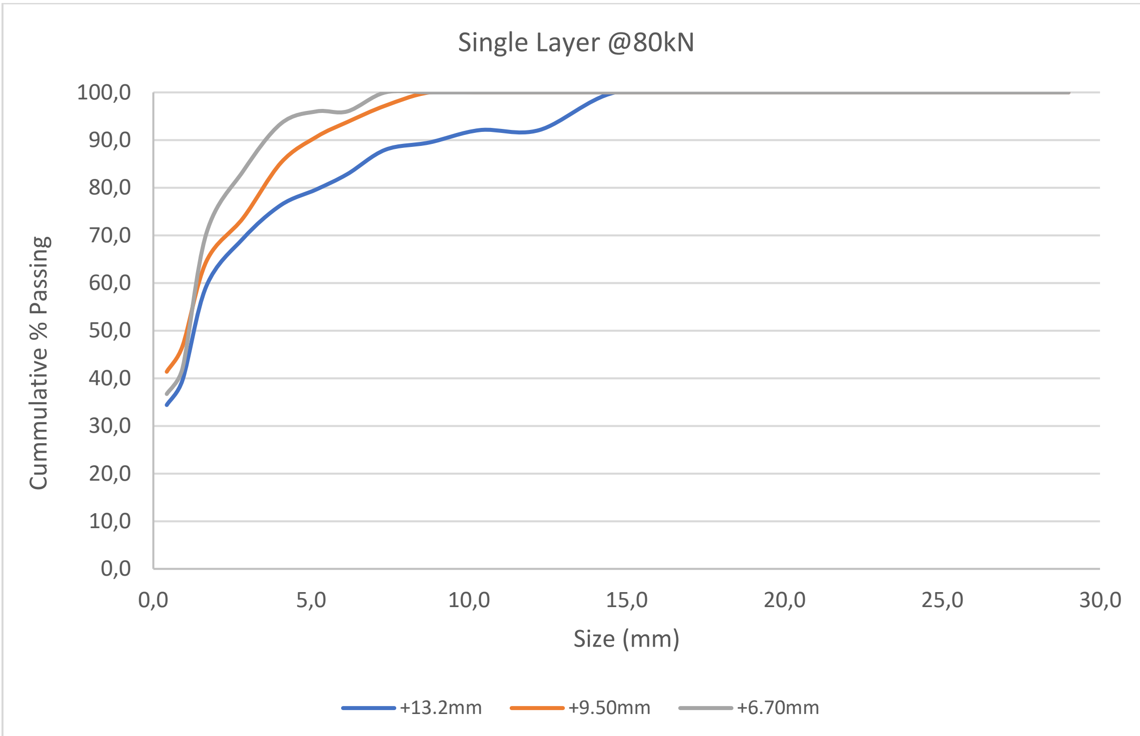

The single layer at 80kN indicates a similar characteristic behavior to what was obtained at 50kN. The smaller particles display greater particle breakage than the larger particles.

Figure 4-16: Normalized data for 80kN single layer applied force

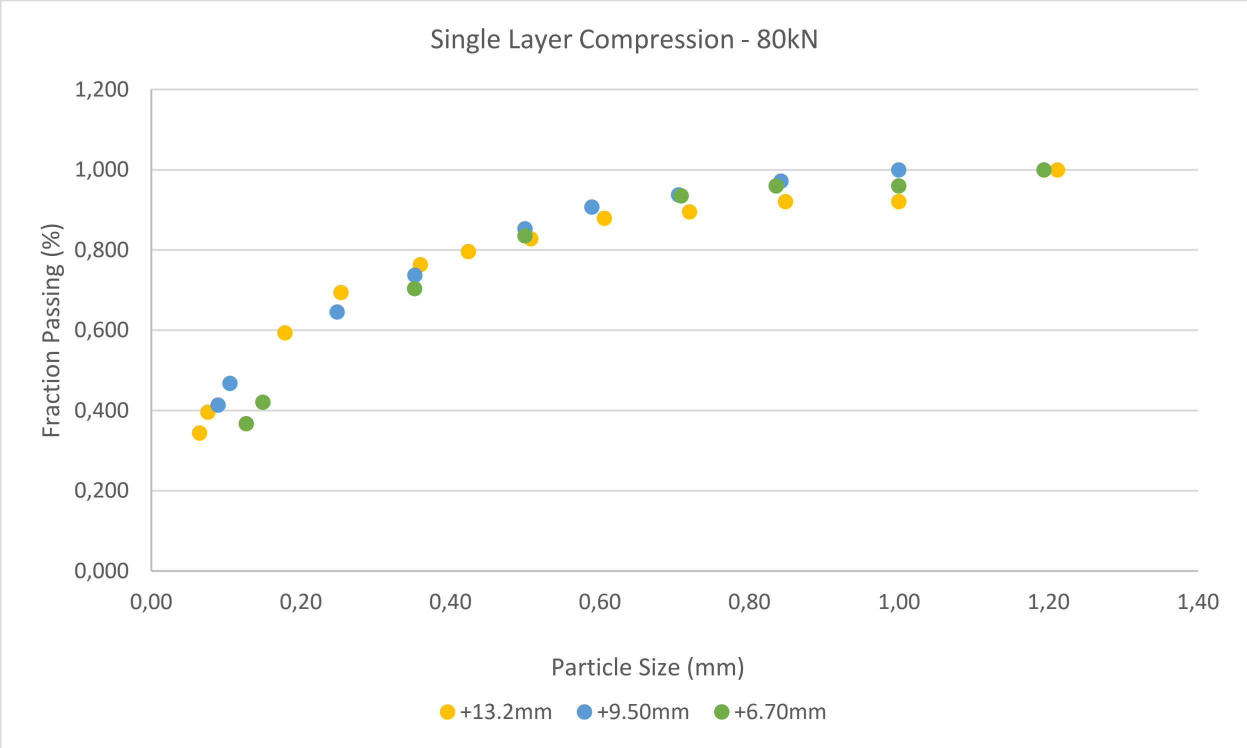

For the three-layer compression system at 80kN, we see a similar behavior for the +6.70mm and +9.50mm sized particles, while the +13.20mm sized particles suggest a different behavior.

4.2.3. Analysis of Single Particle Layer at 50kN compressive force (High Pressure Compression)

The specific energy employed in each compression force is a product of the input energy and the mass of the particle(s) employed:

Specific Energy Input (SI) = Input Energy (J) / Sample Mass (g)

The calculated specific energy employed for single particle layer compression at 50kN is detailed in the table below.

Table 4-17:Specific Energy Employed for Single Particle Layer (50kN)

Initial Particle Size (mm)	Input Energy (J)	Sample Mass (g)	Specific Input Energy (J/g)
26,50	97,35	59,46	1,637235
19,00	122,40	60,87	2,010843
16,00	101,91	49,94	2,040649
13,20	101,15	45,42	2,226993
9,50	72,48	37,61	1,927147
6,70	64,85	25,71	2,522365

The energy adsorbed by the particle layer is indicated in the table below:

Table 4-18: Energy Employed for the Comminution of Single Particle Layer (50kN)

Initial Particle Size (mm)	Feed (mm)	Feed (microns)	Product d80 (mm)	Product d80 (microns)	W (J/g)
+26.5	28,89	28892,04	10,30	10 300	2,0081
+19.0	22,44	22438,81	8,80	8 800	2,0153
+16.0	17,44	17435,60	10,10	10 100	1,2024
+13.2	14,53	14532,72	5,10	5 100	2,8869
+9.50	11,20	11198,21	4,70	4 700	2,5981
+6.70	7,98	7978,10	3,60	3 600	2,7672

The ratios of SI employed to computed W achieved are recorded in Table 4.19:

Ratio of Energy Applied to Energy employed (EP) = SI/W

The greater the EP value, the greater the energy required to effect comminution, as suggested in Table 4.19 the energy required to effect comminution increases with decreasing particle size.

Table 4-19: Ratio of Energy Applied (SI) to Energy Employed (W) in Comminution of Single Particle Layer (50kN)

Feed Size (mm)	Ratio of Energy Employed to Energy Adsorbed
26,50	0,8153
19,00	0,9978
16,00	1,6972
13,20	0,7714
9,50	0,7417
6,70	0,9115

The EP value trend, for single particles and 24.34J of energy input is shown graphically in Figure 4.17:

Figure 4-17:Relationship between energy applied and energy employed with 50kN compression on single particle layer

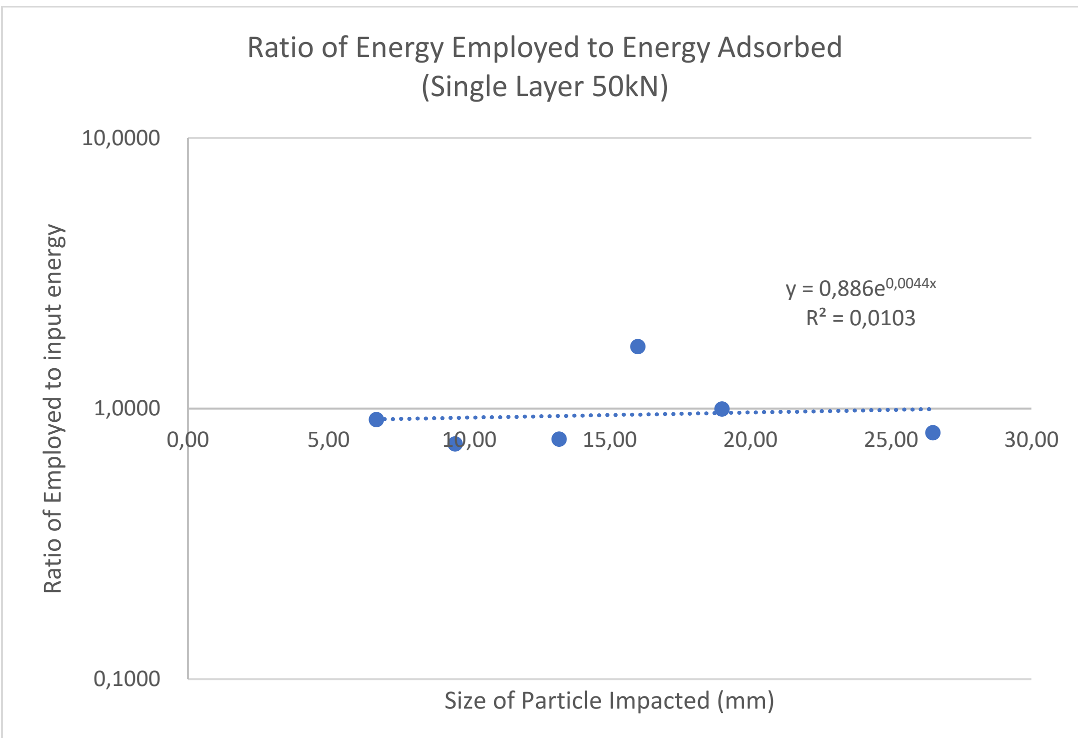

4.2.4. Analysis of Single Particle Layer at 80kN compressive force (High Pressure Compression)

The high pressure compression tests were repeated using layers of single size particles but, this time, employing only 80kN of compressive force.

The values obtained for SE, W and EP are recorded in Tables 4-20, 4-21 and 4-22.

Table 4-20:Specific Energy Employed for Particle Layer (80kN)

Initial Particle Size (mm)	Input Energy (J)	Sample Mass (g)	Specific Input Energy (J/g)
13,20	131,08	38,71	3,386205
9,50	116,43	26,85	4,336313
6,70	107,36	20,64	5,201550

Table 4-21:Energy Employed for the Comminution of Particles Layer (80kN)

Initial Particle Size (mm)	Feed (mm)	Feed (microns)	Product d80 (mm)	Product d80 (microns)	W (J/g)
+13.2	14,53	14532,72	5,60	5 600	2,5633
+9.50	11,20	11198,21	4,15	4 150	3,0718
+6.70	7,98	7978,10	3,00	3 000	3,5718

Table 4-22:Ratio of Applied and Employed Energy in Comminution of Particle Layer (80kN)

Feed Size (mm)	Ratio W/Specific Energy (J/g)
13,20	1,3210
9,50	1,4117
6,70	1,4563

The EP results obtained for both the 50kN and 80kN energy inputs suggest that there is a considerable increase in EP values when transiting from the lower to the higher energy inputs.

Figure 4-18: Relationship between energy applied and energy employed with 80kN compression on single particle layer

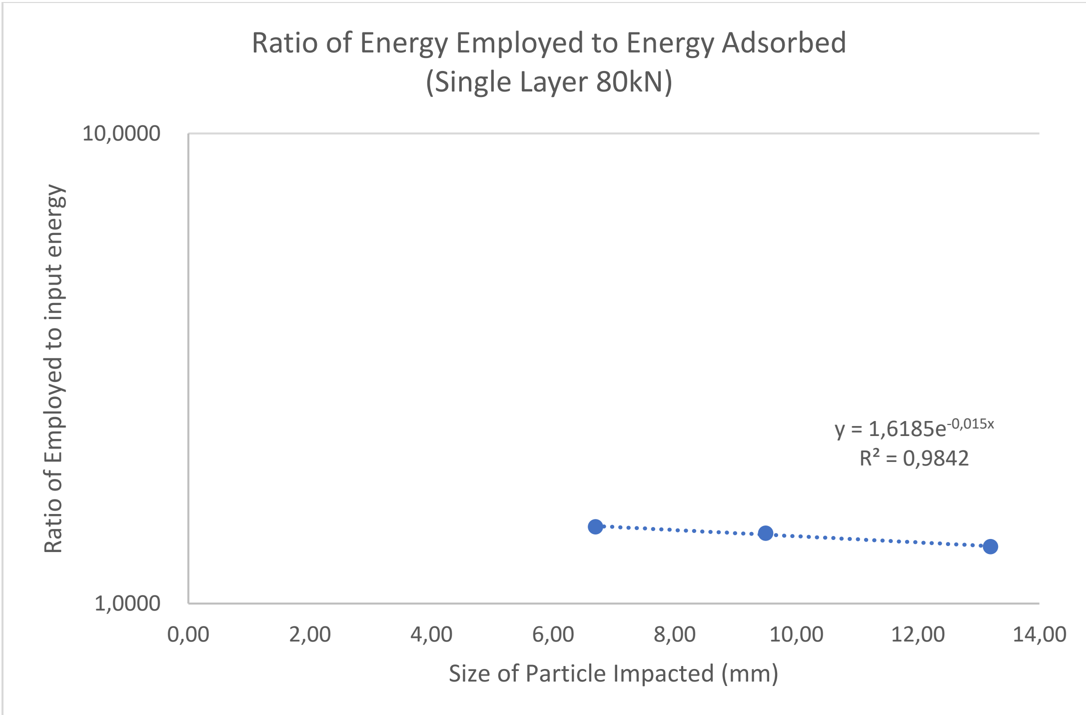

4.2.5. Three Particle Layer at 50kN of compressive force

The same test was conducted at a force of 50kN on a three-layer particle system. In this case, the high pressure test was conducted at a plunger travel rate of 3mm/min and was conducted only for the -16.0+13.2mm, -13.2+9.50mm and the -9.50+6.70mm size classes. The fragments obtained from the test per size class were screened for sizing and resulted in the following distribution:

Figure 4-19: Three-layer high pressure at 50kN applied force particle size distribution

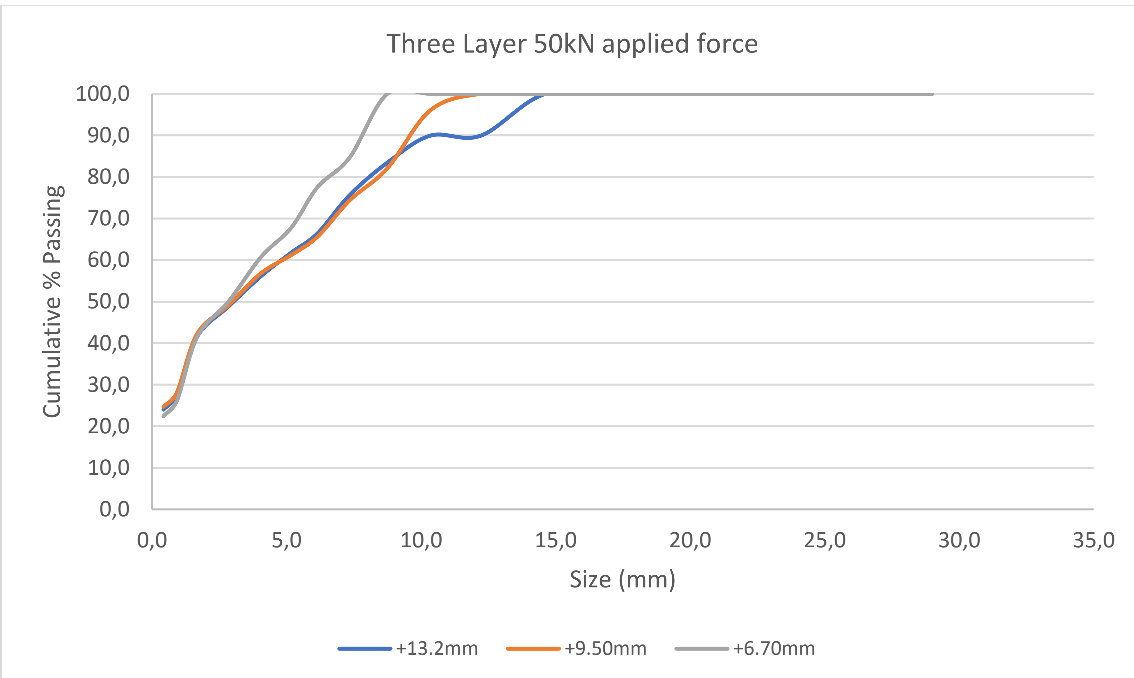

From the above it can be noted that the finer particles experience a greater extent of breakage when compared to the larger particle classes. However, it is clear that the degree of particle breakage is a function of the initial particle size.

Figure 4-20: Normalized data for 50kN three layer applied force

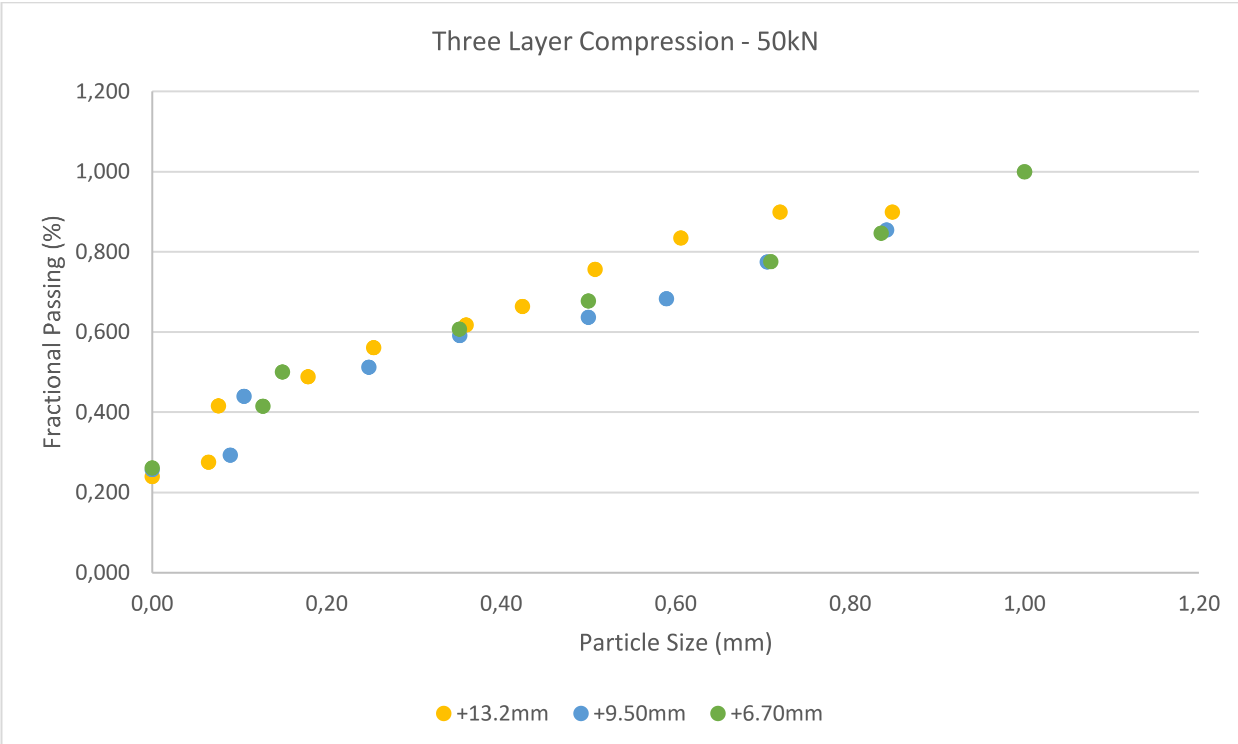

The figure above shows that for multiple layer system at 50kN applied force, the smaller particles behave in a similar manner, while the +13.20mm sized particles behave differently.

4.2.6. Three Particle Layer at 80kN of compressive force

The test was then conducted at 80kN on a three-layer system at a plunger loading rate of 3mm/min. The test was conducted on size class 4 (-16.00 +13.20mm), class 5 (-13.20 +9.50mm) and class 6 (-9.50 +6.70mm). This is the size distribution obtained:

Figure 4-21: Three-layer high pressure system at 80kN applied force particle size distribution

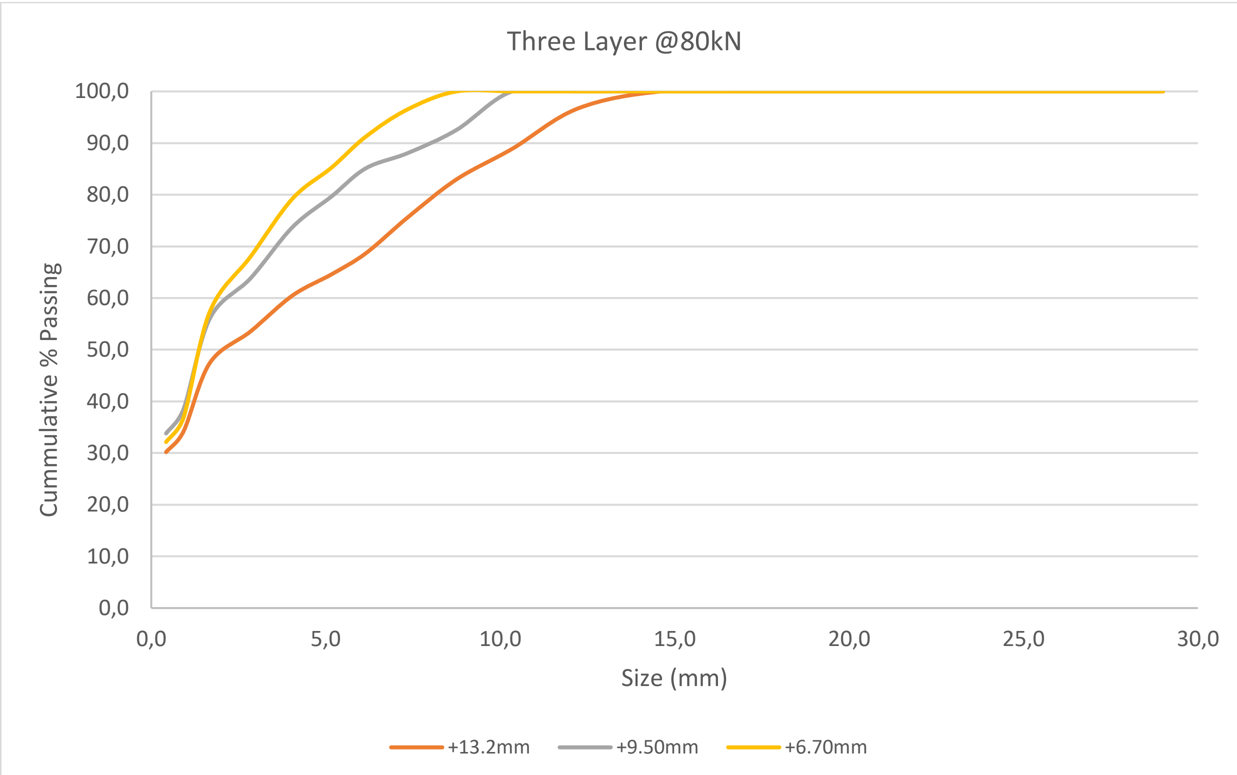

The three scenarios discussed above indicate that the smaller initial particle sizes result in a finer size distribution than the larger particles when the load is induced at a rate of 3mm/min. The same particle sizes display varying characteristics when subject to 50kN in comparison with 80kN compression load with the size distribution obtained.

The size distribution obtained resulted in a finer distribution in the 80kN test when compared to the 50kN. Thus, higher pressure input results in a higher degree of particle breakage.

Figure 4-22: Normalized data for 80kN three layer applied force

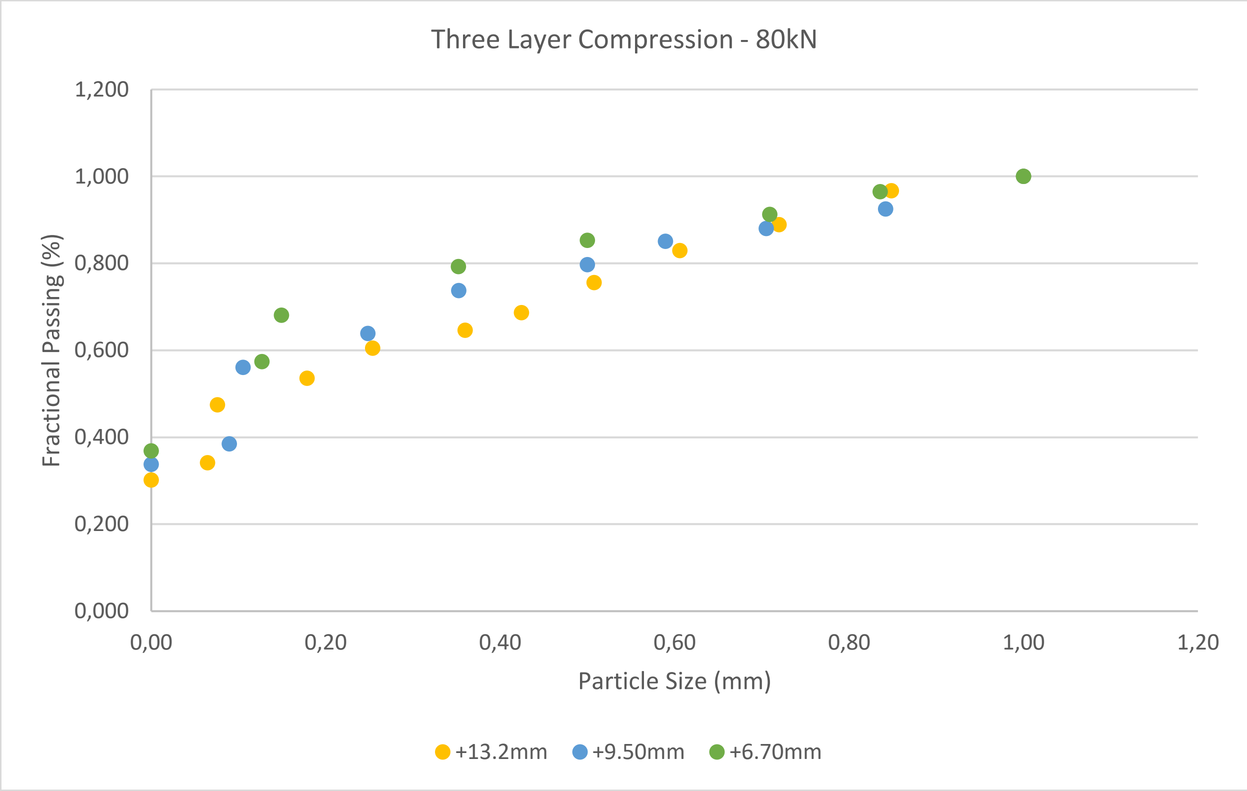

For the three-layer system at 80kN compressive force shows that the particle breakage for the +13.20mm sized particles is different to that obtained for the finer size distributions. The particle breakage is finer for the smaller particles than it is for the larger initial particle size.

Below see the normalized data behavior for the different applies force conditions:

Figure 4-23: Normalized data for +13.2mm particle size

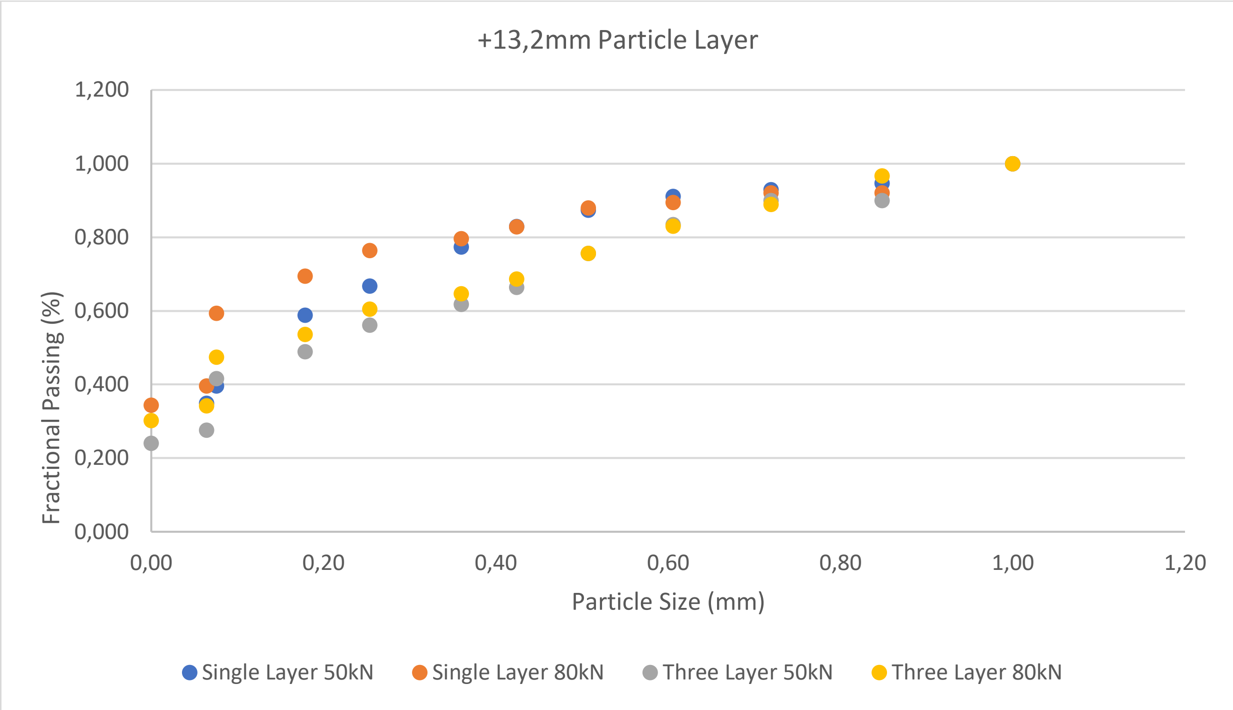

For the +13.20mm sized particles above it can be seen that the resultant particle breakage is finer for the single layer force conditions than it is for the multiple layer systems. This shows that in the single layer systems, more of the applied force is directly used towards the particle breakage, while in the multiple layer system the applied force is also used to facilitate particle movement from one level to the other.

Figure 4-24: Normalized data for +6.70mm particle size

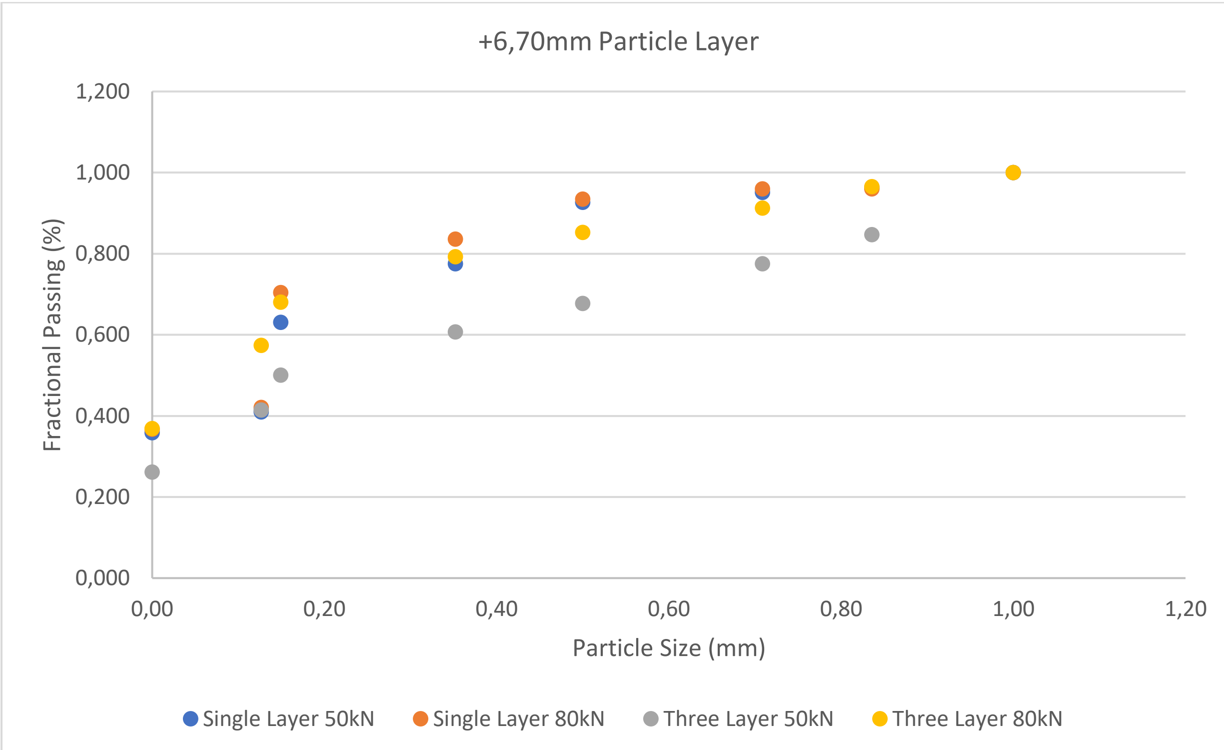

Looking at the +6.70mm sized particle setup above, we see that finer resultant breakage is obtained for the single layer system than that of the multiple layer system. This is similar to the relationship obtained in the coarser particle size distribution (+13.20mm). Looking at the difference in the applied forces we see that higher particle breakage is evident for the 80kN applied force than that of the 50kN applied force.

4.2.7. Analysis of Three Particle Layer at 50kN compressive force (High Pressure Compression)

The sequence of high pressure compression experiments was repeated, this time onto three layers of a mono-sized particle, rather than a single particle layer.

The specific energy (SE) applied to particle layers composed of the same particle size is recorded in Table 4-23. The values for energy absorbed are calculated, from data in Table 4-23, using a modified Bond equation. The results are recorded in Table 4-24.

The resulting EP values are calculated for the data in Tables 4-23 and 4-24 and recorded in Table 4-25.

Again the trend in EP values confirms the increasing energy requirements with smaller particle sizes.

Table 4-23: Specific Energy Employed for Three Particle Layer (50kN):

Initial Particle Size (mm)	**Input Energy (J)**	**Sample Mass (g)**	**Specific Input Energy (J/g)**
13,20	170,39	90.00	1,893222
9,50	147,55	65,73	2,244789
6,70	88,20	49,70	1,774648

The energy absorbed by each sized layer is computed as follows using the relationship determined for W above**.**

Table 4-24:Energy Employed for the Comminution of Three Particles Layer (50kN)

Initial Particle Size (mm)	**Feed (mm)**	**Feed (microns)**	**Product d80 (mm)**	**Product d80 (microns)**	**W (J/g)**
+13.2	14,53	14532,72	8,80	8 800	1,1961
+9.50	11,20	11198,21	7,40	7 400	1,1001
+6.70	7,98	7978,10	6,20	6 200	0,7609

Table 4-25:Ratio of Applied and Employed Energy in Comminution of Three Particle Layer (50kN)

Feed Size (mm)	**Ratio of Energy Employed to Energy Adsorbed**
13,20	1,5828
9,50	2,0406
6,70	2,3323

The relationship between EP and size employed in the particle layer is illustrated by Figure 4-25.

Figure 4-25:Relationship between Energy Applied and Energy Employed with 50kN of compression on Three Particle Layers

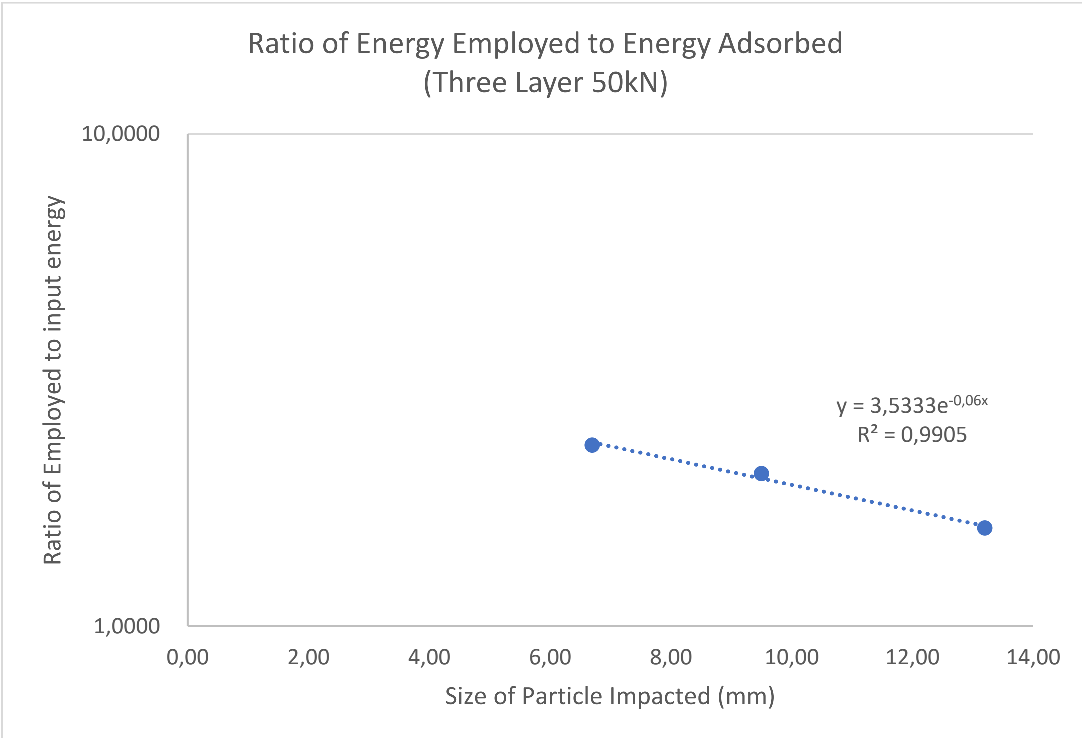

4.2.8. Analysis of Three Particle Layer at 80kN compressive force (High Pressure Compression)

The high pressure compression tests were repeated using three layers of single size particles but, this time, employing 80kN high pressure compressive force.

The values obtained for SE, W and EP are recorded in Tables 4-26, 4-27 and 4-28.

Table 4-26:Specific Energy Employed for Three Particle Layer (80kN)

Initial Particle Size (mm)	Input Energy (J)	Sample Mass (g)	Specific Input Energy (J/g)
13,20	295,49	121,84	2,425230
9,50	182,40	60,40	3,019868
6,70	147,12	48,03	3,063086

Table 4-27:Energy Employed for the Comminution of Three Particles Layer (80kN)

Initial Particle Size (mm)	Feed (mm)	Feed (microns)	Product d_{80} (mm)	Product d_{80} (microns)	W (J/g)
+13.2	14,53	14532,72	7,40	7 400	1,6841
+9.50	11,20	11198,21	5,20	5 200	2,2344
+6.70	7,98	7978,10	4,10	4 100	2,2365

Table 4-28:Ratio of Applied and Employed Energy in Comminution of Three Particle Layer (80kN)

Feed Size (mm)	Ratio W/Specific Energy (J/g)
13,20	1,4401
9,50	1,3515
6,70	1,3696

Figure 4-26: Relationship between energy applied and energy employed with 80kN of compression on three particle layers

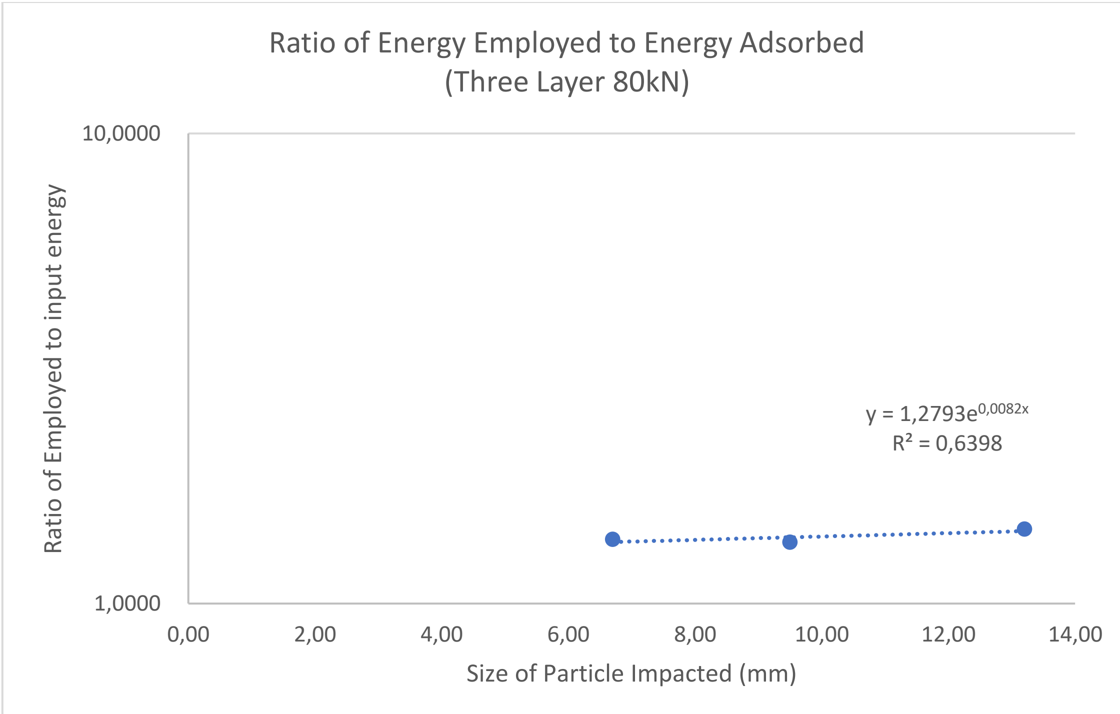

The EP values again support the additional energy required for finer particles.

The data obtained in the single and three layer experiments employing 50kN and 80kN were employed in the derivation of algorithms. It is intended that the data provided by the algorithms removes some of the outliers resulting from experimental inaccuracies.

The results provided by the algorithms are recorded in Table 4-29 and are shown graphically in Figure 4-27.

Table 4-29:Comparison of EP Values for Single Particle Layer and Three Particle Layer Responses to 50kN and 80kN Energy Inputs

Ratio of Energy Applied to Energy Employed				
Particle Size (mm)	**Single Layer 50kN**	**Three Layer 50kN**	**Single Layer 80kN**	**Three Layer 80kN**
4,00	0,902	3,596	1,647	1,302
8,00	0,918	3,660	1,676	1,325
12,00	0,934	3,725	1,706	1,349
16,00	0,951	3,791	1,737	1,373
20,00	0,968	3,858	1,767	1,397
24,00	0,985	3,927	1,799	1,422
28,00	1,002	3,997	1,831	1,447

Figure 4-27:Graphic Representation of Single and Three Layer Particles compressed by 50kN and 80kN

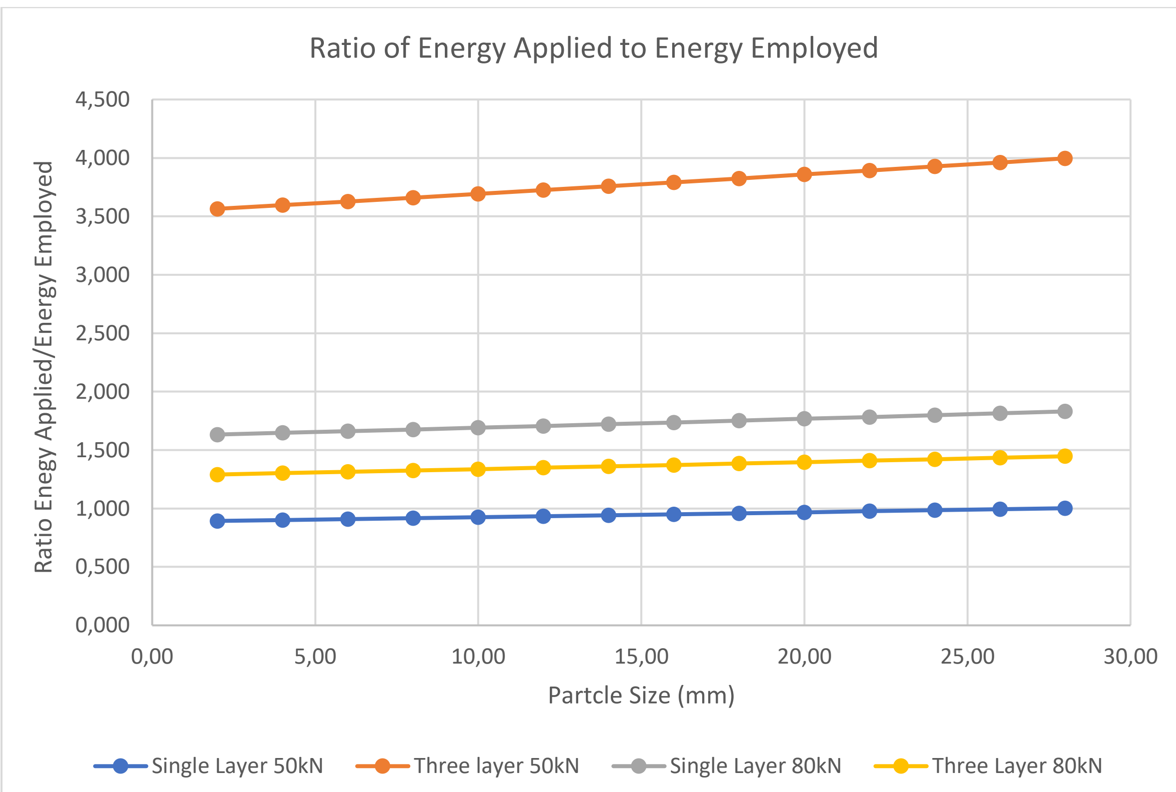

The algorithms indicate that with high pressure compression test does not rely entirely on the cracks initiated on the particles for energy conversion to comminution.

If the data obtained for the compression test on single particle layer and three particle layer at two energy levels is examined the relationships shown in Table 4-30, 4-31 and Figure 4-28, 4-29 can be established.

Table 4-30:Size Reduction Accomplished on Single Particles Layer using Two Level of Energy

High Pressure Compression - Single Particle Layer at Two Energy Levels		
Particle Size (mm)	**D_{80} @ 50kN (mm)**	**D_{80} @80kN (mm)**
26,50	10,30	
19,00	8,80	
16,00	10,10	
13,20	5,10	5,60
9,50	4,70	4,15
6,70	3,60	3,00

Figure 4-28:Graphic Representation of Size Reduction Accomplished on Single Particle layer using Two Levels of Energy

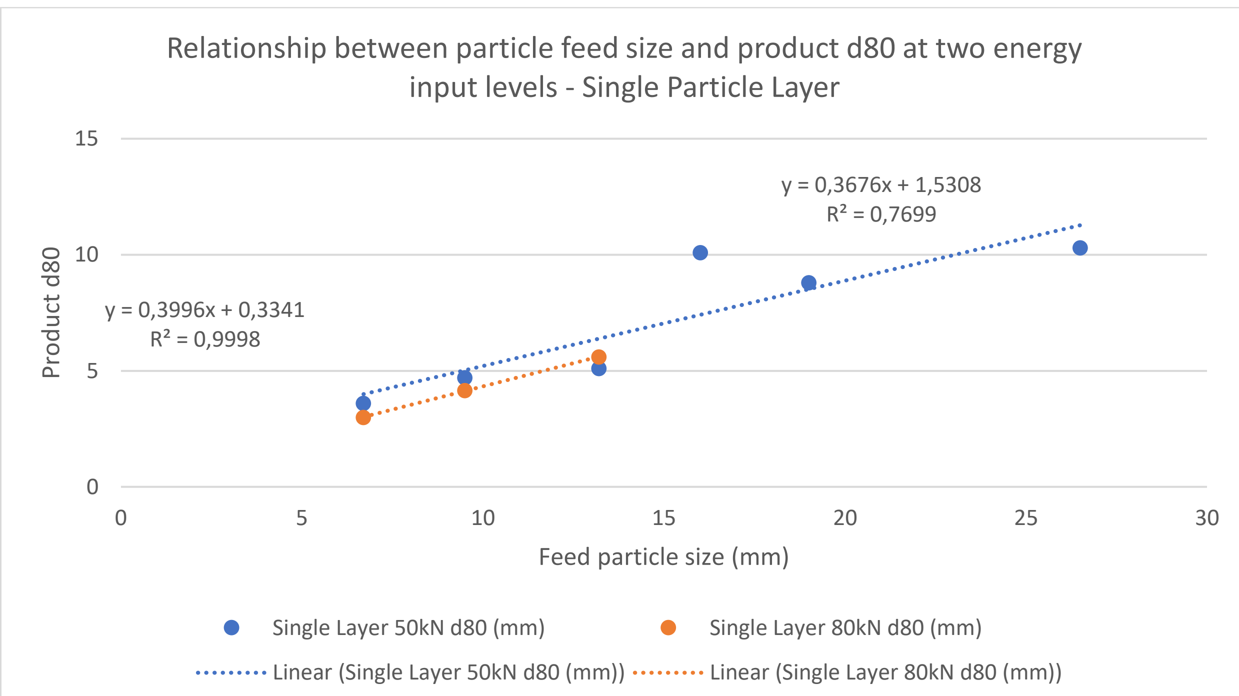

Table 4-31:Size Reduction Accomplished on Three Particles Layer using Two Level of Energy

High Pressure Compression - Three Particle Layer at Two Energy Levels		
Particle Size (mm)	**D_{80} @ 50kN (mm)**	**D_{80} @80kN (mm)**
13,20	8,80	7,40
9,50	7,40	5,20
6,70	6,20	4,10

Figure 4-29:Graphic Representation of Size Reduction Accomplished on Three Particle layer using Two Levels of Energy

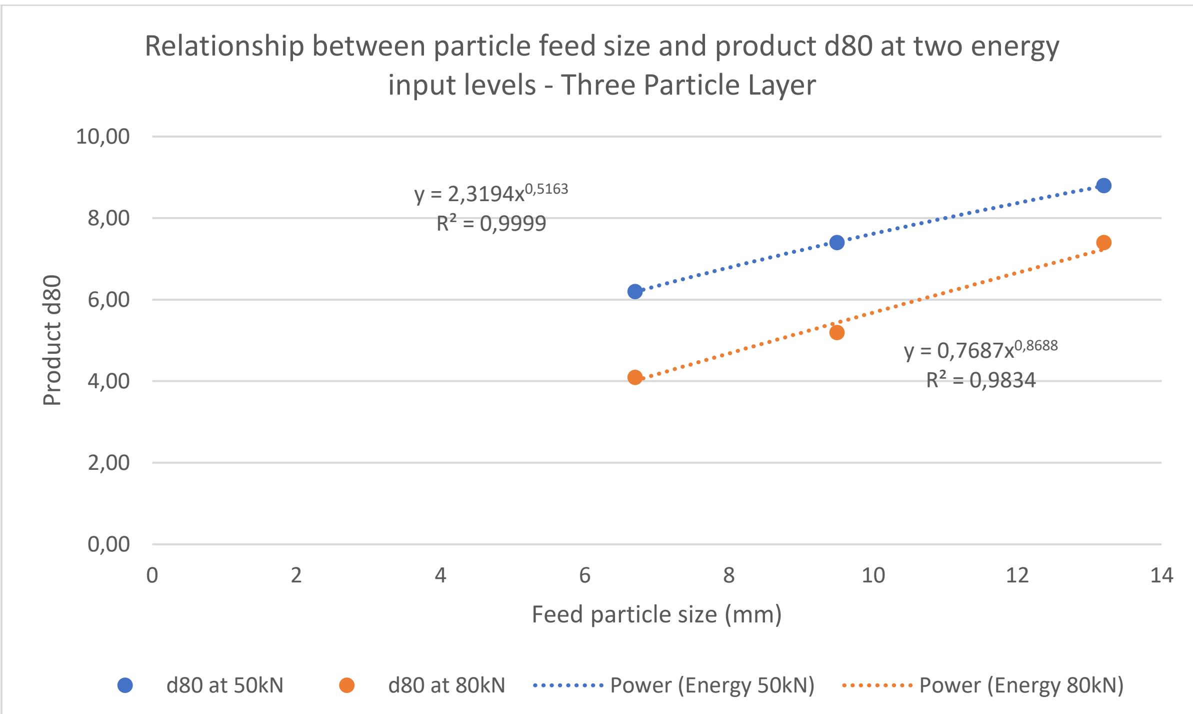

The situation can also be interpreted in terms of single particle layer and three particle layers as shown in Figure 4-30 and 4-31:

Figure 4-30:Degree of Comminution Employing 50kN of Energy

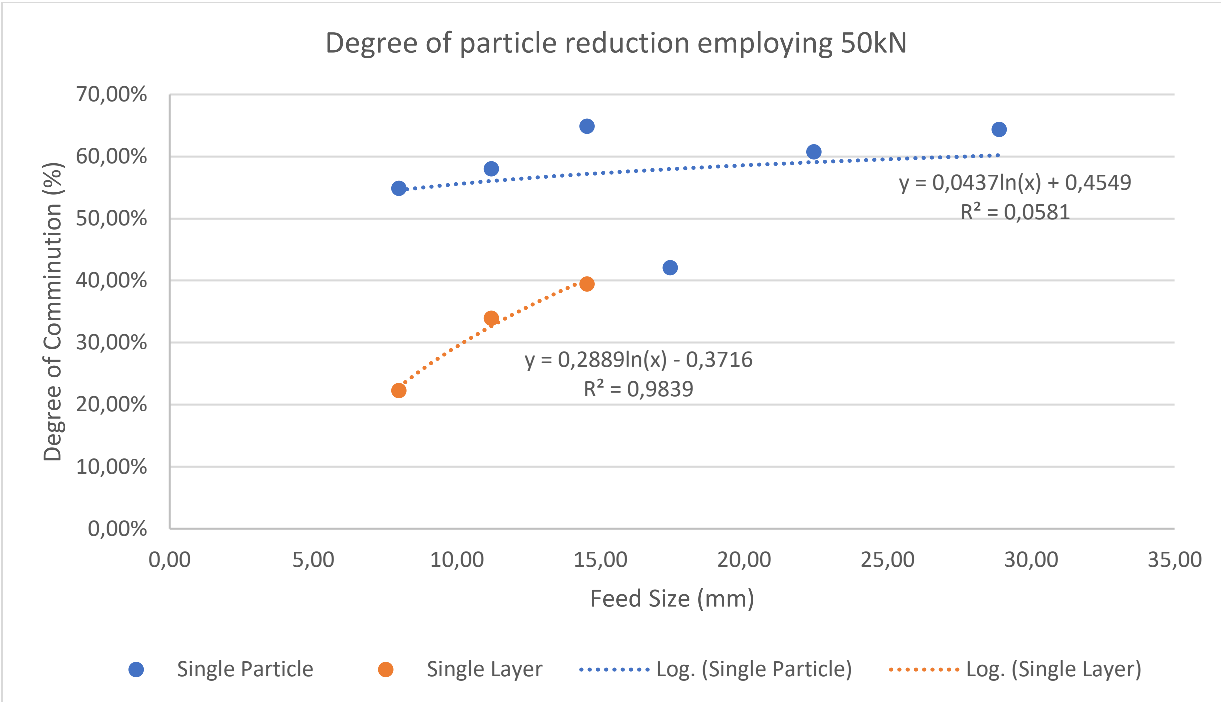

Figure 4-31:Degree of Comminution Employing 80kN of Energy

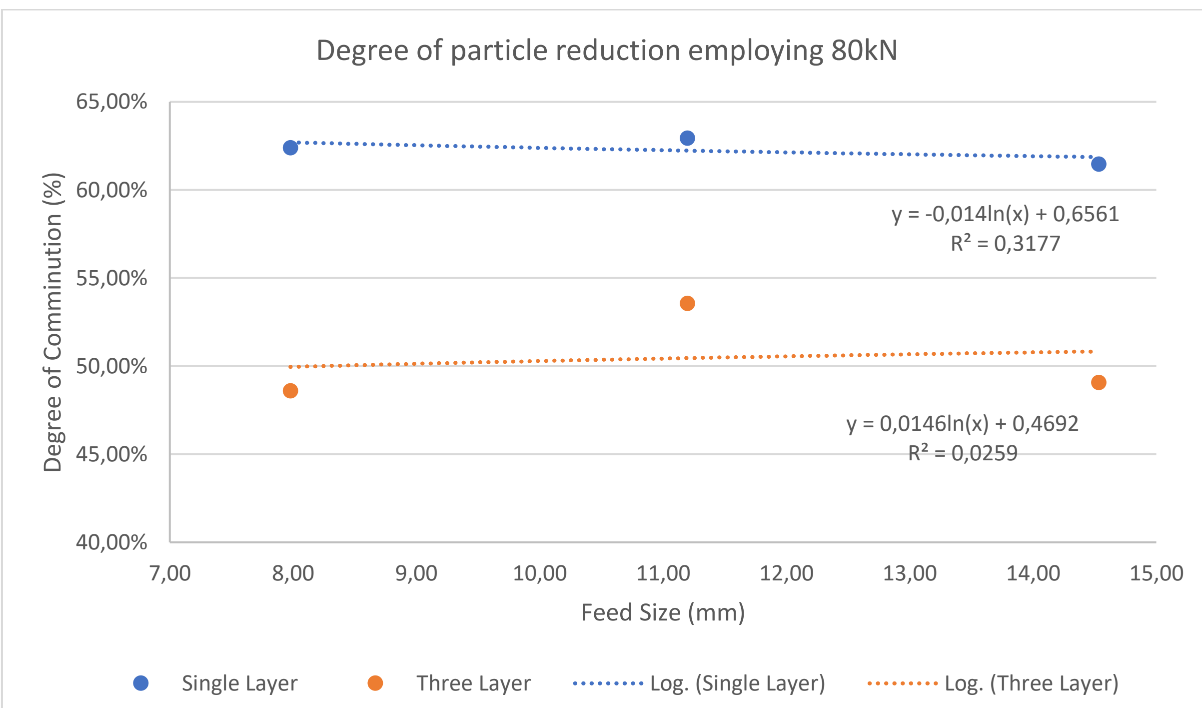

Looking at the single layer high pressure impact at 24.34J and the single layer high pressure compression at 50 kN, the ratio of the energy applied to the energy employed results in the following:

Table 4-32: :Ratios of energy applied to energy employed

Initial Particle Size (mm)	Single Particle Layer Impact (24,34J)	Single Particle Layer 50kN
+26.5	0,194	0,815
+19.0	0,258	0,998
+16.0	0,499	1,697
+13.2	1,745	0,771
+9.50	6,797	0,742
+6.70	1,971	0,912

Figure 4-32:Energy applied to energy employed graphical representation

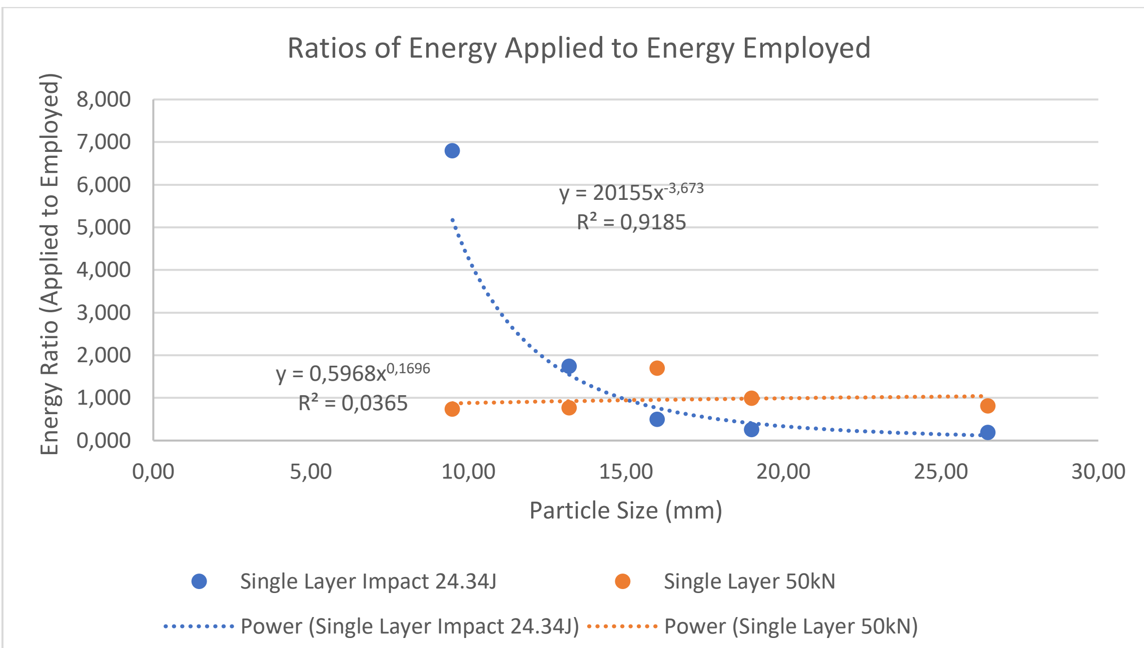

Looking at the above graphs we see that the single layer impact and single layer compression result in different energy ratio relationship for the impact and the high pressure compression test. The relationship between the impact and compression in terms of the energy applied to the energy employed results in the following relationship:

Table 4-33: Ratio of energy in high pressure compression compared to impact.

Initial Particle Size (mm)	Ratio of Energy in Pressure vs Impact
+26.5	4,21
+19.0	3,87
+16.0	3,40
+13.2	0,44
+9.50	0,11
+6.70	0,46

Figure 4-33: Relationship between impact and compression

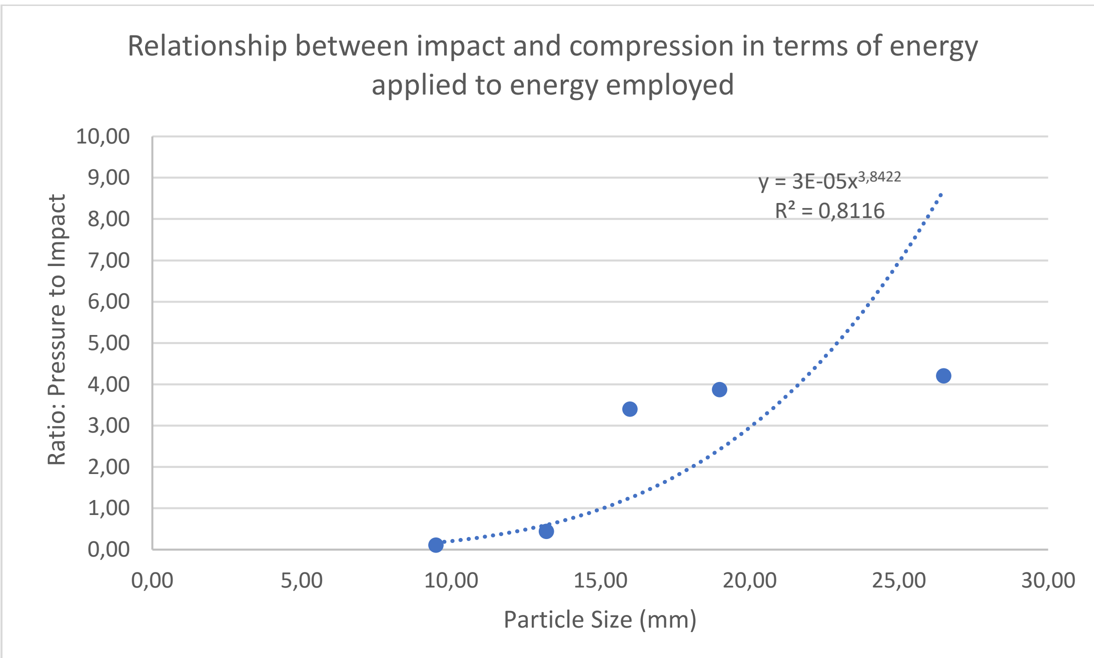

The figure above indicates that in the high pressure compression there is more energy available compared to the impact test at the coarser particle size, while for the smaller particles the two modes of comminution converge to less surplus energy.

5. General Discussion

Particle breakage is a function of various conditions. The particle properties, size and shape all play a role in the breakage characteristics thereof and this work has demonstrated the effect of size However, the extent of breakage can be influenced by the process the particle is subjected to.

In the drop weight test, the specific energy employed in the single particle comminution increased with decreasing particle size, while the EP ratio, which is the ratio of the energy applied to energy employed, from the 24.34J and 16.06J energy input suggest that there is a considerable increase in EP values when transiting from the lower to the higher energy inputs. The single particle layer drop weight test, the ratio of energy applied to energy employed showed a decreasing effect with increasing particle size at both energy inputs. From the drop weight test, the degree of comminution is shown to be higher for singe particle impact than that obtained for the particle layer impact. The larger particles resulted in a greater degree of particle comminution than the smaller particles at similar energy input levels.

In the high-pressure compression test, the specific input energy and the energy employed for comminution increased with decreasing particle size for the single particle layer high-pressure compression. The EP results obtained for both the 50kN and 80kN energy inputs suggest that there is an increase in the ratio of energy applied to energy employed values when transiting from the lower to the higher energy inputs. For the three-layer system, the energy employed for comminution increases with decreasing particle size, while the ratio of applied to employed energy in comminution increases with decreasing particle size. The degree of comminution in the three layer systems resulted in higher comminution values for the single particle layer than it is for the three layer comminution, indicating a greater ease of particle breakage in the single layer system than in the multiple layer system.

In both the drop weight and the high-pressure compression tests, it was noted that an increase in the input energy results in a greater degree of particle comminution. The same can be said about the number of particles present, whereby the less the number of particles present, the higher breakage being achieved. The input energy was also better controlled in the high pressure test due to the better control at which force was exerted onto the particles, which was a result of the contained particulate set-up as compared to the drop impact test. There are factors which contribute to the degree of breakage obtained and these include the initial particle size, number of particle layers and the applied compressive force. In both tests when the similar energy was input into the system the different initial particle sizes resulted in different product particle size distribution.

O Ozcan, et al. [38] has demonstrated that compression particle tests have been shown to result in a finer product distribution than that obtained from impact breakage more so with particles above the

75micron size fraction. In his test, less than 75micron, mineral liberation obtained did not show significant differentiation between the impact and the high-pressure breakage of particles of the same size. The particle breakage obtained in the coarser particles can be attributed to the micro cracking at the grain boundaries of the particles because of the high stresses in compression breakage. The stress in compression breakage is higher along the grain boundaries and this is why higher particle breakage is obtained in piston-die presses. [25]

In both impact and pressure tests it was noted that an increase in the input energy results in a greater degree of particle breakage as compared to that achieved at lower input energy. The same can be said about the number of particles present, whereby the lesser number of particles present resulted in higher particle breakage being achieved. The input energy was also better controlled in the high-pressure test, which was a result of the contained particulate set-up as compared to the drop impact test.

Figure 4-32 and 4-33 showed that in the high pressure compression there is more energy available compared to the impact test at the coarser particle size, while for the smaller particles the two modes of comminution converge to less surplus energy. This indicates that high pressure compression breakage supplies higher energy towards comminution than that obtained from the drop weight impact particle breakage.

6. Conclusions and Recommendation

6.1. Concluding Remarks

When particles of a particular size are subjected to impact breakage, the forces generated will allow for a varying degree of breakage of the particles impacted. This can be attributed to a variance in the resistance of particle, of various size and character, to the variable impact energy inputs.

When particle of various sizes and in various configurations (single, layered) are subjected to impact, or compressive forces, families of daughter products will be formed. It has been found that employment of size analysis provides some indication of the degree to which the various commutative energy inputs have been actually employed in daughter particle production.

With impact breakage, it is found that smaller particles require higher specific impact energy in order to produce any degree of breakage compared to larger particle. The greater energy input required to break the smaller particles is generally thought to be the decreasing presence of cracks, dislocations and other weakening factors with decreasing particle size. This is the reason why, when subjecting particles of different sizes to impact breakage, a relevant application of energy is required to break any of the particles, and all the particles will only break if an adequate quantum of force is applied in the impact process.

An important consideration in the laboratory application of compressive forces is that the energy is constrained by the container resulting in a better employment of available energy in comminution. With compression breakage, increasing the compressive pressure will result in more fracture of a particular particle size. When compression crushing is applied to a bed of particles, the fraction of particles which will fracture at lower bed pressure will produce fragments which have been totally or partially relieved of the bed stress and have therefore lost strain energy to fracture and heat. In order to fracture these, further additional compression force will need to be applied, thus making them appear stronger than the same size particles in the feed. Thus in compressive breakage, one cannot assume that the specific strain energy, after fracture, will remain the same because the product size distribution after fracture will be finer. This same concept is directly applicable to crushing in high pressure grinding rolls. The compression tests indicated that the energy input to breakage does not depict a linear relationship to the particle size and this can be attributed to the same phenomenon. In the impact experiments, the same energy input produces daughter products with rapid attenuation of the input energy. In the high-pressure compression tests, the energy input is prolonged aided by lower but steadier transmission of energy.

In impact breakage, the energy input can be varied by the height from which the load is suspended. This will directly influence the produced particle size distribution. In compressive breakage, the stresses raised need to be monitored and controlled closely by controlling the amount of pressure applied on the particles to directly influence the product particle size distribution. This strain energy can be raised by further compression in order to initiate fracture. As a result of higher stresses required to break smaller particles, the pressure required for fracture increases with decreasing particle size. [24]

The tests conducted between the impact drop weight and to a degree, the high pressure compression unit indicated that the specific input energy increases with decreasing particle size. Smaller particles were noted to require higher stresses to initiate breakage which can be attributed to their higher strength, or the lesser occurrence of cracks that could have propagated.

The drop weight test indicated that reducing the drop height resulted in a difference in the energy used in the breakage obtained. The energy input was varied from 24.34 J to 16.06 J from drop height of 0.94m to drop height of 0.62m. Impact breakage on the single particle resulted in higher comminution degree at both energy inputs when compared to the single layer drop weight test at the same specific energy.

Compression breakage thus allows for more intensive crack formation and propagation due to its gradual but consistent force application on the particles, while drop weight impact breakage results in immediate fracture because of the high forces with which it occurs and the quicker stress application. At the same time, the drop weight impact breakage results in a rapid attenuation of force.

The high-pressure test indicated that the change in the energy input does have an effect on the degree of breakage obtained and the number of particles subject to the breakage does affect the degree of particle breakage. The increase in the input force resulted in a higher breakage of the smaller sized particles at the single layer set-up when compared to the multiple layers setting. As the number of particle layers increased, the resultant particle breakage was reduced due to the reduction in the particle contact to the direct applied pressure as well as the initial particle breakage which causes particle re-arrangement and between the particle layers.

Looking at both the drop weight test and the high-pressure test the highest particle breakage efficiency was obtained with the high-pressure single layer test at 80kN. At this setting higher particle breakage was obtained, as was indicated by the degree of comminution obtained. As R. Mariano, *et al* [16] established, random particle breakage can be summarized as “the independence of breakage from ore properties and mechanical properties during comminution.” This was seen in the energy utilization obtained from both the high-pressure compression and drop weight impact test.

Looking at the energy used per mass of particles subject to breakage it indicated, for both tests, that more energy is used for the small particle size breakage. From the experimental data, energy was certainly more effectively used in the high-pressure compression breakage than in the drop weight impact. For drop weight test, the ratio of energy applied to energy employed indicate that there is a considerable increase in EP values when transiting from the lower to the higher energy inputs. This was also noted with the high-pressure compression test. The degree of comminution for both the drop weight impact and the high pressure compression generally increases with decreasing particle size. The presence of multiple particles however, also resulted in a reduced the degree of comminution for both the impact and the high-pressure compression test.

It should be noted however, that differential degree of comminution is less related to the particle size, in the case of compression, than is the case with impact comminution. The steady application of force in a constrained space eliminates, to a degree the apparent differences exhibited by individual particles in the application of energy through impact.

6.2. Recommendations

This work involved a wide exploration of the effect applying energy either by drop weight or high pressure compression and it is seen that the inter relationship between energy and breakage is complex. For future studies it is recommended to have narrower approach and use more repeats to have more data quality to test thoroughly some of the findings reported in this paper. It will also be very interesting to extend these tests to a totally different material. We also recommend varying the energy input more and try as much as possible to maintain similar specific energy as energy size relationship is a feature that has emerged from these studies. The sample size for the particles also needs to be increased as these kind of data shows a lot of scatter.

7. References

I. http://www.crystallinesilica.eu/what-are-main-uses-silica 8 August 2017
II. http://www.mdpi.com/2075-163X/5/2/276/htm , Bench-Scale Grindability Tests
III. https://www.911metallurgist.com/blog/bond-work-index-test-procedure-and-method
IV. http://www.bbc.co.uk/schools/gcsebitesize/science/add_ocr_pre_2011/chemicals/rocksmineralsrev3.shtml,18 July 2018
V. https://www.ausimmbulletin.com/feature/comminution-energy-efficiency/
VI. https://www.slideshare.net/medishettiswetha/bpharmacy-ii-yr-chapter-11-size-reduction
VII. https://www.azom.com/properties.aspx?ArticleID=1114
VIII. https://www.911metallurgist.com/blog/wp-content/uploads/2015/06/Bond-Work-Index-Test-Report-Example-1.pdf

(1) Abouzeid A., Fuerstenau DW., (2009) Grinding of Mineral Mixtures in High Pressure Grinding Rolls, International Journal of Mineral Processing, Vol 93, pp 59-65.

(2) Arbiter, N., Harris, C.C. and Stamboltzis, G.A. (1969). Single fracture of brittle spheres. Trans. AIME 244, pp 118-133.

(3) Asim. M.E., (1984), Investigations of Cement Clinker Grindability Using Drop-Weight Tests and its Relation to Tube Mill Performance, Zement-Kalk-Gips, No.11, pp 577-584.

(4) Austin L.G., (2002), A treatment of impact breakage of particles. Powder Technology Vol 126, 2002 pp 85–90.

(5) Austin L.G., Cho H., (2003), An equation for the breakage of particles under impact. Powder Technology Vol 132, pp 161– 166.

(6) Bemrose, C.R and Bridgewater, J. (1987). A review of the attrition and attrition test methods. Powder Technology Vol 49, pp 97-126.

(7) Bhondayi C., Danha G., Legodi D., Hlabangana N., Hildebrandt D. A fundamental investigation on the breakage of a bed of silica sand. Department of Chemical, Metallurgical and Materials Engineering, College of Engineering and Technology, Botswana International University of Science and Technology.

(8) Bond, F.C., Crushing Tests by Pressure and Impact. Trans. AIME (1946), Vol 169, pp 58–65.

(9) Bourgeois F.S., Banini G.A., A portable load cell for in-situ ore impact breakage testing, Julius Kruttschnitt Mineral Research Centre, Isles Road, Indooroopilly, QLD 4068, Australia

(10) Broadbent S.R, Callcott T.G. (1956). I. A new analysis of coal breakage process. II. A Matrix representation of breakage. Inst. Fuel Vol 29, pp 524-539.

(11) Brown J.G., Jones T.F,. (1996) Fractal description of the progeny of single impact single particle breakage, Minerals Engineering, pp 715-726

(12) Butler I., Ooi JY., Wang L., (2015) Interpretation of particle breakage under Compression using x-ray computed tomography and digital image correlation, Powder Technology Procedia Engineering, Vol 102, pp 240-248.

(13) Bwalya M.M., (2005) Using the discrete element method to guide the modelling of semi and fully autogenous milling, University of the Witwatersrand, Johannesburg.

(14) Committee on comminution and Energy Consumption. (1981), Comminution and Energy Consumption, US Department of Energy Bureau of Mines, US Department of Interior National Science Foundation.

(15) Drzymala J., (2007) Mineral Processing Foundations of Theory and Practice of Minerallurgy, 1st English edition, Wroclaw University of Technology, pp 123 – 126.

(16) Evans C.L., Mariano R.A., Manlapig E., (2016) Definition of random and non-random breakage in mineral liberation – A review. The University of Queensland, Australia.

(17) Fang H.Y, Yang J.H, Chen Q. (2018), Particle size distribution and energy consumption during impact crushing of single granite particles. Journal of the Southern African Institute of Mining and Metallurgy, Vol 118, pp 555-561.

(18) Fuerstenau D.W., Rashidi S., Rajamani R.K., (2017). A Review of the modelling of High Pressure Grinding Rolls, Powder Technology Foundation.

(19) Gaudin A.M., Principles of Mineral Dressing, size reduction laws.

(20) Genc O., Ergun L., Benzer H., (2004). Single particle impact breakage characterization of materials by drop weight testing. Physicochemical Problems of Mineral Processing, Vol 38, pp 241-255.

(21) Ghadiri, M. and Papadopoulos, D.G. (1995). Impact attrition of particulate solids. IFPRI Final Report FRR 16-05, University of Surrey, U.K.

(22) Ghadiri, M., Papadopoulos, D.G. and Bassam, F. (1995). Attrition of particulate solids. IFPRI Annual Report ARR 16-07, University of Surrey, U.K.

(23) Golekwang M, Murray M B, Revisiting the drop weight model for predicting particle breakage probability. The University of the Witwatersrand, Johannesburg

(24) Griffith A., (1921), The Phenomena of Rupture and Flow in Solids, Royal Society of London. Series A, Containing Papers of a Mathematical or Physical Character, Vol. 221, pp. 163-198.

(25) Huang J., Xu S., Hu S., (2014), Influence of particle breakage on the dynamic compression responses of brittle granular materials, University of Science and Technology of China.

(26) Jankovic A., Dundar H., Mehta R., (2010). Relationships between comminution energy and product size for a magnetite ore. The Journal of The Southern African Institute of Mining and Metallurgy, Vol 110, pp 141-146.

(27) Jeswiet J., Szekeres A. , (2016) Energy Consumption in Mining Comminution, 23rd CIRP Conference on Life Cycle Engineering, Vol 48, pp 140-145

(28) Kafui, K.D. and Thornton, C. (1993). Computer simulated impact of agglomerates. In Powders and Grains 93 (ed. C. Thornton). Rotterdam, Balkema, pp 401-406.

(29) Kalman, H., (2000) Particle breakage and Attrition. Department of Mechanical Engineering Ben-Gurion University of the Negev, pp 108-120.

(30) King, R.P. (2001) Modeling and Simulation of Mineral Processing Systems, Department of Metallurgical Engineering, University of Utah, Chapter 5.

(31) Klymowsky R., (2009) HPGR-Accepted Technology in Mining, Mining Magazine Congress, Canada.

(32) Komnitas K., Petrakis E., (2017), Improved modelling of the grinding process through the combined use of matrix and population balance models, Minerals 2017, Vol 7, pp 67-84.

(33) Kuts M. , (2002), The Handbook of Materials Selection, John Wiley and Sons, pp556-557

(34) Kwade A., (2015), Comminution processes: Basics and application to energy efficiency, Institute for Particle Technology, Technische Universität Braunschweig.

(35) Man Y.T., (2000), A Model-based scale-up procedure for Wet, Overflow Ball Mills., Julius KruttschnittMineral Research Centre., Department of Mining, Minerals and Materials Engineering, The University of Queensland

(36) Mwanga, A., Rosenkranz, J., Lamberg, P. (2015) Testing of Ore Comminution Behavior in the Geometallurgical Context—A Review. Minerals, Vol 5, pp 276-297.

(37) Okuda, S. and Choi, W.S., (1981). Mechanism of cutting fracture of polypropylene by impact on wedge-shaped target. J Chem. Eng. Japan Vol 14(2), pp 149-153.

(38) Ozcan O, Benzer H., (2013), Comparison of different breakage mechanisms in terms of product particle size distribution and mineral liberation, Minerals Engineering Volume 49, pp 103-108.

(39) Ozgur O, Hakan B., (2013), Comparison of different breakage mechanisms in terms of product particle size distribution and mineral liberation. Minerals Engineering Volume 49, pp 103-108.

(40) Nakata,Y., Kato,Y., Hydo,M., Hyde,A.F.L., Murata,H. , (2001), One-dimensional compression behavior of uniformly graded sand related to single particle crushing strength. Soils and Foundations, Vol 41, pp 39-51.

(41) Napier-Munn, T.J., Morrell, S., Morrison, R.D., and Kojovic, T., (1996) Mineral Comminution Circuits: their Operation and Optimisation. Julius Kruttschnitt Mineral Research Centre, University of Queensland.

(42) Narayanan S.S., Whiten W.J., (1988), Determination of comminution characteristics from single particle breakage tests and its application to ball-mill scale-up. University of Queensland

(43) Narayanan, S.S., (1985) Development of a Laboratory Single Particle Breakage Technique and Its Application to Ball Mill Scale-Up. Ph.D. Thesis, University of Queensland, Queensland, Australia

(44) Norazirah A., Fuad S.H.S., Hazizan M.H.M., (2015) The Effect of Size and Shape on Breakage Characteristic of Mineral. School of Material and Mineral Resources Engineering, Engineering Campus,University Science Malaysia.

(45) Petruk W. , (2000), Applied Mineralogy in the Mining Industry, Elsevier Science, Ottawa, Ontario, Canada.

(46) Potapov A., Campbell C., (2001). Parametric Dependence of Particle Breakage Mechanisms. Department of mechanical engineering, University of Southern California, Los Angeles. Powder Technology, Vol 120, pp 164 – 174.

(47) Rizk, A.M.E., El-Sageer, H.A.A. and Doheim, M.A. (1994). Examination of single and repetitive impact breakage. Minerals Eng., Vol 7(4), pp 479-490.

(48) Rumpf, H. and Schonert, K. (1973). Single particle crushing of polymers. In H. Heywood Memorial Symp., Loughborough University of Technology.

(49) Schonert K., (1988) A First Survey of Grinding with High-Compression Roller Mills, International Journal of Mineral Processing, Vol 22, pp 401-412.

(50) Schonert K., (1996) The Influence of Particle Bed Configurations and Confinements on Particle Breakage, International Journal of Mineral Processing, 44-45, pp 1-16.

(51) Shi D., Zheng L., Xue J., Sun J., (2016), DEM Modelling of Particle Breakage in Silica Sands under One-Dimensional Compression, Acta Mechanica Solida Sinica, Vol 29 (1), pp78-94.

(52) Stixrude, L., Cohen, R., Hemley, R., (1998) Theory of Minerals at High Pressure. Chapter 19, University of Michigan, pp 639-671.

(53) Tavares L.M., (2007), Breakage of Single Particles: Quasi-static, in Salman AD, Ghardi M and Hounslow M.J., (Eds): Handbook of Powder Technology, Volume 12, Particle Breakage, pp 12-18. Elsevier Scientific Publishing Co.

(54) Tuğcan Tuzcudama Engineering,Particle Internal Fracture Energy Measurement by Ultrafast Load Cell E. Head of Mining and Metallurgy, 06810, Ankara

(55) Weedon, D.M.; Wilson, F., (2000), Modelling Iron Ore Degradation Using a Twin Pendulum Breakage Device. Int. J. Miner. Process. Vol 59, pp 195–213.

(56) Weichert R., (1992) Anwendung von Fehlstellenstatistik und Bruchmechanik zur Beschreibung von Zerkleinerungsvorga¨ngen, Zement-Kalk-Gips, Vol 45 (1), pp 1 – 8.

(57) Wills B.A and Atkinson, K. (1993). Some observations on the fracture and liberation of mineral assemblies, Minerals Engineering, Vol. 6(7), pp697-706.

(58) Wills B., Napier-Munn T., (2006), Mineral Processing Technology, Elsevier Science and Technology Books Publisher.

8. Appendices

8.1. Appendix A: Drop Weight Test

8.1.1. Single Particle impact test

Table 8-1:Particle size distribution – single particle impact

Initial Particle size (mm)		26,5	19	16	13,2	9,5	6,7
Top Size	Bottom Size	Mass % Passing	Mass % Passing	Mass % Passing	Mass % Passing	Mass % Passing	Mass % Passing
-19,0	+16,0	100,0%	100,0%	100,0%	100,0%	100,0%	100,0%
-16,0	-13.2	56,7%	90,7%	90,9%	100,0%	100,0%	100,0%
-13.2	-11.2	46,0%	76,1%	85,6%	100,0%	95,8%	100,0%
-11.2	-9.5	39,9%	67,9%	77,0%	83,9%	93,0%	100,0%
-9.5	-8.0	34,7%	66,6%	73,9%	80,0%	88,8%	100,0%
-8.0	-6.7	29,8%	59,4%	67,6%	74,1%	83,1%	89,2%
-6.7	-4.8	23,9%	52,3%	55,2%	65,3%	74,4%	77,9%
-4.8	-3.4	18,8%	44,3%	44,6%	57,3%	64,8%	64,7%
-3.4	+2.4	14,9%	38,6%	36,4%	47,7%	54,3%	55,2%

8.1.2. Single Particle layer impact test

Table 8-2:Particle size distribution – single particle layer impact

Initial Particle size (mm)		26,5	19	16	13,2	9,5	6,7
Top Size	Bottom Size	% Passing	% Passing	% Passing	% Passing	% Passing	% Passing
19,0	16,0	100,00%	100,00%	100,00%	100,00%	100,00%	100,00%
16,0	13,2	15,47%	31,68%	24,63%	39,30%	100,00%	100,00%
13,2	11,2	11,42%	26,60%	20,64%	27,55%	54,06%	100,00%
11,2	9,5	11,42%	21,99%	15,23%	21,90%	23,06%	99,02%
9,5	8,0	9,35%	19,88%	13,53%	20,32%	15,80%	78,25%
8,0	6,7	8,57%	17,46%	11,13%	16,22%	11,58%	44,42%
6,7	4,8	5,63%	13,89%	8,24%	11,73%	7,94%	29,12%
4,8	3,4	4,53%	12,45%	6,80%	9,21%	6,15%	19,05%
3,4	2,4	3,51%	10,78%	4,97%	7,58%	4,62%	14,16%

8.2. Appendix B: High Pressure Compression - sizing

8.2.1. High pressure compression at 50kN

8.2.1.1. Single Layer

+26.50mm

Table 8-3: +26.50mm Single layer impact

Particle size (mm)		Representative Size (mm)	Mass (g)
Top Size	Bottom Size		
31,50	26,50	29,00	0,00
26,50	19,00	22,75	0,00
19,00	16,00	17,50	4,71
16,00	13,26	14,63	2,47
13,26	11,20	12,23	1,25
11,20	9,50	10,35	6,68
9,50	8,00	8,75	4,96
8,00	6,70	7,35	3,24
6,70	5,60	6,15	7,01
5,60	4,75	5,18	2,79
4,75	3,35	4,05	4,28
3,35	2,36	2,86	3,82
2,36	1,00	1,68	6,42
1,00	0,85	0,93	1,28
0,85	0,00	0,43	9,64
			58,55

+19.0mm

Table 8-4:+19.00mm Single layer impact

Particle size (mm)		Representative Size (mm)	Mass (g)
Top Size	Bottom Size		
	26.50	29.00	0
26.50	19.00	22.75	0
19.00	16.00	17.50	0
16.00	13.26	14.63	0
13.26	11.20	12.23	4.45
11.20	9.50	10.35	4.65
9.50	8.00	8.75	6.43
8.00	6.70	7.35	3.74
6.70	5.60	6.15	2.54
5.60	4.75	5.18	5.38
4.75	3.35	4.05	5.65
3.35	2.36	2.86	3.42
2.36	1.00	1.68	9.05
1.00	0.85	0.93	1.59
0.85	0	0.43	12.99
			59.89

+16.0mm

Table 8-5: +16.00mm Single layer impact

Particle size (mm)		Representative Size (mm)	Mass (g)
Top Size	Bottom Size		
	26.50	29.00	0
26.50	19.00	22.75	0
19.00	16.00	17.50	4.94
16.00	13.26	14.63	2.41
13.26	11.20	12.23	0.04
11.20	9.50	10.35	4.98
9.50	8.00	8.75	2.11
8.00	6.70	7.35	1.83
6.70	5.60	6.15	2.09
5.60	4.75	5.18	2.33
4.75	3.35	4.05	4.74
3.35	2.36	2.86	3.31
2.36	1.00	1.68	7.88
1.00	0.85	0.93	1.7
0.85	0	0.425	11.17
			49.53

+13.2mm

Table 8-6: +13.20mm Single layer impact

Particle size (mm)		Representative Size (mm)	Mass (g)
Top Size	Bottom Size		
	26.50	29.00	0
26.50	19.00	22.75	0
19.00	16.00	17.50	0
16.00	13.26	14.63	0
13.26	11.20	12.23	2.38
11.20	9.50	10.35	0.78
9.50	8.00	8.75	0.81
8.00	6.70	7.35	1.66
6.70	5.60	6.15	1.96
5.60	4.75	5.18	2.48
4.75	3.35	4.05	4.75
3.35	2.36	2.86	3.49
2.36	1.00	1.68	8.57
1.00	0.85	0.93	2.08
0.85	0	0.425	15.55
			44.51

+9.50mm

Table 8-7: +9.50mm Single layer impact

Particle size (mm)		Representative Size (mm)	Mass (g)
Top Size	Bottom Size		
	26.50	29.00	0
26.50	19.00	22.75	0
19.00	16.00	17.50	0
16.00	13.26	14.63	0
13.26	11.20	12.23	0
11.20	9.50	10.35	0
9.50	8.00	8.75	2.81
8.00	6.70	7.35	0
6.70	5.60	6.15	2.12
5.60	4.75	5.18	2.42
4.75	3.35	4.05	4.97
3.35	2.36	2.86	3.19
2.36	1.00	1.68	8.13
1.00	0.85	0.93	2.94
0.85	0	0.425	10.38
			36.96

+6.70mm

Table 8-8: +6.70mm Single layer impact

Particle size (mm)		Representative Size (mm)	Mass (g)
Top Size	Bottom Size		
	26.50	29.00	0
26.50	19.00	22.75	0
19.00	16.00	17.50	0
16.00	13.26	14.63	0
13.26	11.20	12.23	0
11.20	9.50	10.35	0
9.50	8.00	8.75	0
8.00	6.70	7.35	0.93
6.70	5.60	6.15	0.3
5.60	4.75	5.18	0.63
4.75	3.35	4.05	3.85
3.35	2.36	2.86	3.65
2.36	1.00	1.68	5.61
1.00	0.85	0.93	1.3
0.85	0	0.425	9.1
			25.37

8.2.1.2. Three Layer

+13.2mm

Table 8-9: +13.20mm Three layer Impact

Particle size (mm)		Reprsentative Size (mm)	Mass (g)
Top Size	Bottom Size		
31.5	26.50	29.00	0
26.50	19.00	22.75	0
19.00	16.00	17.50	0
16.00	13.26	14.63	8.94
13.26	11.20	12.23	0
11.20	9.50	10.35	5.78
9.50	8.00	8.75	6.93
8.00	6.70	7.35	8.21
6.70	5.60	6.15	4.11
5.60	4.75	5.18	5.02
4.75	3.35	4.05	6.42
3.35	2.36	2.86	6.5
2.36	1.00	1.68	12.44
1.00	0.85	0.93	3.18
0.85	0	0.43	21.32
			88.85

+9.50mm

Table 8-10: +9.50mm Three layer Impact

Particle size (mm)		Reprsentative Size (mm)	Mass (g)
Top Size	Bottom Size		
	26.50	29.00	
26.50	19.00	22.75	
19.00	16.00	17.50	
16.00	13.26	14.63	
13.26	11.20	12.23	2.79
11.20	9.50	10.35	9.83
9.50	8.00	8.75	5.43
8.00	6.70	7.35	6.19
6.70	5.60	6.15	3.1
5.60	4.75	5.18	3.08
4.75	3.35	4.05	5.36
3.35	2.36	2.86	4.89
2.36	1.00	1.68	9.96
1.00	0.85	0.93	2.42
0.85	0	0.43	17.39
			70.44

+6.70mm

Table 8-11: +6.70mm Three layer Impact

Particle size (mm)		Reprsentative Size (mm)	Mass (g)
Top Size	Bottom Size		
	26.50	29.00	0
26.50	19.00	22.75	0
19.00	16.00	17.50	0
16.00	13.26	14.63	0
13.26	11.20	12.23	0
11.20	9.50	10.35	0
9.50	8.00	8.75	8.39
8.00	6.70	7.35	3.93
6.70	5.60	6.15	5.34
5.60	4.75	5.18	3.87
4.75	3.35	4.05	5.83
3.35	2.36	2.86	4.71
2.36	1.00	1.68	8.42
1.00	0.85	0.93	2.02
0.85	0	0.43	12.3
			54.81

8.2.2. High pressure compression at 80kN

8.2.2.1. Single Layer

+13.2mm

Table 8-12: +13.2mm single layer

Particle size (mm)		Representative Size (mm)	Mass (g)
Top Size	Bottom Size		
31.5	26.50	29.00	0
26.50	19.00	22.75	0
19.00	16.00	17.50	0
16.00	13.26	14.63	3.04
13.26	11.20	12.23	0
11.20	9.50	10.35	1
9.50	8.00	8.75	0.59
8.00	6.70	7.35	1.96
6.70	5.60	6.15	1.23
5.60	4.75	5.18	1.26
4.75	3.35	4.05	2.68
3.35	2.36	2.86	3.87
2.36	1.00	1.68	7.58
1.00	0.85	0.93	2.01
0.85	0	0.43	13.22
			38.44

+9.50mm

Table 8-13: +9.50mm single layer

Particle size (mm)		Representative Size (mm)	Mass (g)
Top Size	Bottom Size		
31.5	26.50	29.00	0
26.50	19.00	22.75	0
19.00	16.00	17.50	0
16.00	13.26	14.63	0
13.26	11.20	12.23	0
11.20	9.50	10.35	0
9.50	8.00	8.75	1.1
8.00	6.70	7.35	1.35
6.70	5.60	6.15	1.22
5.60	4.75	5.18	2.13
4.75	3.35	4.05	4.56
3.35	2.36	2.86	3.62
2.36	1.00	1.68	7.01
1.00	0.85	0.93	2.12
0.85	0	0.43	16.31
			39.42

+6.70mm

Table 8-14: +6.70mm single layer

Particle size (mm)		Representative Size (mm)	Mass (g)
Top Size	Bottom Size		
31.5	26.50	29.00	0
26.50	19.00	22.75	0
19.00	16.00	17.50	0
16.00	13.26	14.63	0
13.26	11.20	12.23	0
11.20	9.50	10.35	0
9.50	8.00	8.75	0
8.00	6.70	7.35	0.82
6.70	5.60	6.15	0
5.60	4.75	5.18	0.52
4.75	3.35	4.05	2.04
3.35	2.36	2.86	2.71
2.36	1.00	1.68	5.82
1.00	0.85	0.93	1.11
0.85	0	0.43	7.55
			20.57

8.2.2.2. Three Layer

+13.2mm

Table 8-15: +13.20mm three layer

Particle size (mm)		Representative Size (mm)	Mass (g)
Top Size	Bottom Size		
	26.50	29.00	0
26.50	19.00	22.75	0
19.00	16.00	17.50	0
16.00	13.26	14.63	3.98
13.26	11.20	12.23	9.4
11.20	9.50	10.35	7.15
9.50	8.00	8.75	8.88
8.00	6.70	7.35	8.37
6.70	5.60	6.15	4.87
5.60	4.75	5.18	4.97
4.75	3.35	4.05	8.33
3.35	2.36	2.86	7.41
2.36	1.00	1.68	15.98
1.00	0.85	0.93	4.83
0.85	0	0.43	36.39
			120.56

+9.50mm

Table 8-16: +9.50mm three layer

Particle size (mm)		Representative Size (mm)	Mass (g)
Top Size	Bottom Size		
	26.50	29.00	0
26.50	19.00	22.75	0
19.00	16.00	17.50	0
16.00	13.26	14.63	0
13.26	11.20	12.23	0
11.20	9.50	10.35	4.46
9.50	8.00	8.75	2.68
8.00	6.70	7.35	1.76
6.70	5.60	6.15	3.23
5.60	4.75	5.18	3.57
4.75	3.35	4.05	5.89
3.35	2.36	2.86	4.68
2.36	1.00	1.68	10.5
1.00	0.85	0.93	2.81
0.85	0	0.43	20.21
			59.79

+6.70mm

Table 8-17: +6.70mm three layer

Particle size (mm)		Representative Size (mm)	Mass (g)
Top Size	Bottom Size		
	26.50	29.00	0
26.50	19.00	22.75	0
19.00	16.00	17.50	0
16.00	13.26	14.63	0
13.26	11.20	12.23	0
11.20	9.50	10.35	0
9.50	8.00	8.75	1.65
8.00	6.70	7.35	2.51
6.70	5.60	6.15	2.83
5.60	4.75	5.18	2.87
4.75	3.35	4.05	5.3
3.35	2.36	2.86	5.09
2.36	1.00	1.68	9.75
1.00	0.85	0.93	2.25
0.85	0	0.43	15.27
			47.52

8.3. Appendix C: High Pressure Compression – compression results

8.3.1. High pressure compression at 50kN

8.3.1.1. Single Layer

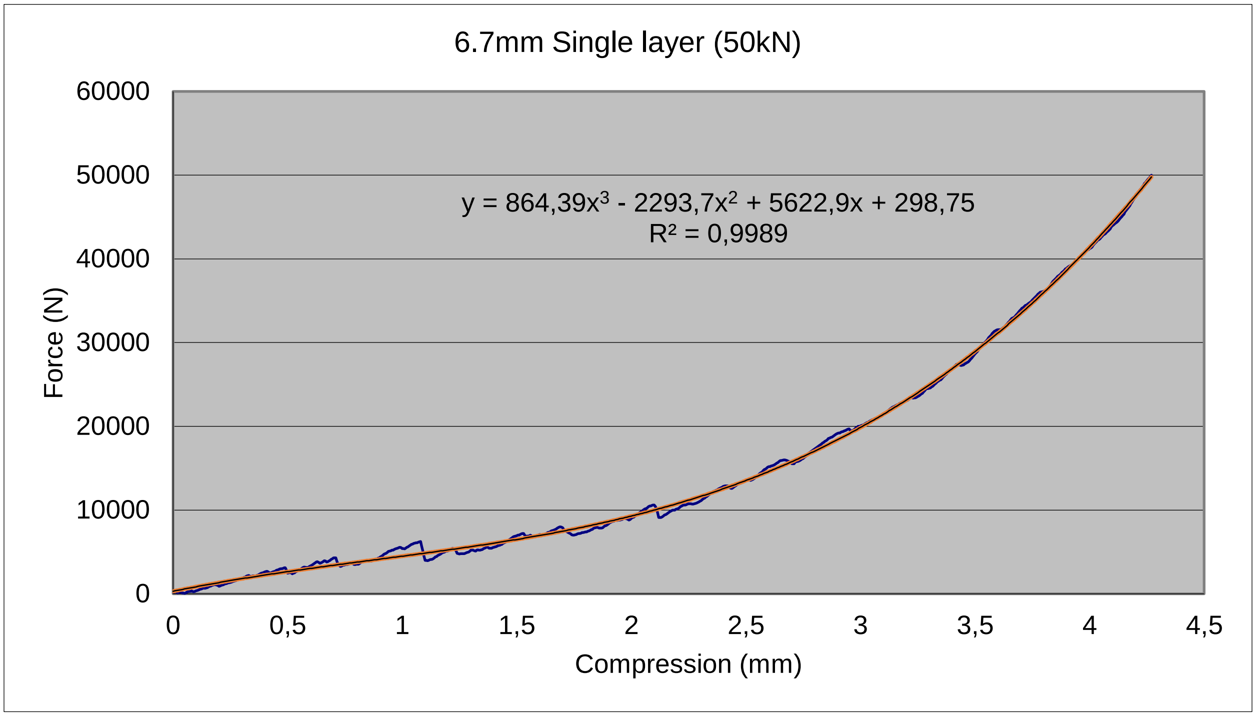

Figure 8-1: 6.70mm Single Layer High Pressure at 50kN

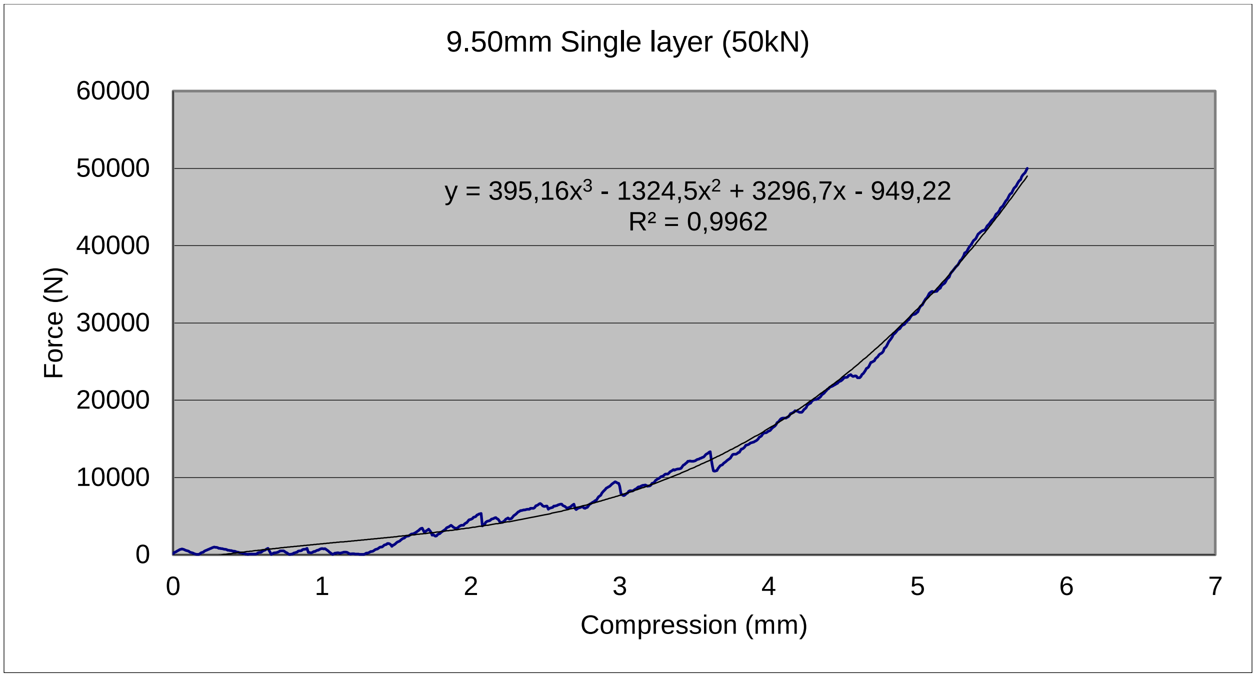

Figure 8-2: 9.50mm Single Layer High Pressure at 50kN

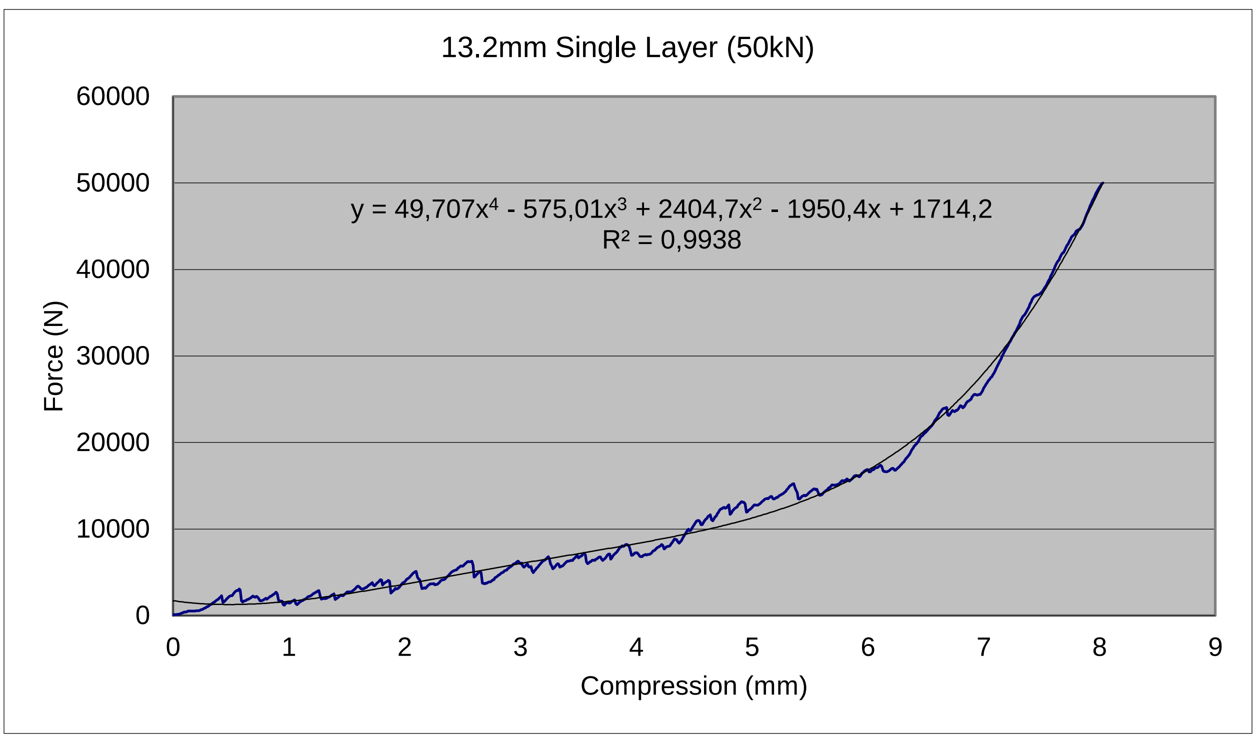

Figure 8-3: 13.20mm Single Layer High Pressure at 50kN

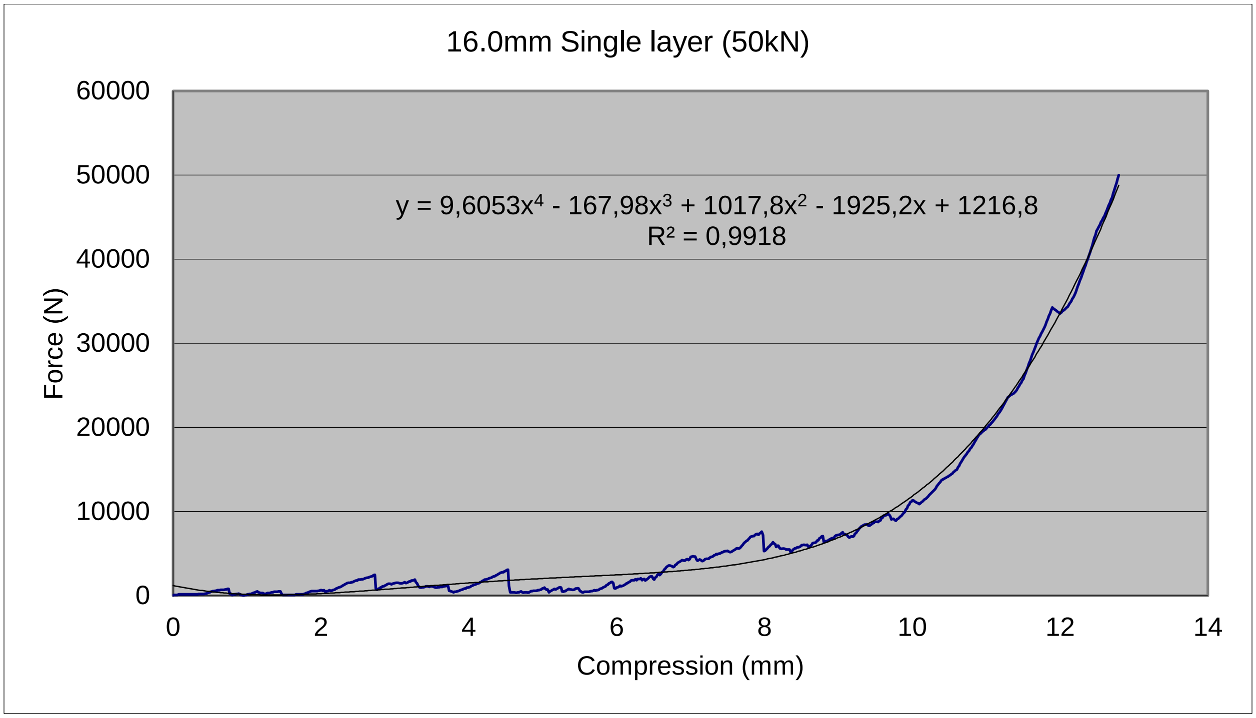

Figure 8-4: 16.0mm Single Layer High Pressure at 50kN

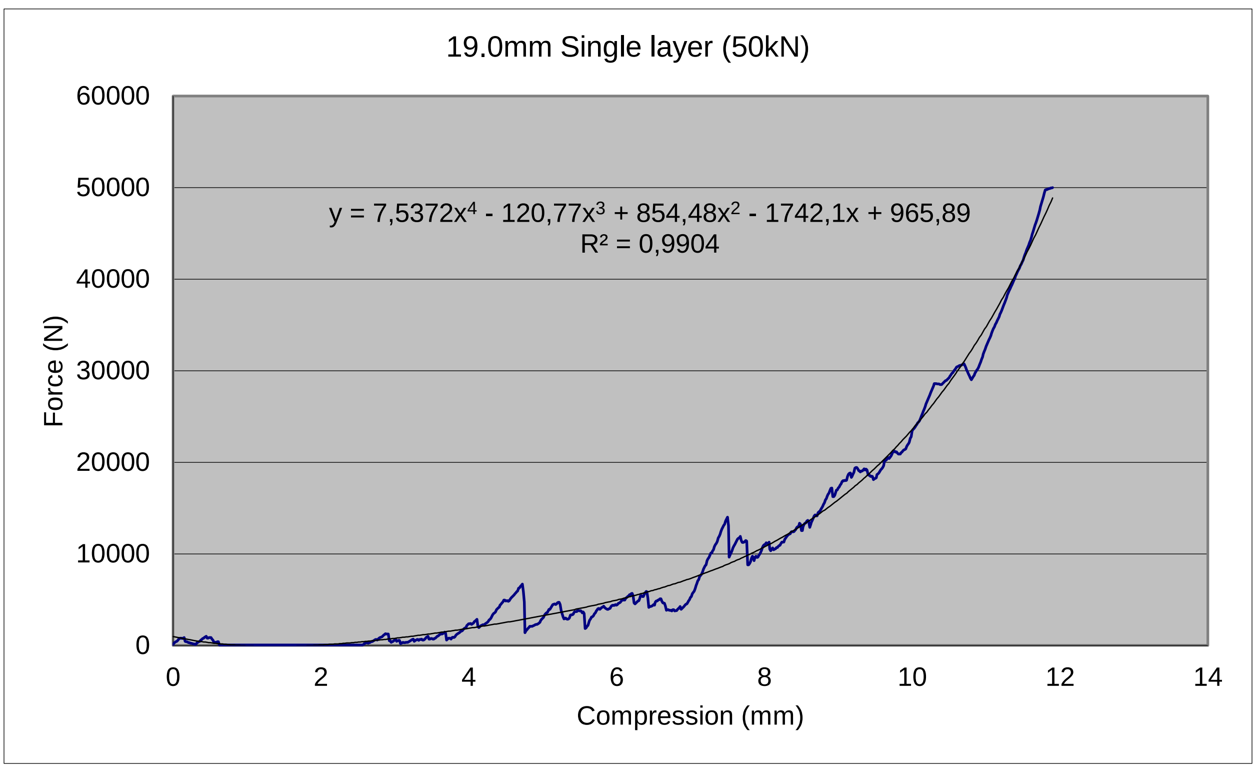

Figure 8-5:19.0mm Single Layer High Pressure at 50kN

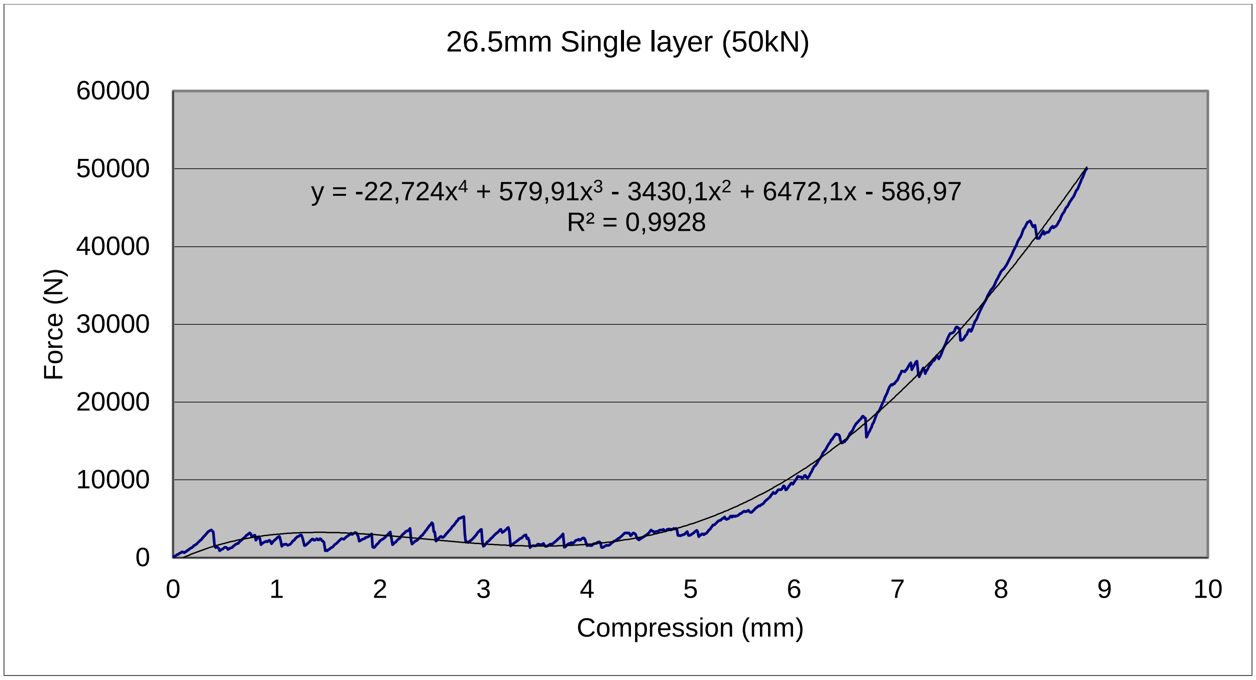

Figure 8-6:26.5mm Single Layer High Pressure at 50kN

8.3.1.2. Three Layer

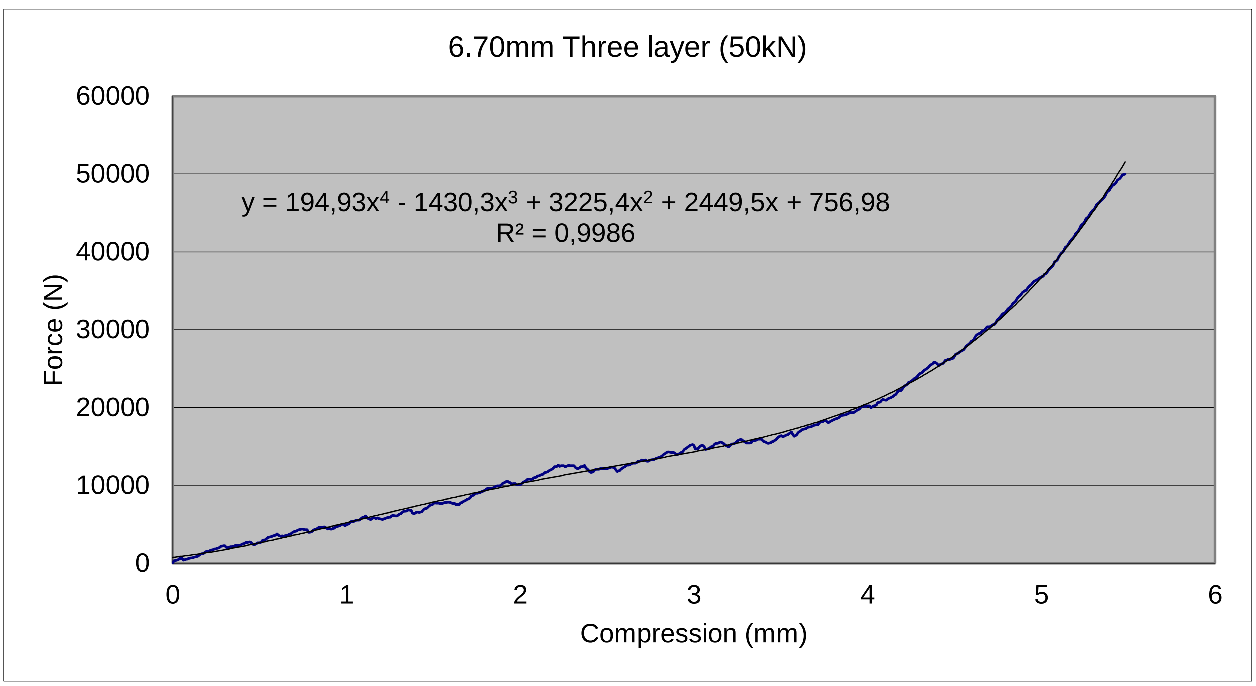

Figure 8-7:6.70mm Three Layer High Pressure at 50kN

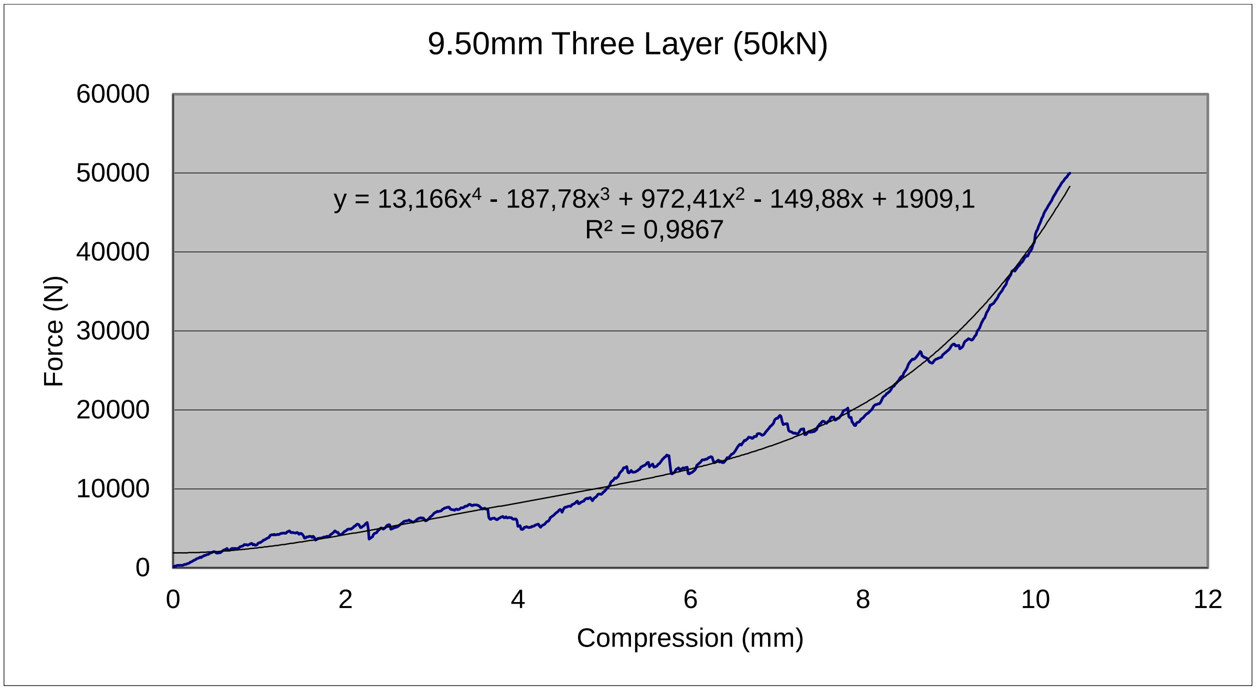

Figure 8-8: 9.50 mm Three Layer High Pressure at 50kN

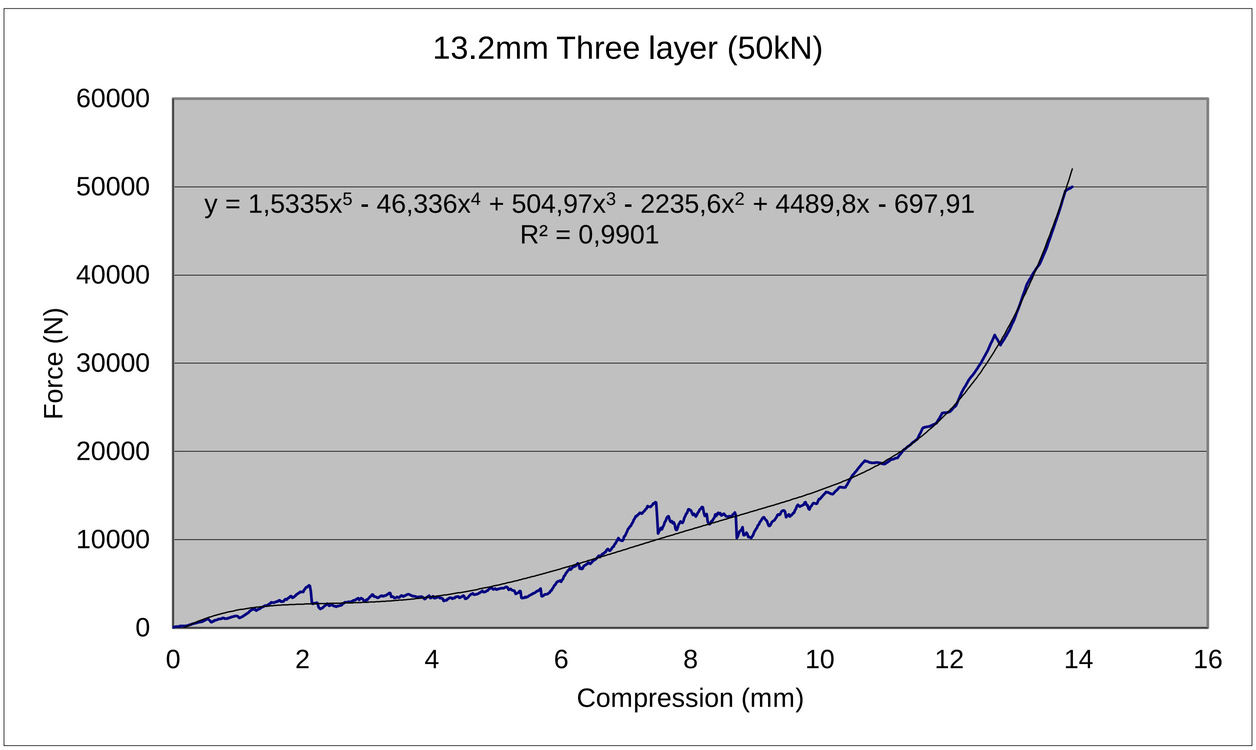

Figure 8-9:13.20 mm Three Layer High Pressure at 50kN

8.3.2. High pressure compression at 80kN

8.3.2.1. Single Layer

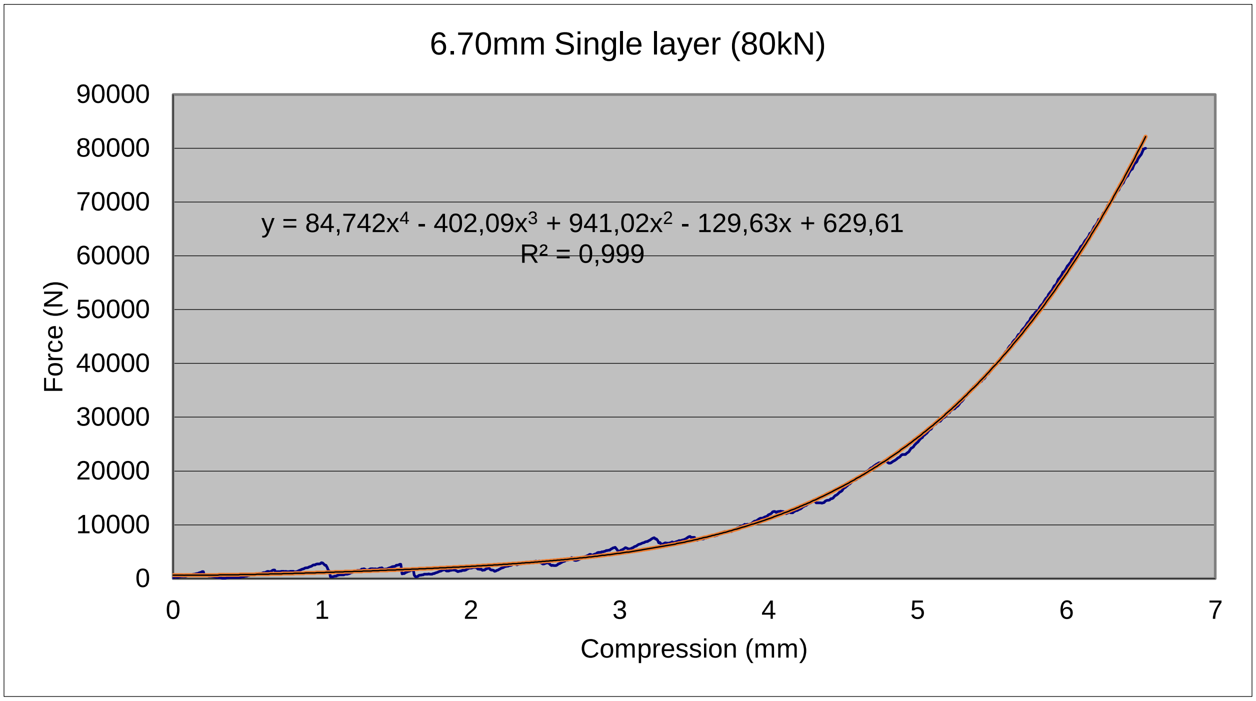

Figure 8-10: 6.70mm Single Layer High Pressure at 80kN

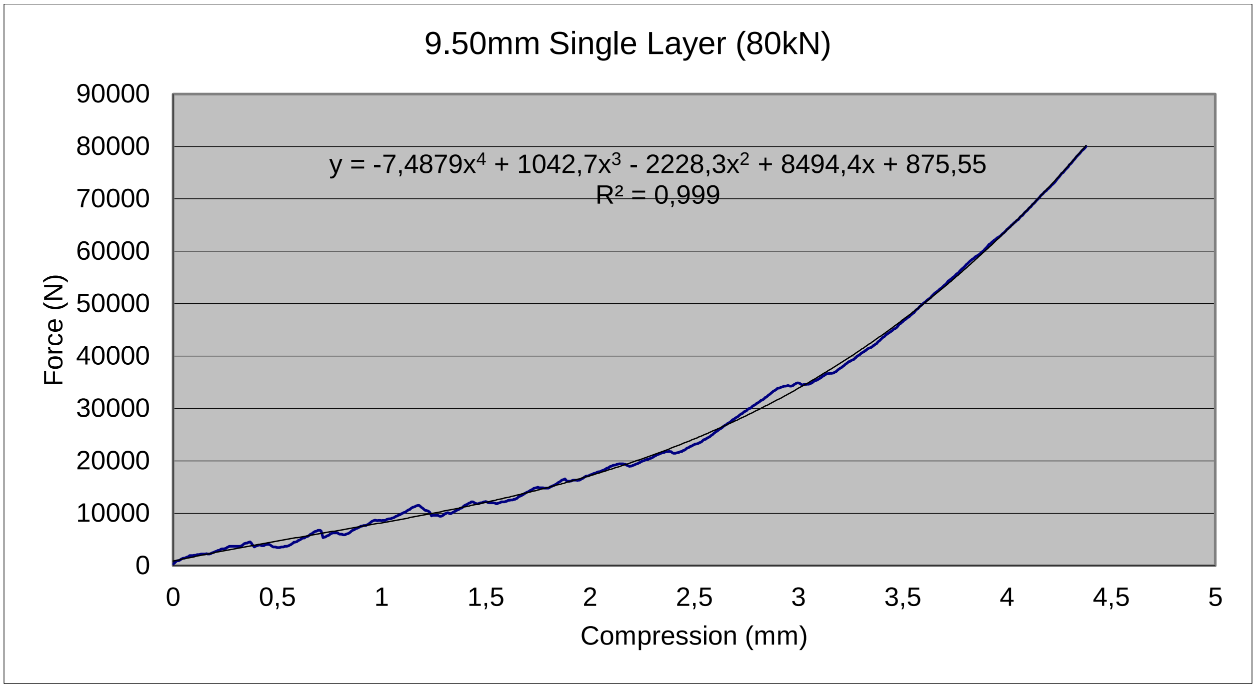

Figure 8-11: 9.50mm Single Layer High Pressure at 80kN

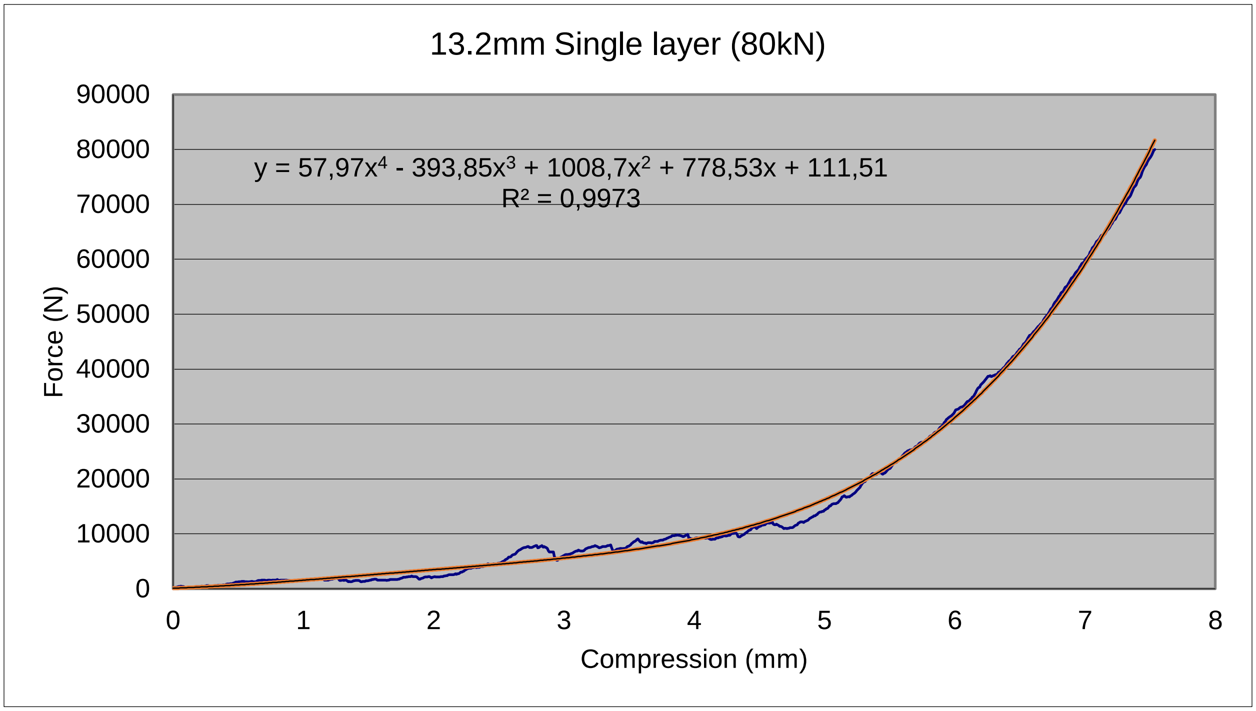

Figure 8-12: 13.2mm Single Layer High Pressure at 80kN

8.3.2.2. Three Layer

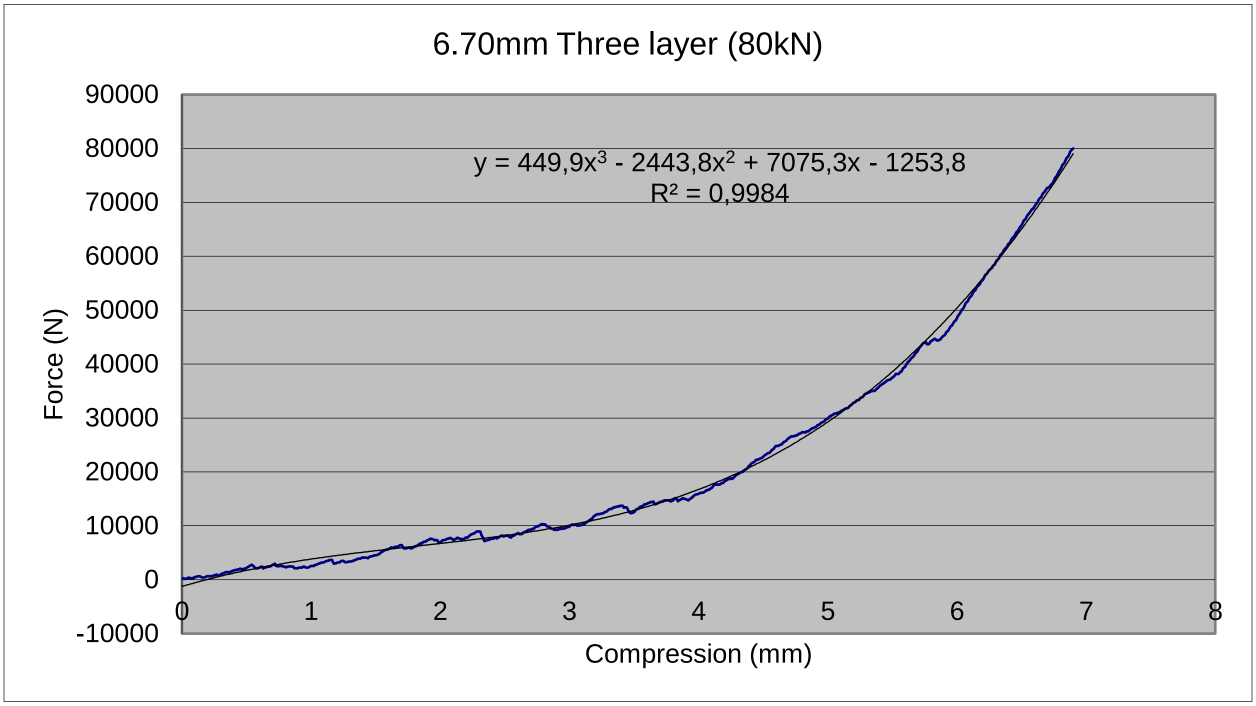

Figure 8-13: 6.70mm Three Layer High Pressure at 80kN

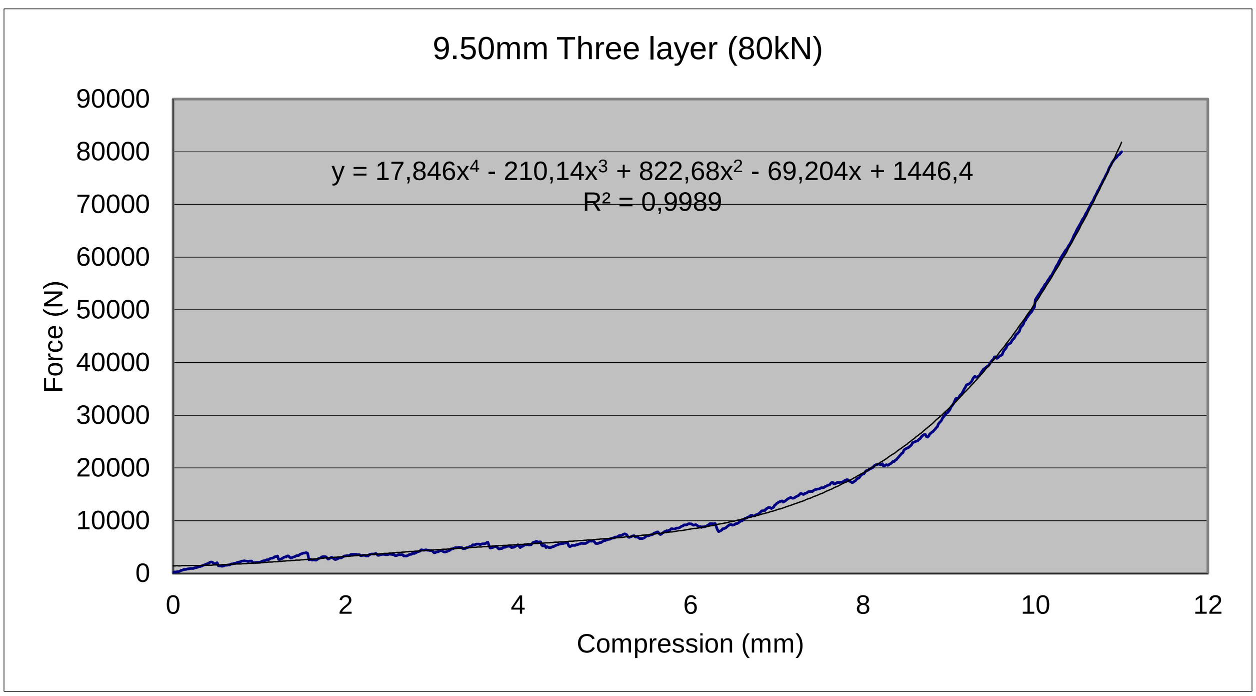

Figure 8-14: 9.50mm Three Layer High Pressure at 80kN

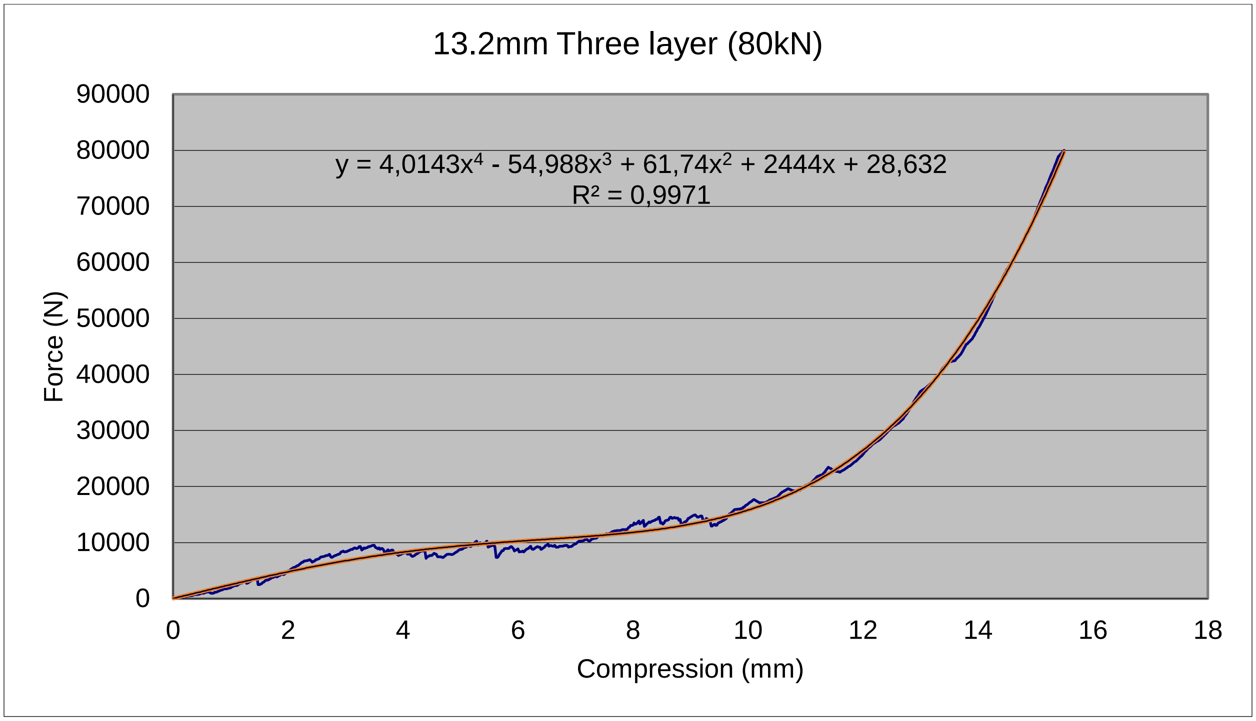

Figure 8-15: 13.2mm Three Layer High Pressure at 80kN